Thermohaline variability in the Mediterranean and Black Seas as observed by Argo floats in 2000-2009

by

Giulio Notarstefano and Pierre-Marie Poulain

Istituto Nazionale di Oceanografia e di Geofisica Sperimentale (OGS)
Trieste, Italy

Partial contribution to Task 4.4 of the Euro Argo PP project.

Produced by the Mediterranean Argo Regional Centre (MED-ARC), OGS, Trieste, Italy

Approved for release by: ……

Dr. Alessandro Crise
Director, Department of Oceanography

Table of contents

1. Introduction

Since 2000, numerous Argo floats have been deployed in the Mediterranean and Black Seas under various programs and by different institutions/countries. Different cycling and sampling characteristics have been chosen to monitor these marginal seas, including cycles of 5 to 10 days, parking depths between 350 and 650 m for the Mediterranean and between 200 and 1550 m for the Black Sea, and maximum profiling depths between 700 and 2000 m. This report contains the description of the thermohaline variability obtained using all the historical Argo data in the Mediterranean (section 2) and Black Sea (section 3). The intrinsic variability of the temperature and salinity is first described for most of the Mediterranean sub-basins and the Black Sea by means of monthly statistics. Second, the Argo dataset is sub-sampled (reduced number of floats) and the same statistics are computed. Third, the temporal decorrelation scales of temperature and salinity following floats are estimated. Conclusions are included in section 4.

2. Argo data in the Mediterranean Sea

In total, 88 Argo floats have been operated in the Mediterranean Sea between December 2000 and June 2009, out of which 27 correspond to the MFSTEP project (Poulain et al. 2007). The maximum density of floats was obtained in May 2006 with 31 floats running simultaneously. Figure 1 depicts the temporal evolution of the float population in the Mediterranean, whereas details on the number of floats and profiles are listed in Table 1.

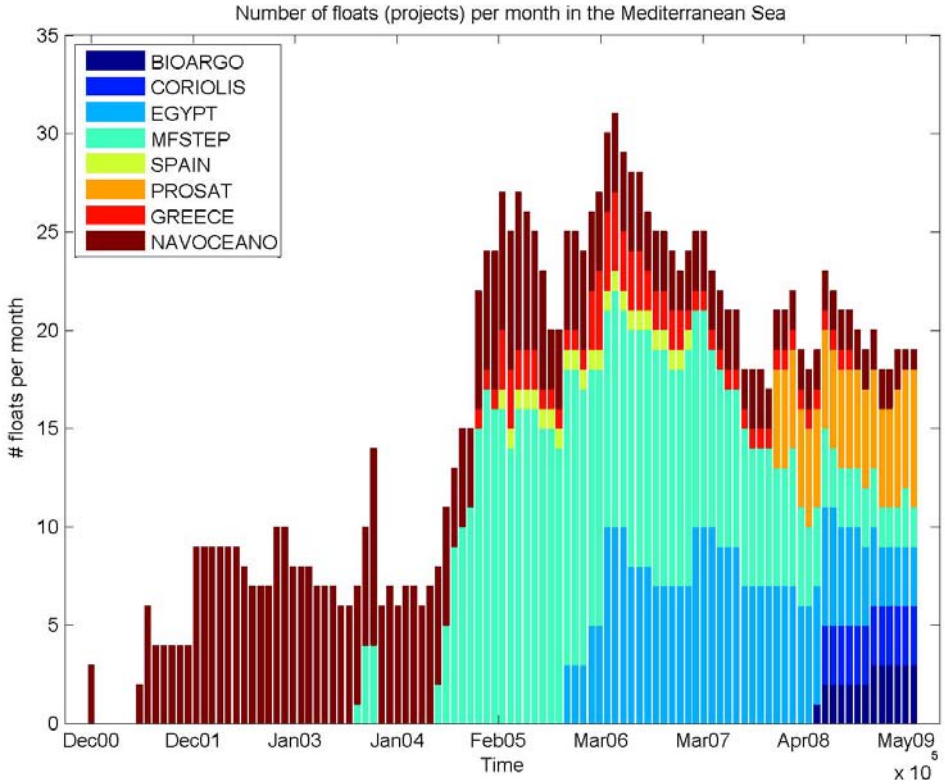

Figure 1. Number of Argo floats per month in the Mediterranean between December 2000 and June 2009.

Program/Agency/Country	Number of floats	Number of CTD profiles
MFSTEP	27	3105
SPAIN	1	138
NAVOCEANO	29	2502
FRANCE (EGYPT, PROSAT, BIOARGO, CORIOLIS)	27	1650
GREECE	4	392
TOTAL	88	7787

Table 1. Number of floats and CTD profiles for the Argo program in the Mediterranean between December 2000 and June 2009.

The Mediterranean Argo floats were operated by the following countries or agencies: U.S. Naval Oceanography Office (NAVOCEANO), European Commission (MFSTEP FP5 project), France (EGYPT, PROSAT, BIOARGO and CORIOLIS projects), Spain and Greece.

The Mediterranean Argo database used to estimate the statistics presented in this report was downloaded from the Argo Global Data Assembly Center (GDAC; http://www.coriolis.eu.org/) in June 2009. They include a total of 7787 CTD profiles spanning the period December 2000 and June 2009. The temporal distribution of the number of profiles per month in the Mediterranean Sea is depicted in Figure 2. The month with the maximal data density (more than 160 profiles per month) is April 2006. The Levantine sub-basin is in general the most populated with data spanning continuously between June 2001 and June 2009.

Figure 3 shows the geographical coverage of the Argo profiles considered and the division of the Mediterranean Sea in several sub-basins. The following sub-basins were relatively well sampled by the floats: Catalan, Algerian, Ligurian, Tyrrhenian, Ionian, Cretan and Levantine. The Alboran and Aegean seas and the Sicily Channel area have limited Argo data. No data are available in the Adriatic Sea. The numbers of the CTD profiles per sub-basin are posted in the figure and listed in Table 2.

Mediterranean sub-basin	Number of CTD profiles
Alboran	62
Algerian	755
Catalan	384
Ligurian	582
Tyrrhenian	508
Sicily	99
Ionian	1367
Aegean	135
Cretan	845
Levantine	3050
Total	7787

Table 2. Number of CTD profiles for the Argo program in the Mediterranean sub-basins between December 2000 and June 2009.

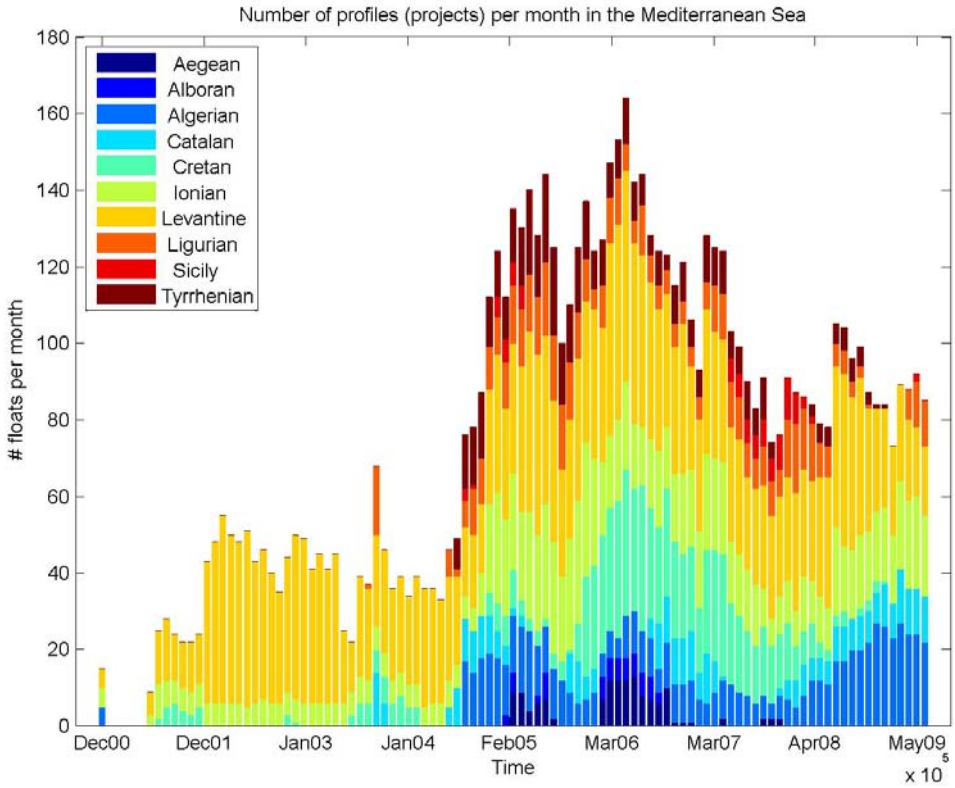

Figure 2. Number of CTD profiles per month provided by Argo floats in the Mediterranean between December 2000 and June 2009. Colors indicate various sub-basins of the Mediterranean (see Figure 3).

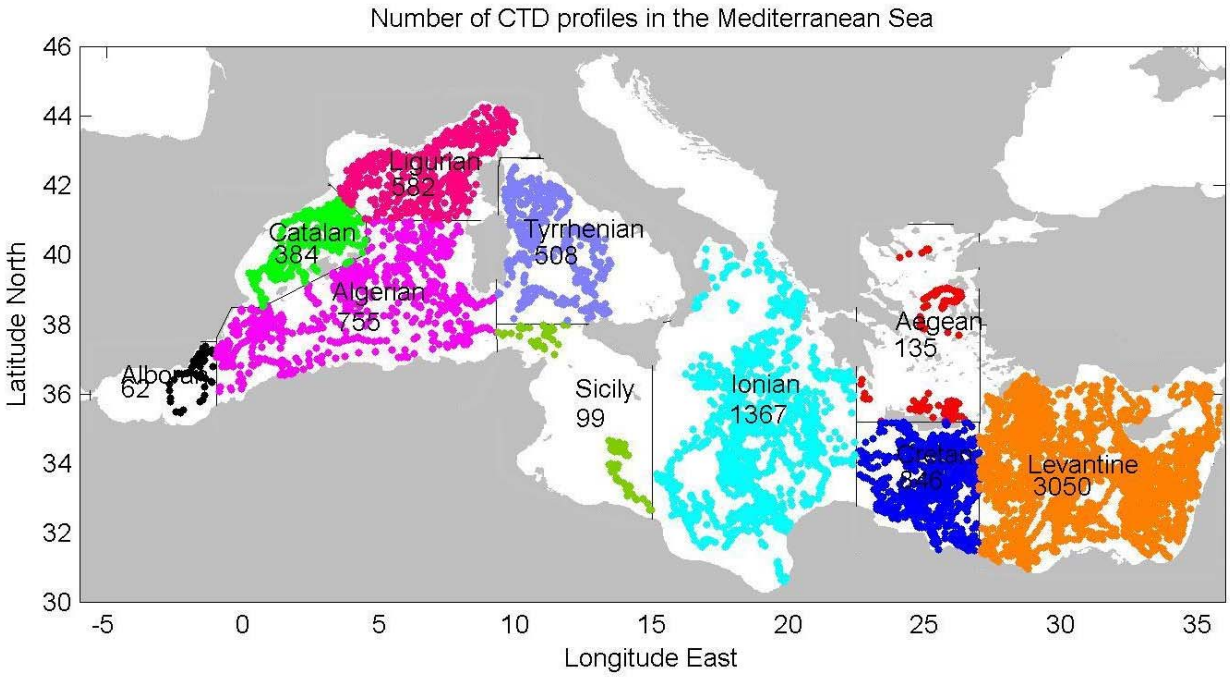

Figure 3. Geographical distribution of the CTD profiles provided by Argo floats in the Mediterranean between December 2000 and June 2009. Colors indicate various sub- basins of the Mediterranean defined in the figure.

2.1 Thermohaline characteristics of the Mediterranean sub-basins.

The following statistics have been calculated using the above-mentioned Argo data in the Mediterranean sub-basins:

- number of observations, mean and standard deviation of potential temperature (θ) and salinity (S) near 0, 600 and 2000 m;
- number of observations, mean and standard deviation of potential temperature (θ) and salinity (S) near depth of salinity maximum;
- depth of salinity maximum.

The Alboran, Sicily and Aegean sub-basins are excluded due to their limited number of observations. The depth of 600 m was chosen as a sub-surface level reached by most floats (including the NAVOCEANO floats), bathymetry permitting.

2.1.1 Algerian sub-basin

Figures 4 and 5 illustrate the temporal distribution of the number of active floats and the number of CTD profiles per month in the Algerian sub-basin, respectively.

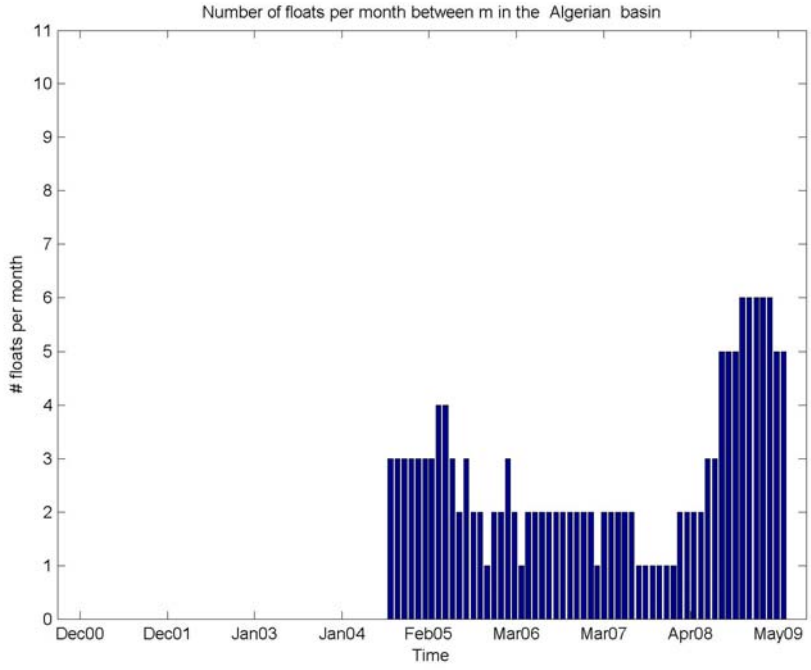

Figure 4. Number of active floats per month in the Algerian sub-basin between December 2000 and June 2009.

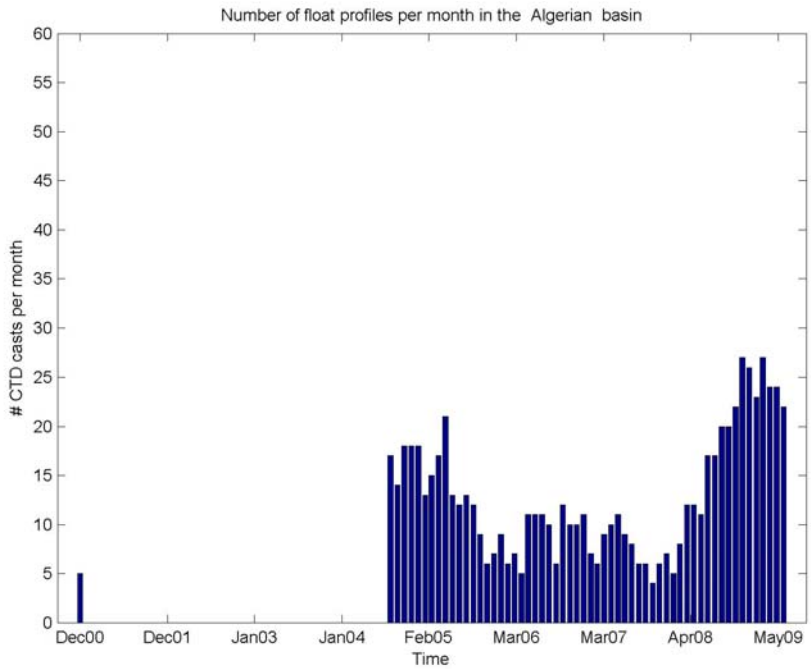

Figure 5. Number of CTD profiles per month in the Algerian sub-basin between December 2000 and June 2009.

The monthly means of θ and S near the surface (0-10 m) are displayed in Figures 6 and 7, respectively. Vertical bars denote the standard deviations and the standard errors. The corresponding numbers of observations are shown in Figure 8.

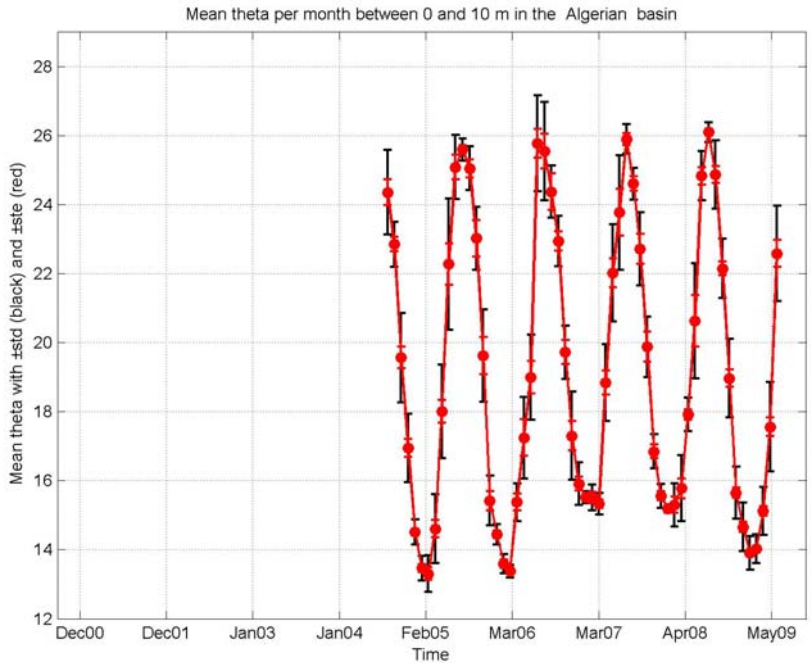

Figure 6. Monthly mean of surface θ in the Algerian sub-basin between December 2000 and June 2009.

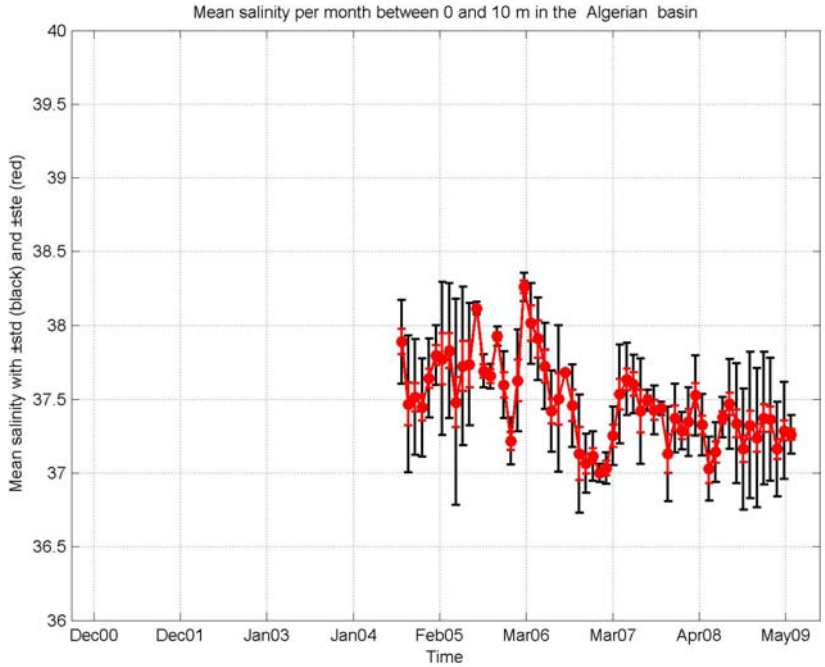

Figure 7. Monthly mean of surface S in the Algerian sub-basin between December 2000 and June 2009.

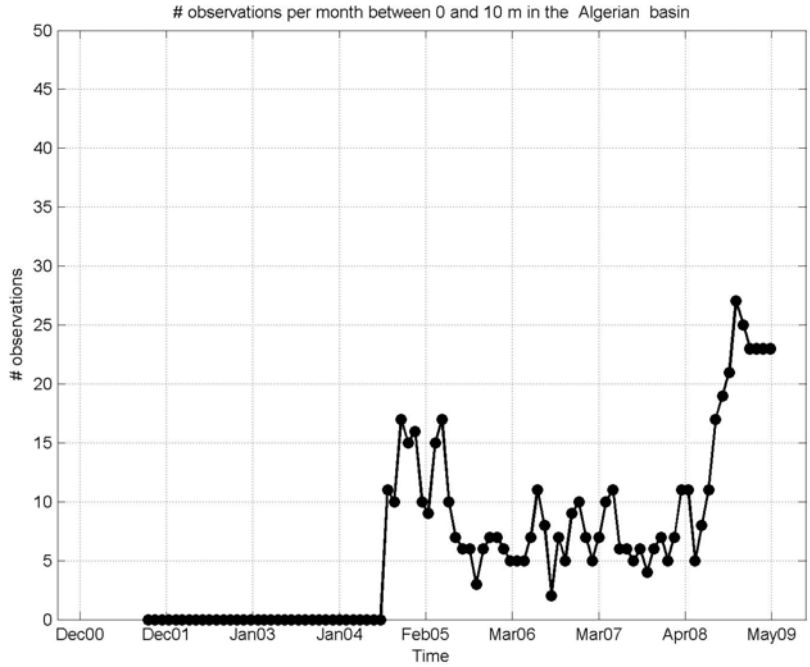

Figure 8. Number of surface observations in the Algerian sub-basin between December 2000 and June 2009.

The monthly means of θ and S near 600 m are displayed in Figures 9 and 10, respectively. Vertical bars denote the standard deviations and the standard errors. The corresponding numbers of observations are shown in Figure 11.

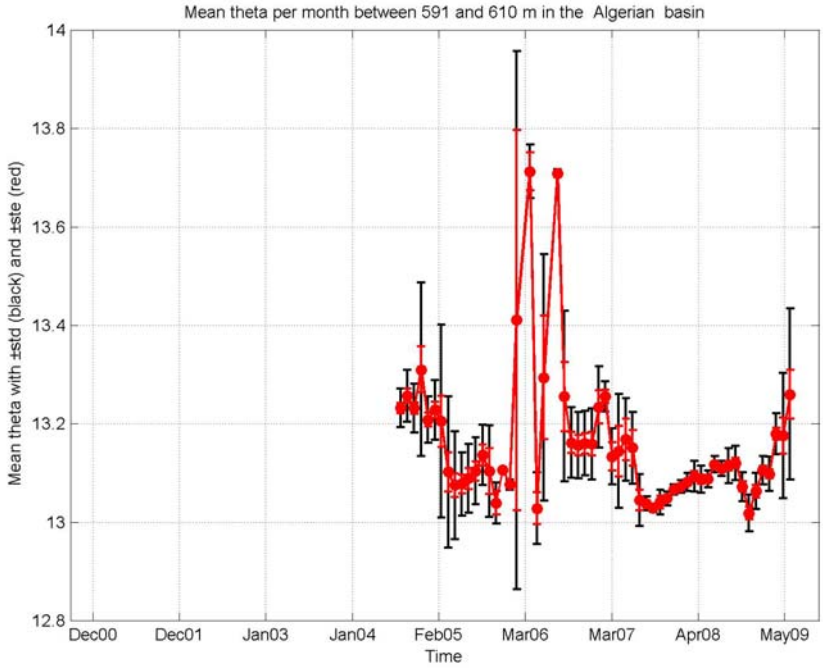

Figure 9. Monthly mean of θ near 600 m in the Algerian sub-basin between December 2000 and June 2009.

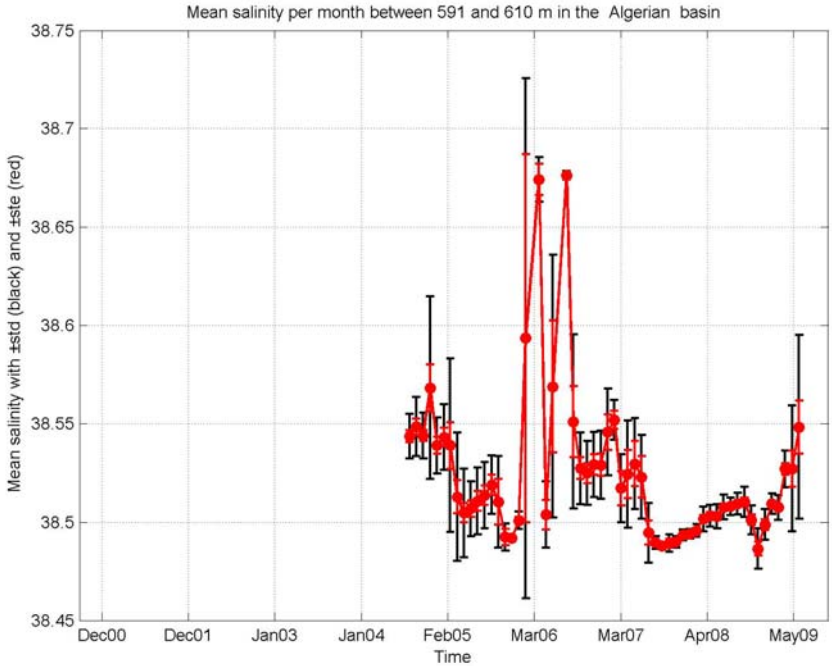

Figure 10. Monthly mean of S near 600 m in the Algerian sub-basin between December 2000 and June 2009.

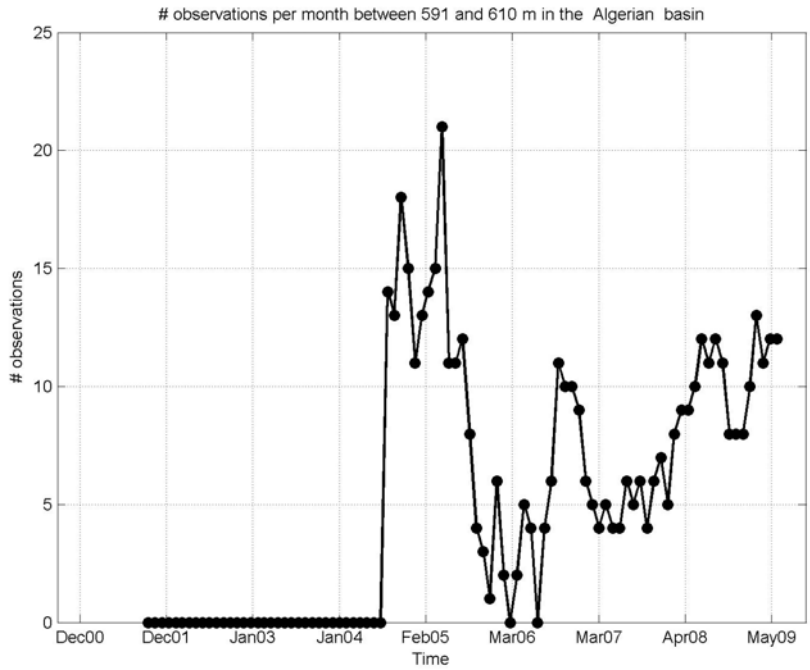

Figure 11. Number of observations near 600 m in the Algerian sub-basin between December 2000 and June 2009.

The monthly means of θ and S near 2000 m are displayed in Figures 12 and 13, respectively. Vertical bars denote the standard deviations and the standard errors. The corresponding numbers of observations are shown in Figure 14.

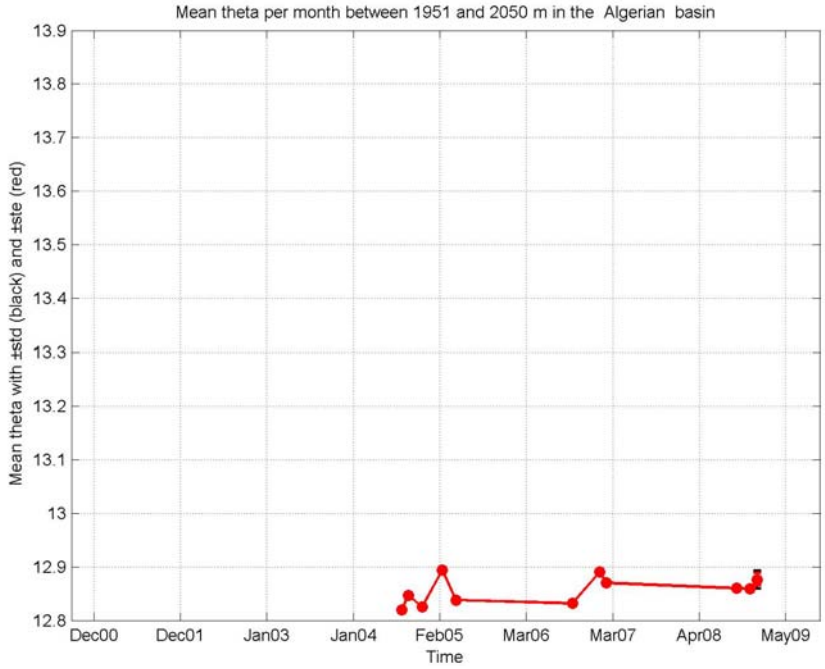

Figure 12. Monthly mean of θ near 2000 m in the Algerian sub-basin between December 2000 and June 2009.

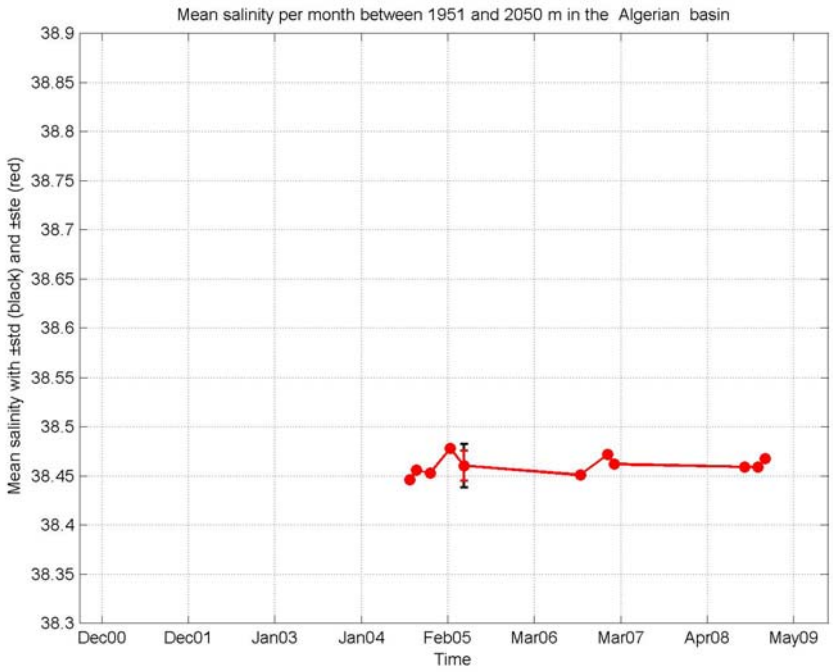

Figure 13. Monthly mean of S near 2000 m in the Algerian sub-basin between December 2000 and June 2009.

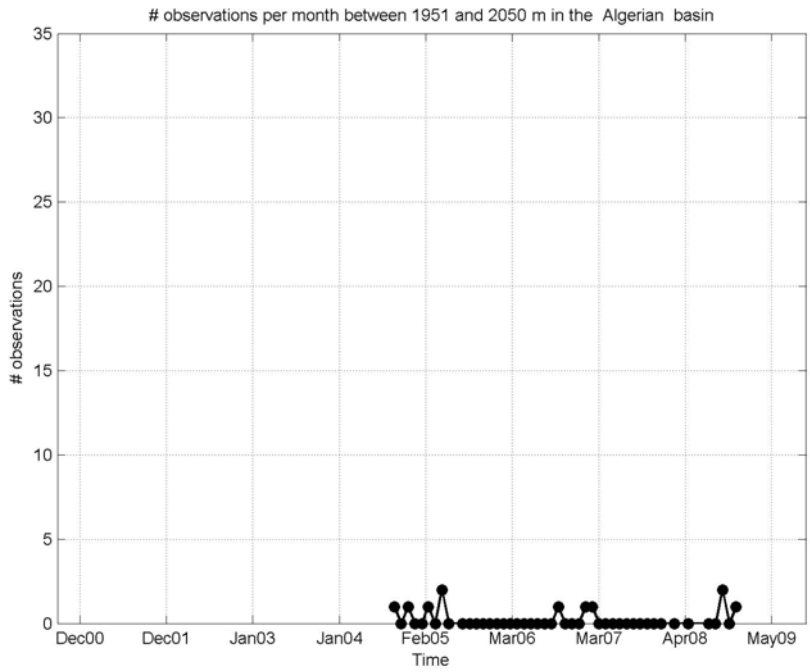

Figure 14. Number of observations near 600 m in the Algerian sub-basin December 2000 and June 2009.

The temporal distributions of the monthly mean of the maximum S and the corresponding depth of the salinity maximum are depicted, respectively in Figures 14 and 15, for the Algerian sub-basin.

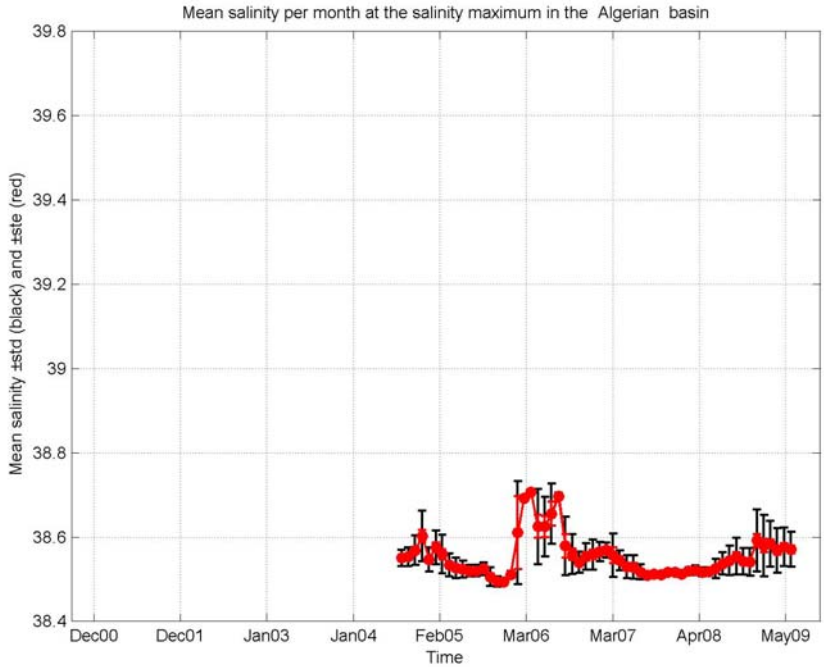

Figure 15. Monthly mean of the maximum S in the Algerian sub-basin December 2000 and June 2009.

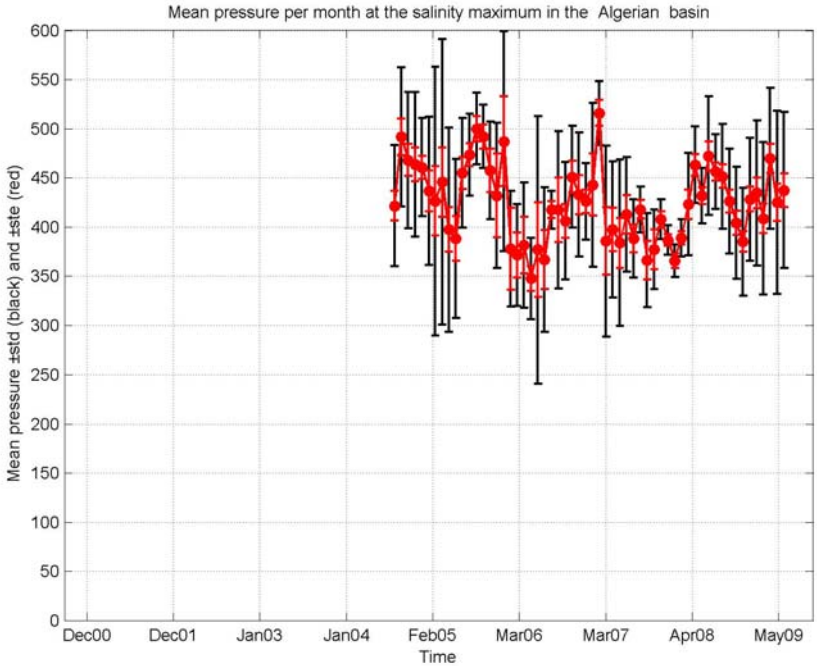

Figure 16. Monthly mean of the depth of the salinity maximum in the Algerian sub-basin between December 2000 and June 2009.

2.1.2 Catalan sub-basin

Figures 17 and 18 illustrate the temporal distribution of the number of active floats and the number of CTD profiles per month in the Catalan sub-basin, respectively.

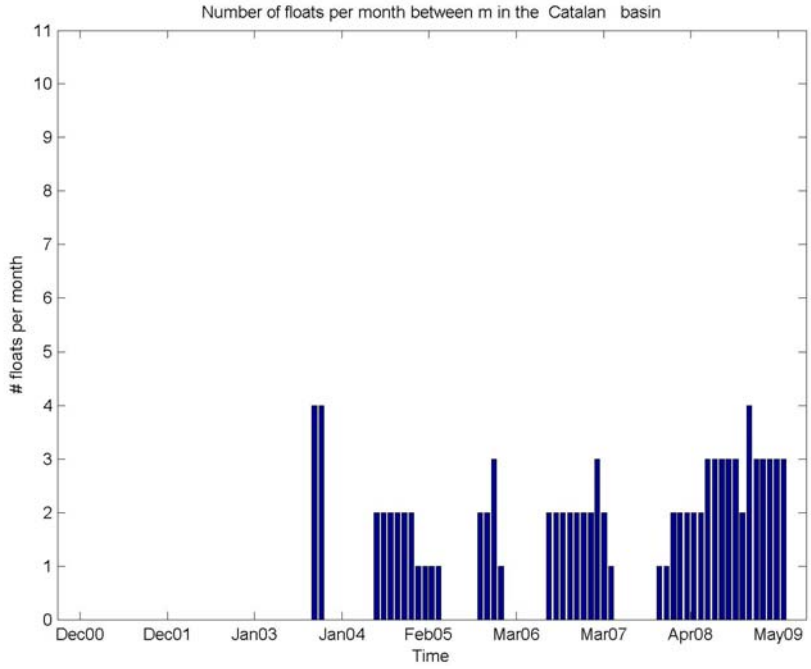

Figure 17. Number of active floats per month in the Catalan sub-basin between December 2000 and June 2009.

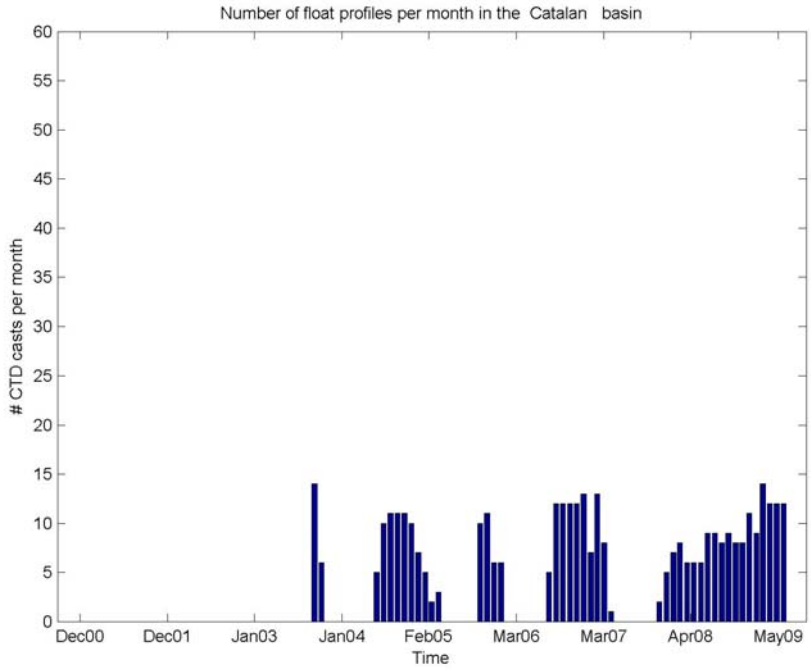

Figure 18. Number of CTD profiles per month in the Catalan sub-basin between December 2000 and June 2009.

The monthly means of θ and S near the surface (0-10 m) are displayed in Figures 19 and 20, respectively. Vertical bars denote the standard deviations and the standard errors. The corresponding numbers of observations are shown in Figure 21.

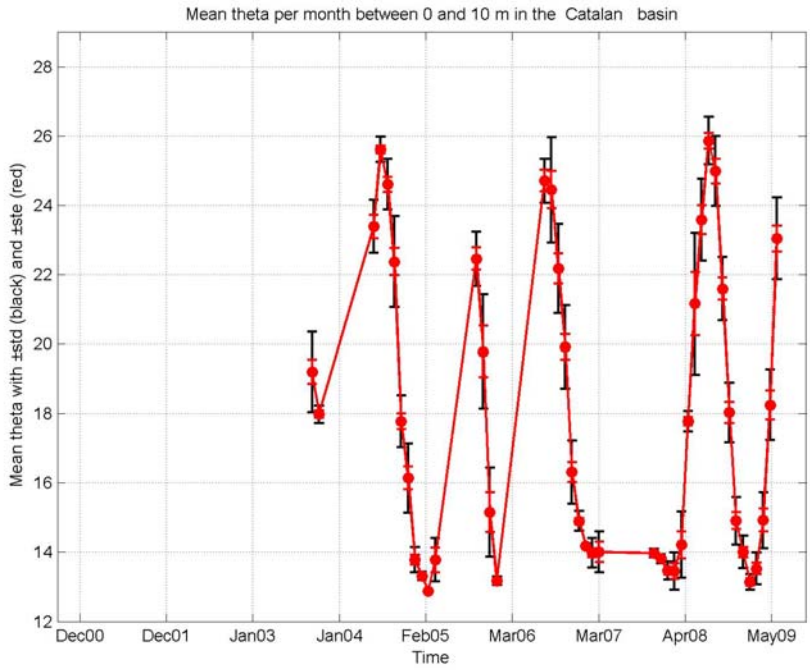

Figure 19. Monthly mean of surface θ in the Catalan sub-basin between December 2000 and June 2009.

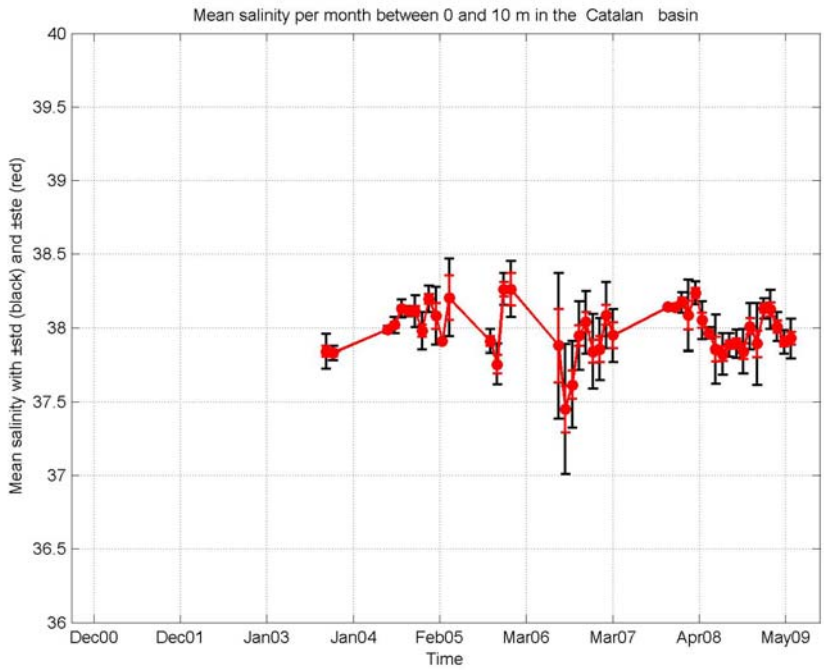

Figure 20. Monthly mean of surface S in the Catalan sub-basin between December 2000 and June 2009.

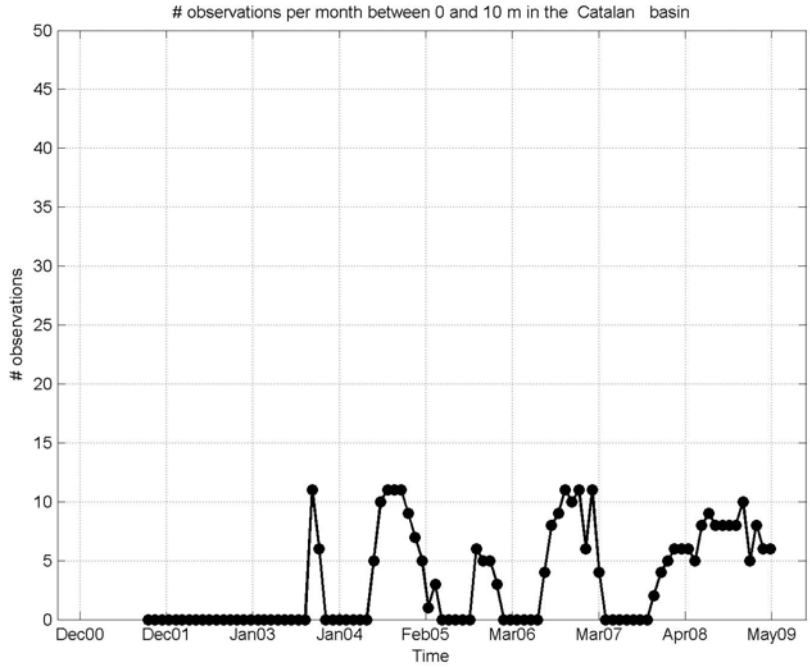

Figure 21. Number of surface observations in the Catalan sub-basin between December 2000 and June 2009.

The monthly means of θ and S near 600 m are displayed in Figures 22 and 23, respectively. Vertical bars denote the standard deviations and the standard errors. The corresponding numbers of observations are shown in Figure 24.

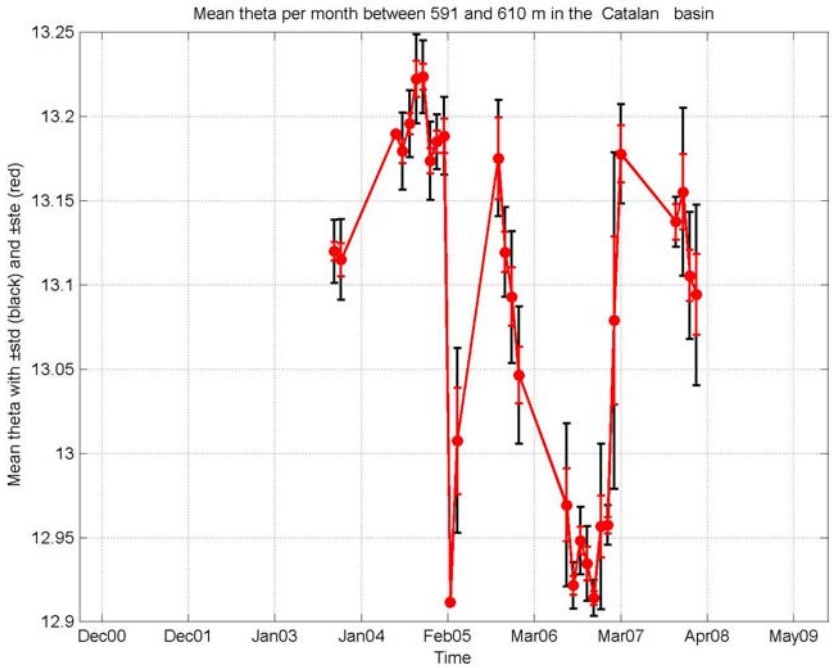

Figure 22. Monthly mean of θ near 600 m in the Catalan sub-basin between December 2000 and June 2009.

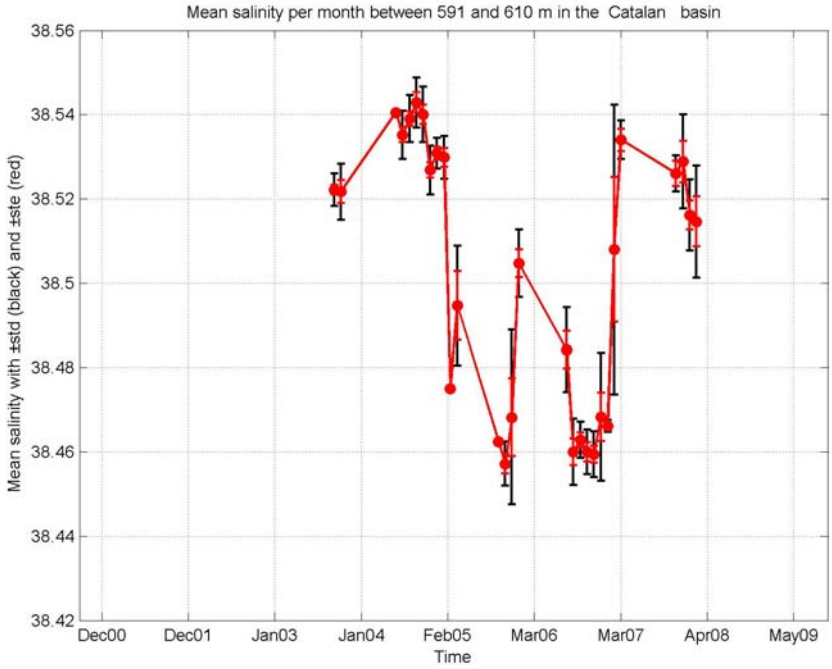

Figure 23. Monthly mean of S near 600 m in the Catalan sub-basin between December 2000 and June 2009.

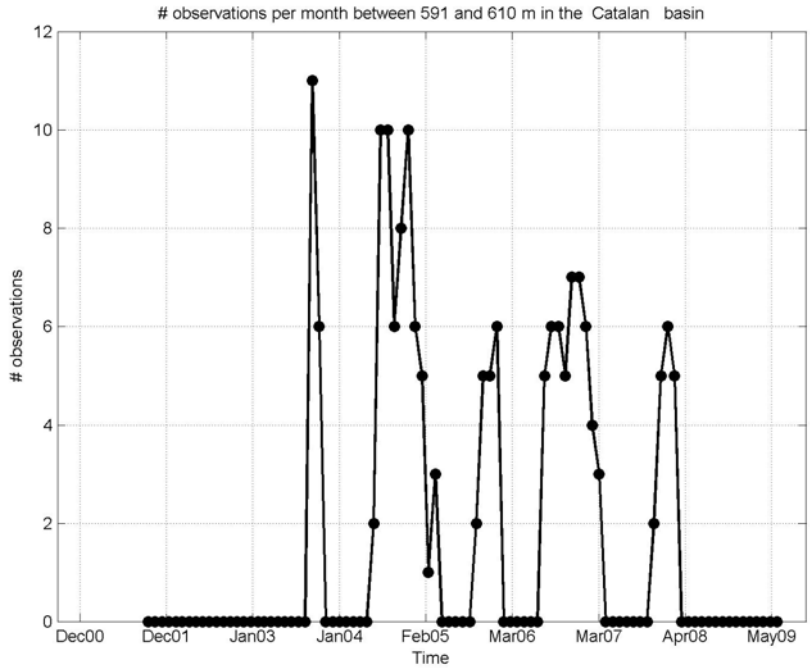

Figure 24. Number of observations near 600 m in the Catalan sub-basin between December 2000 and June 2009.

The monthly means of θ and S near 2000 m are displayed in Figures 25 and 26, respectively. Vertical bars denote the standard deviations and the standard errors. The corresponding numbers of observations are shown in Figure 27

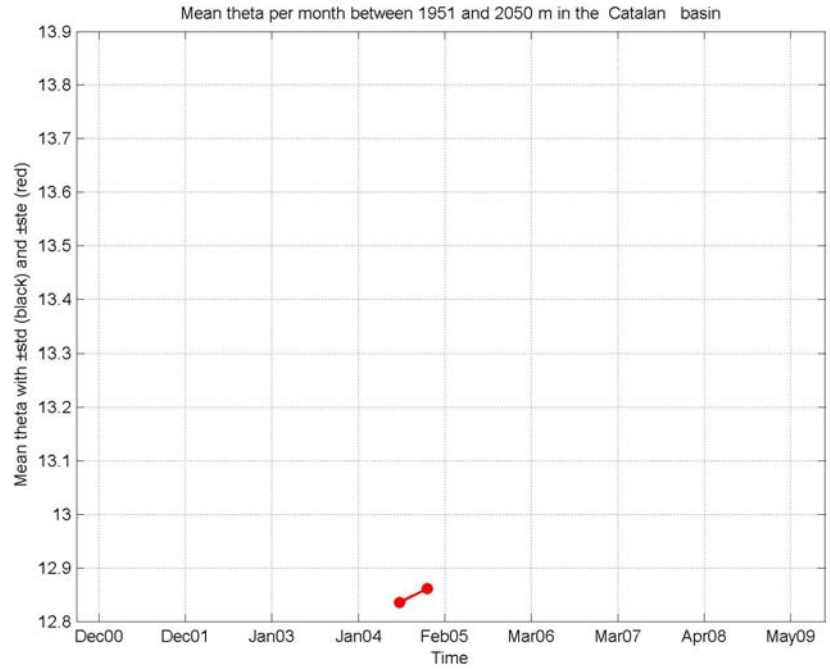

Figure 25. Monthly mean of θ near 2000 m in the Catalan sub-basin between December 2000 and June 2009.

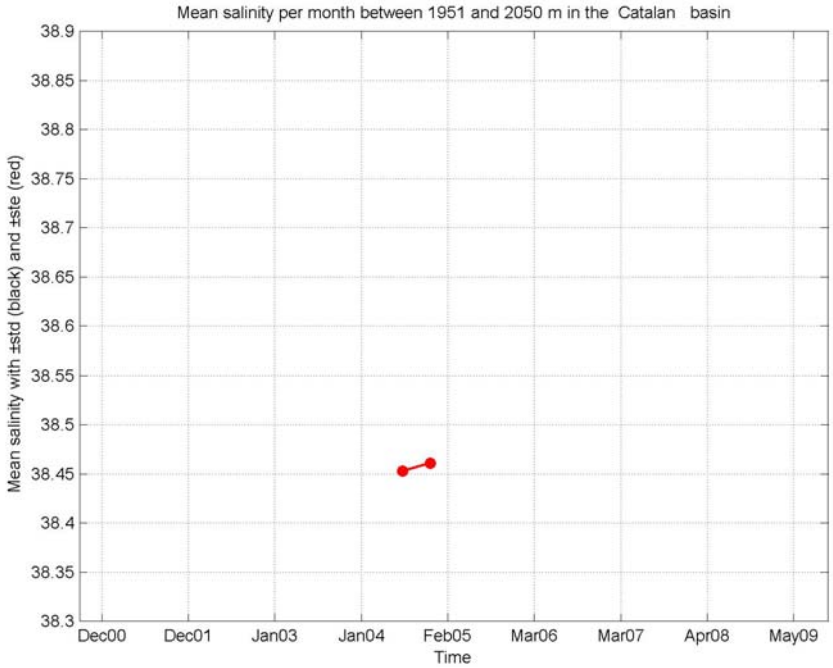

Figure 26. Monthly mean of S near 2000 m in the Catalan sub-basin between December 2000 and June 2009.

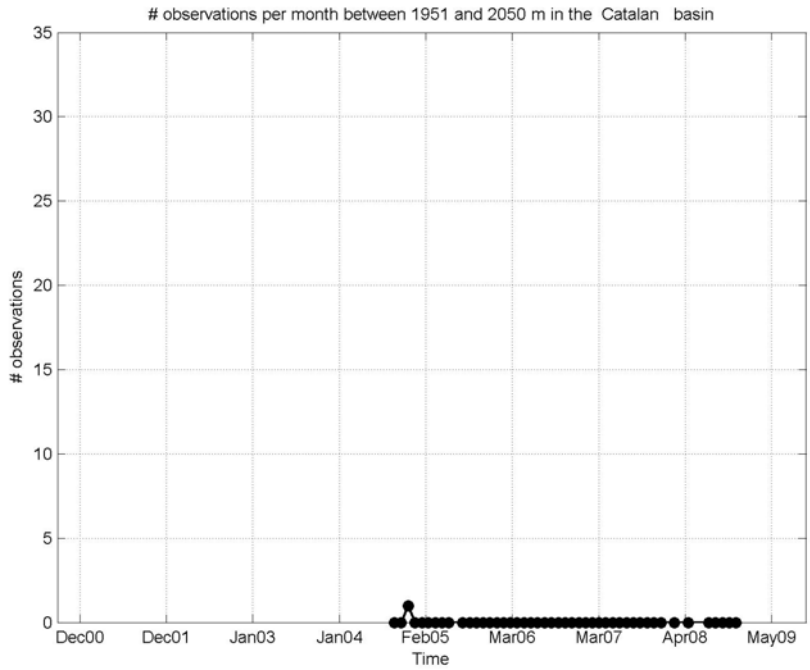

Figure 27. Number of observations near 600 m in the Catalan sub-basin December 2000 and June 2009.

The temporal distributions of the monthly mean of the maximum S and the corresponding depth of the salinity maximum are depicted, respectively in Figures 28 and 29.

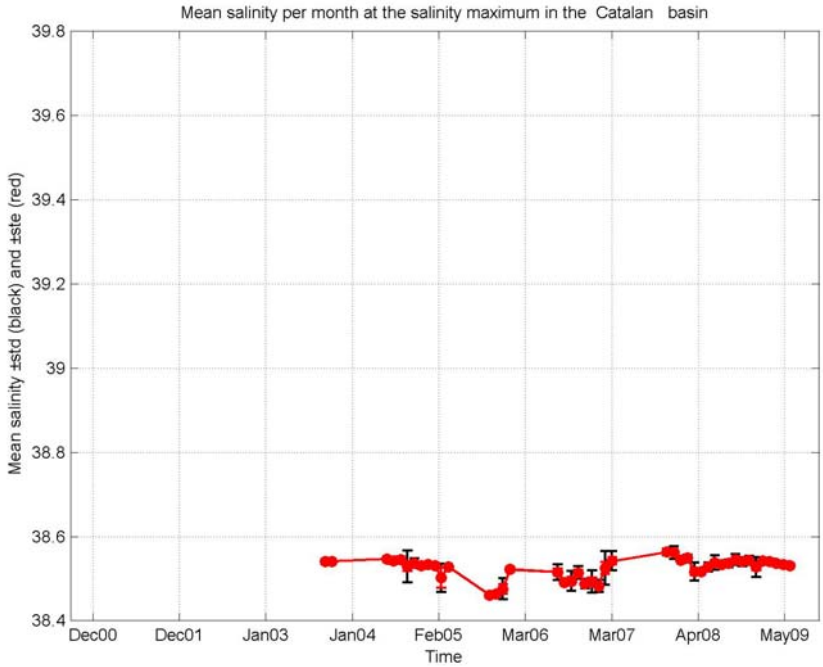

Figure 28. Monthly mean of the maximum S in the Catalan sub-basin December 2000 and June 2009.

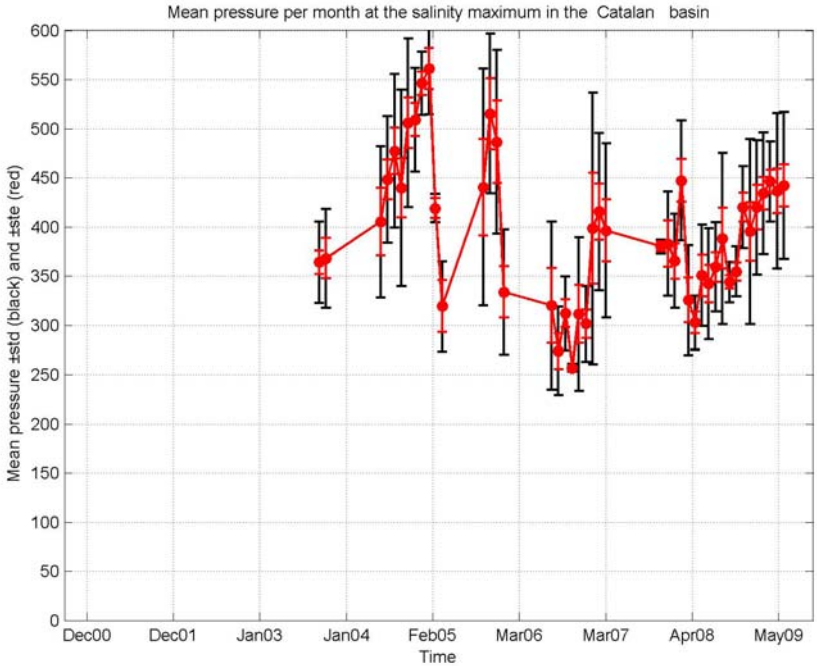

Figure 29. Monthly mean of the depth of the salinity maximum in the Catalan sub-basin between December 2000 and June 2009.

2.1.3 Ligurian sub-basin

Figures 30 and 31 illustrate the temporal distribution of the number of active floats and the number of CTD profiles per month in the Ligurian sub-basin, respectively.

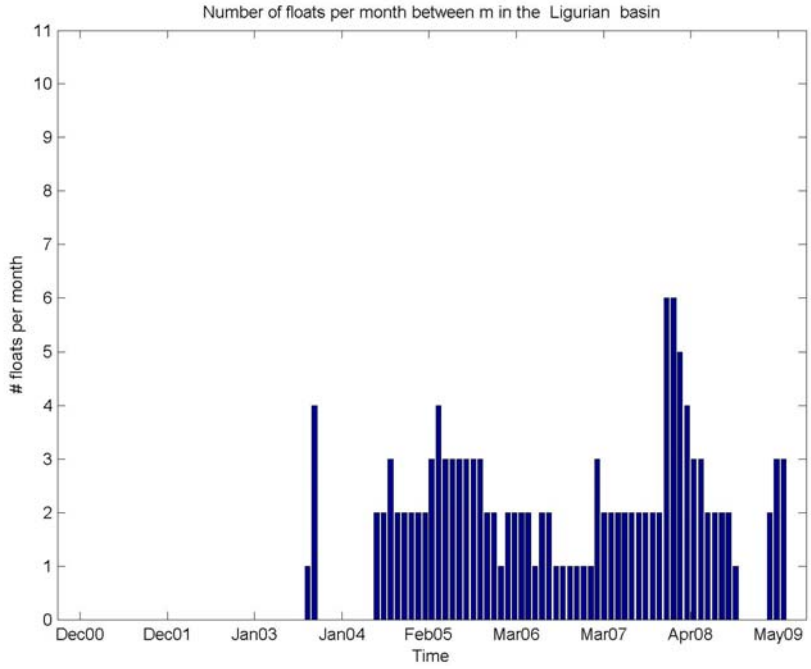

Figure 30. Number of active floats per month in the Ligurian sub-basin between December 2000 and June 2009.

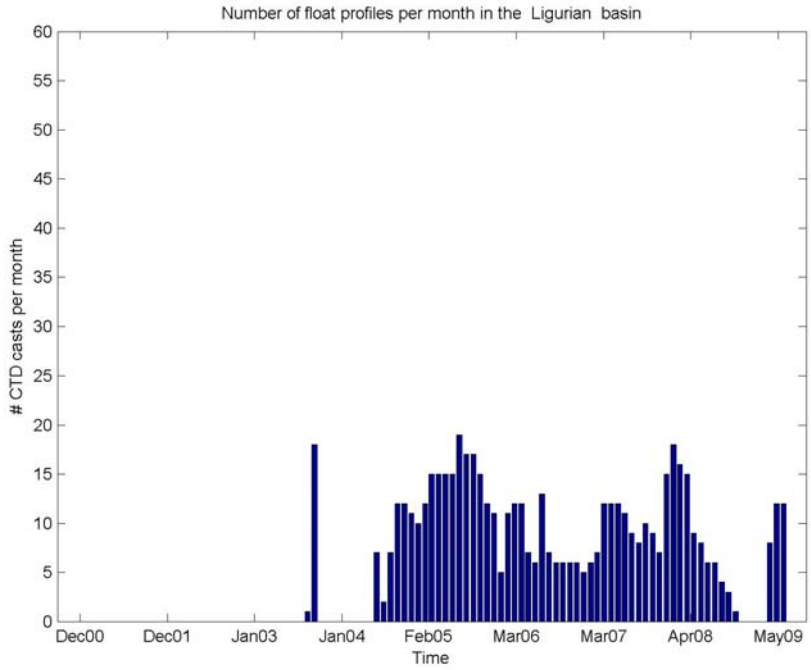

Figure 31. Number of CTD profiles per month in the Ligurian sub-basin between December 2000 and June 2009.

The monthly means of θ and S near the surface (0-10 m) are displayed in Figures 32 and 33, respectively. Vertical bars denote the standard deviations and the standard errors. The corresponding numbers of observations are shown in Figure 34.

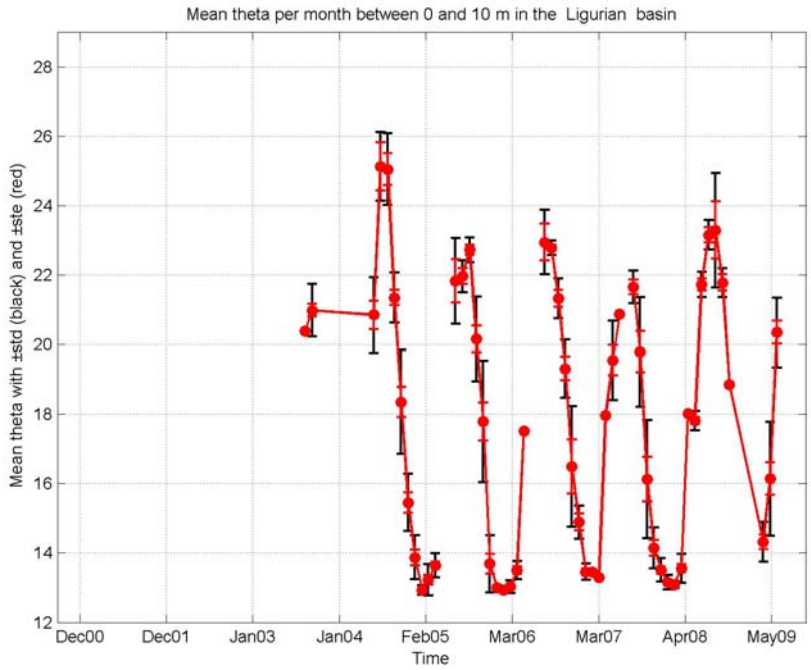

Figure 32. Monthly mean of surface θ in the Ligurian sub-basin between December 2000 and June 2009.

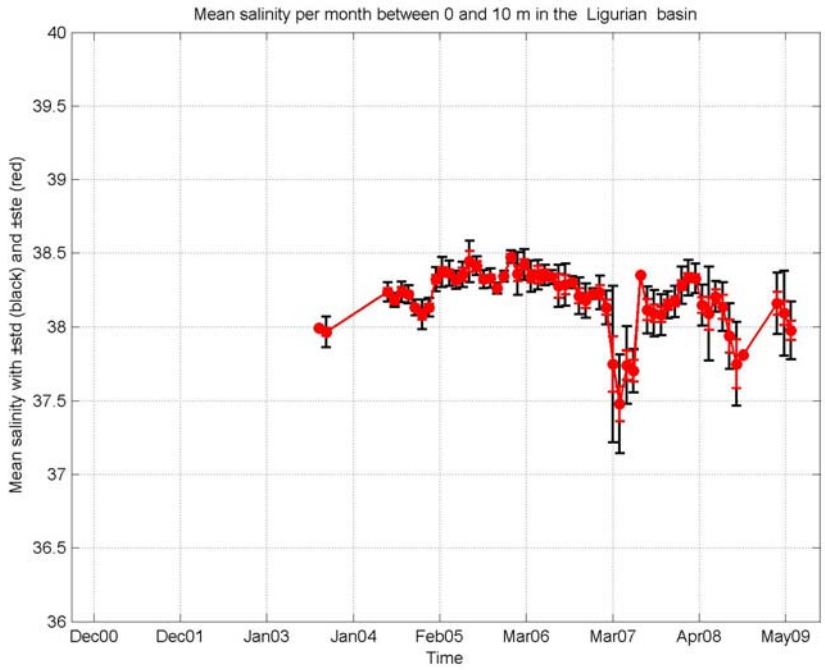

Figure 33. Monthly mean of surface S in the Ligurian sub-basin between December 2000 and June 2009.

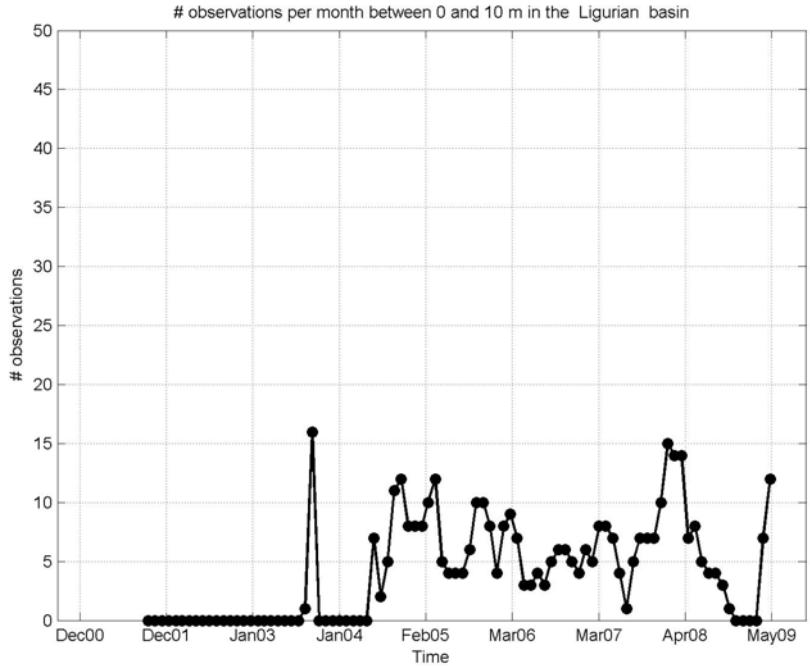

Figure 34. Number of surface observations in the Ligurian sub-basin between December 2000 and June 2009.

The monthly means of θ and S near 600 m are displayed in Figures 35 and 36, respectively. Vertical bars denote the standard deviations and the standard errors. The corresponding numbers of observations are shown in Figure 37.

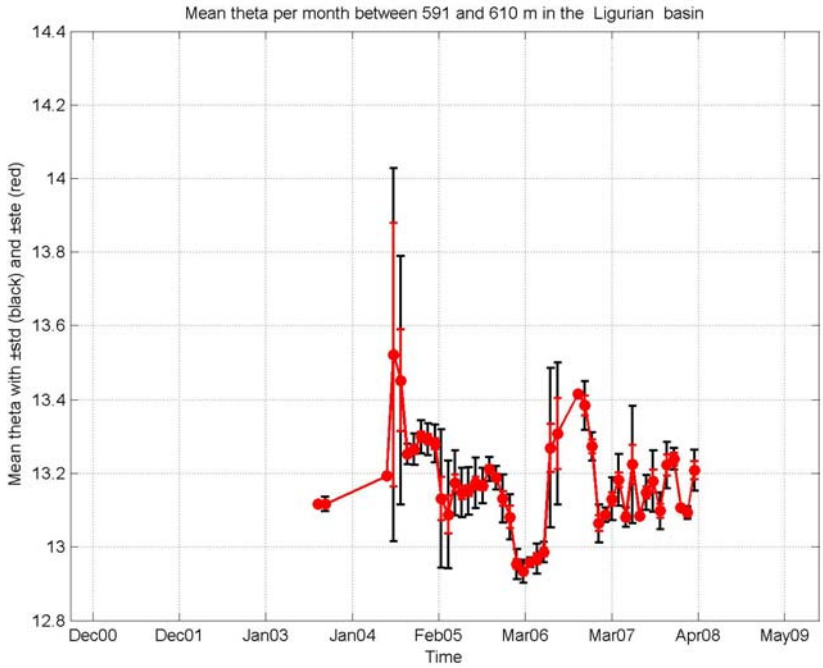

Figure 35. Monthly mean of θ near 600 m in the Ligurian sub-basin between December 2000 and June 2009.

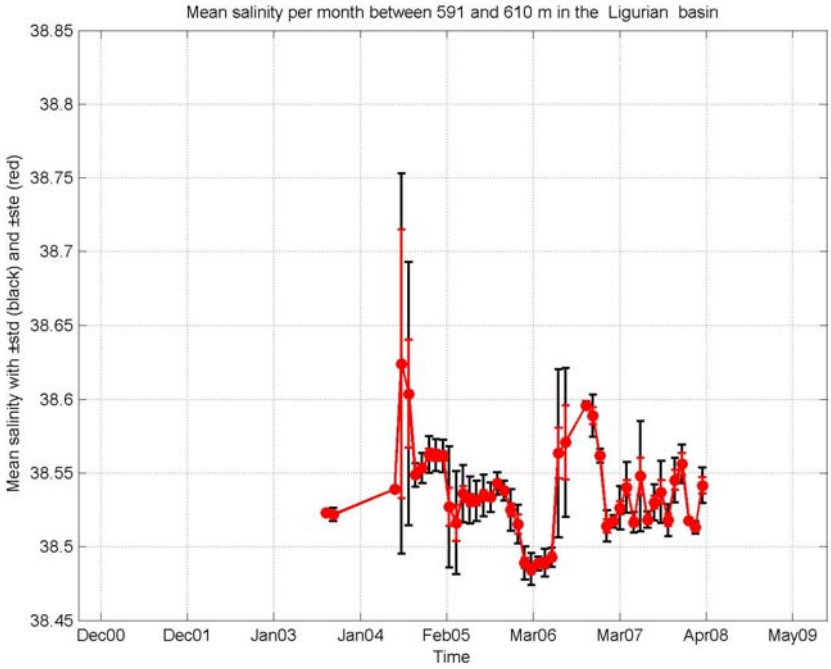

Figure 36. Monthly mean of S near 600 m in the Ligurian sub-basin between December 2000 and June 2009.

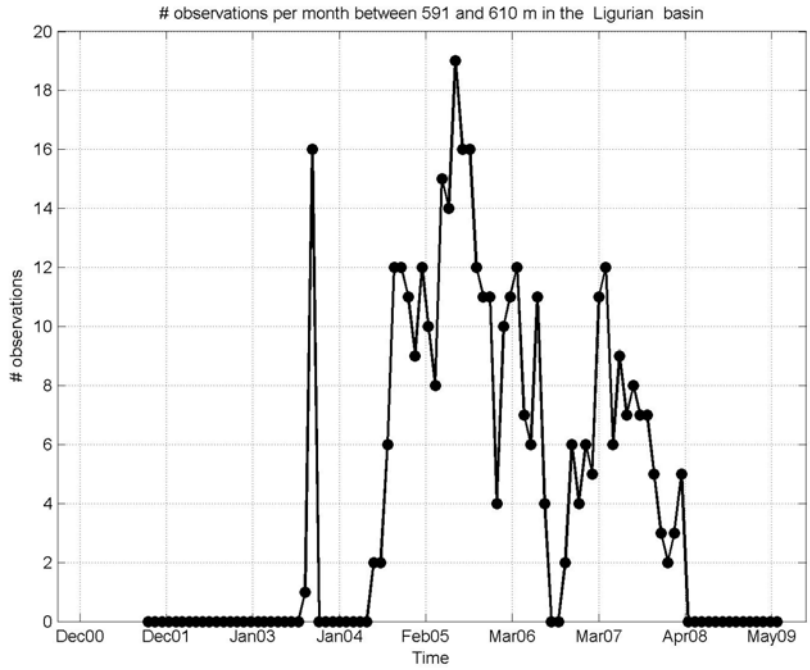

Figure 37. Number of observations near 600 m in the Ligurian sub-basin between December 2000 and June 2009.

The monthly means of θ and S near 2000 m are displayed in Figures 38 and 39, respectively. Vertical bars denote the standard deviations and the standard errors. The corresponding numbers of observations are shown in Figure 40.

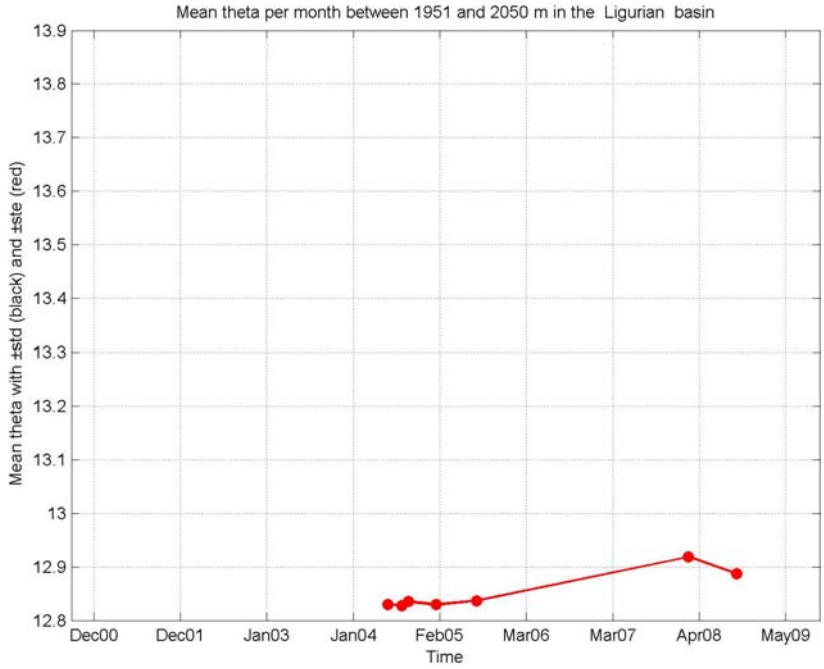

Figure 38. Monthly mean of θ near 2000 m in the Ligurian sub-basin between December 2000 and June 2009.

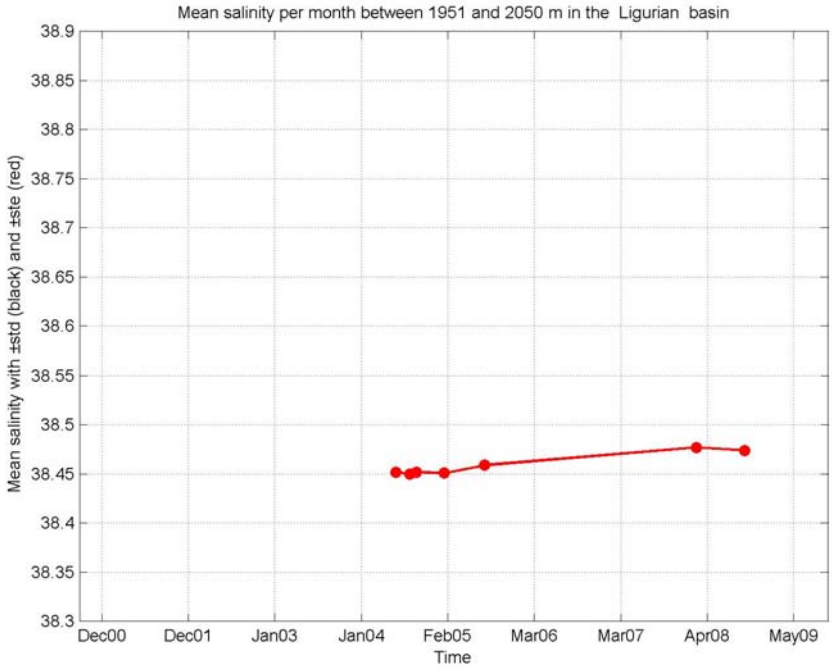

Figure 39. Monthly mean of S near 2000 m in the Ligurian sub-basin between December 2000 and June 2009.

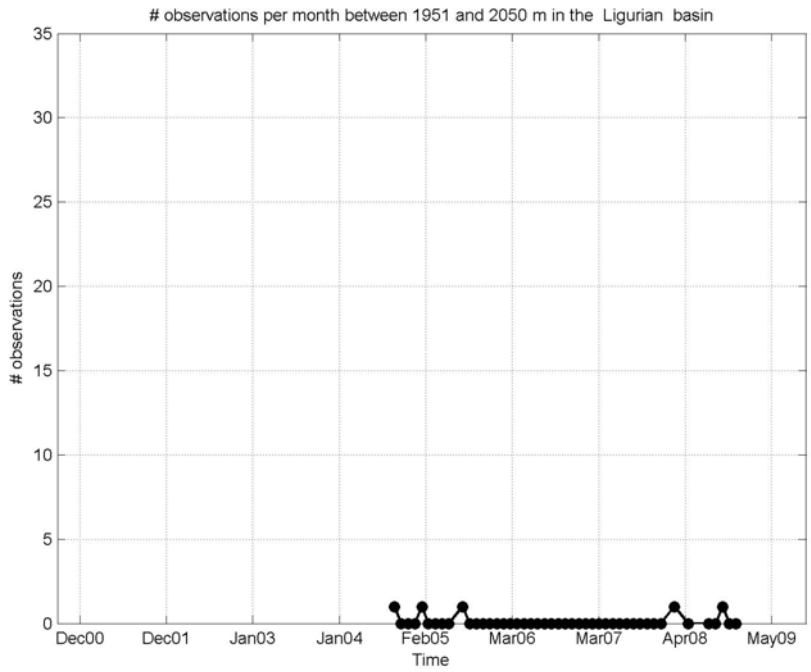

Figure 40. Number of observations near 600 m in the Ligurian sub-basin December 2000 and June 2009.

The temporal distributions of the monthly mean of the maximum S and the corresponding depth of the salinity maximum are depicted, respectively in Figures 41 and 42.

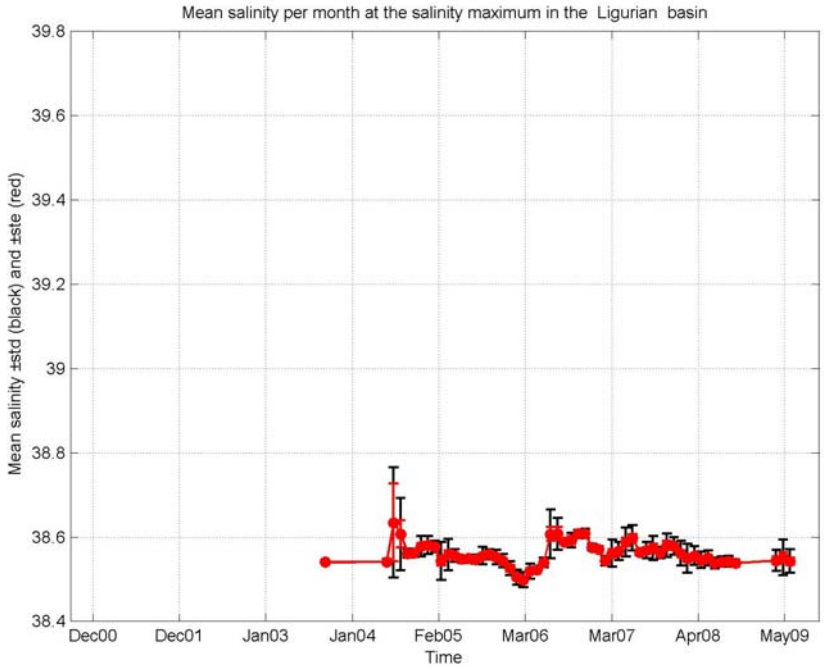

Figure 41. Monthly mean of the maximum S in the Ligurian sub-basin December 2000 and June 2009.

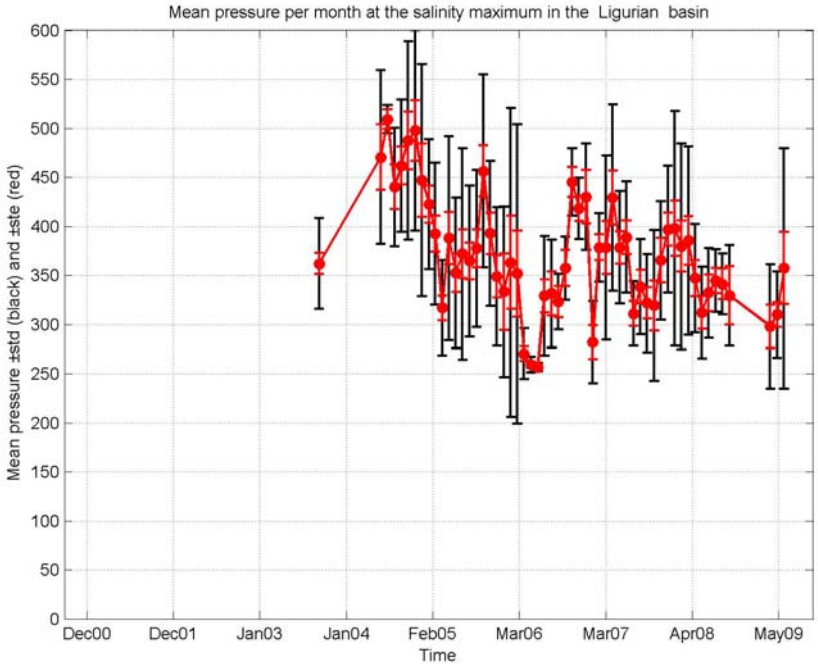

Figure 42. Monthly mean of the depth of the salinity maximum in the Ligurian sub-basin between December 2000 and June 2009.

2.1.4 Tyrrhenian sub-basin

Figures 43 and 44 illustrate the temporal distribution of the number of active floats and the number of CTD profiles per month in the Tyrrhenian sub-basin, respectively.

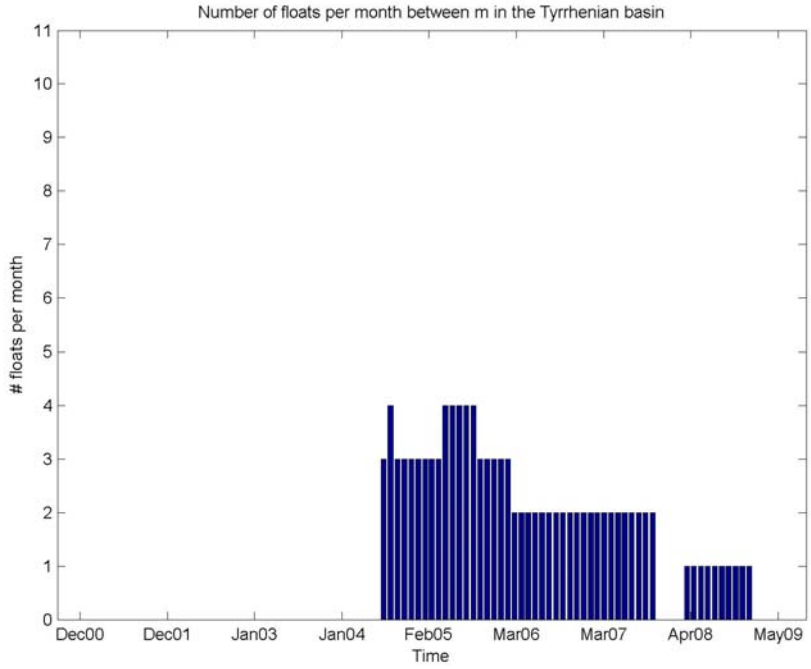

Figure 43. Number of active floats per month in the Tyrrhenian sub-basin between December 2000 and June 2009.

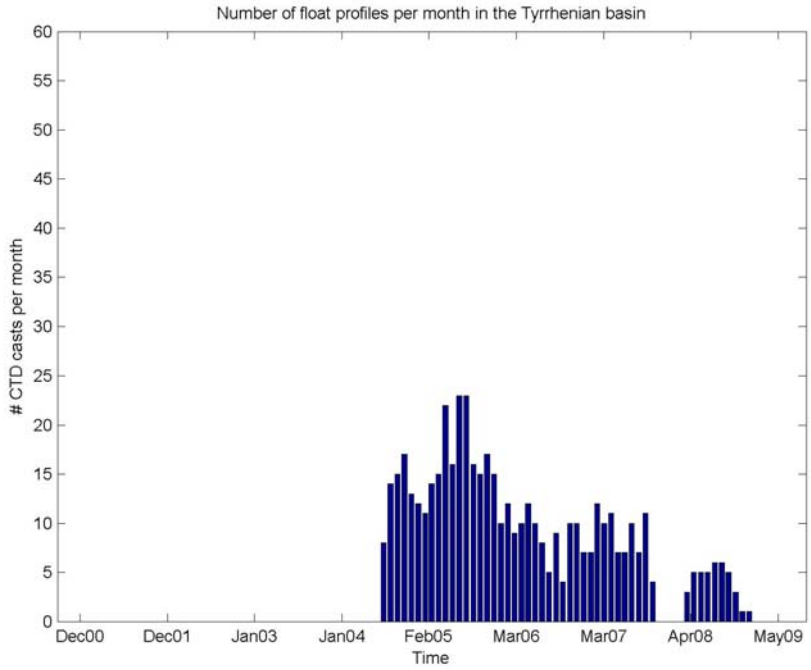

Figure 44. Number of CTD profiles per month in the Tyrrhenian sub-basin between December 2000 and June 2009.

The monthly means of θ and S near the surface (0-10 m) are displayed in Figures 45 and 46, respectively. Vertical bars denote the standard deviations and the standard errors. The corresponding numbers of observations are shown in Figure 47.

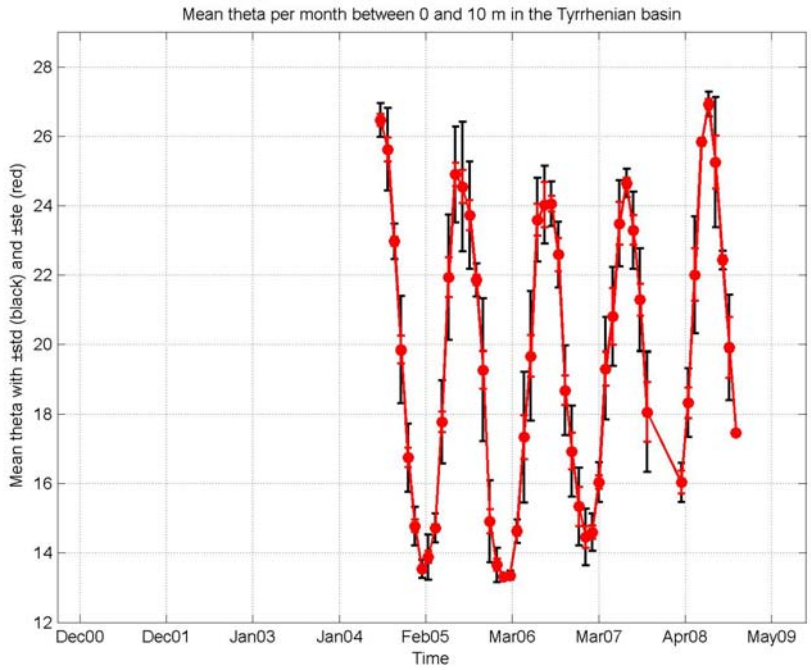

Figure 45. Monthly mean of surface θ in the Tyrrhenian sub-basin between December 2000 and June 2009.

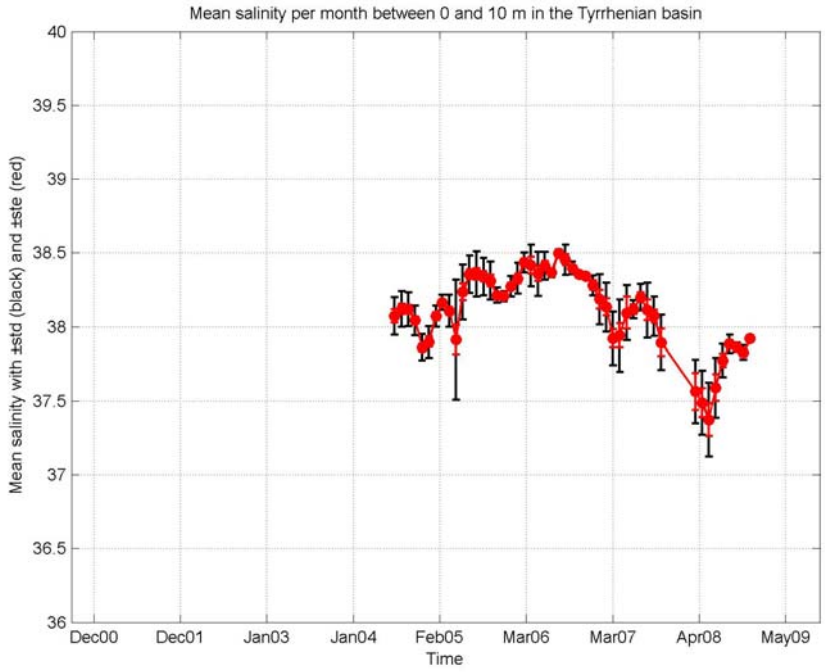

Figure 46. Monthly mean of surface S in the Tyrrhenian sub-basin between December 2000 and June 2009.

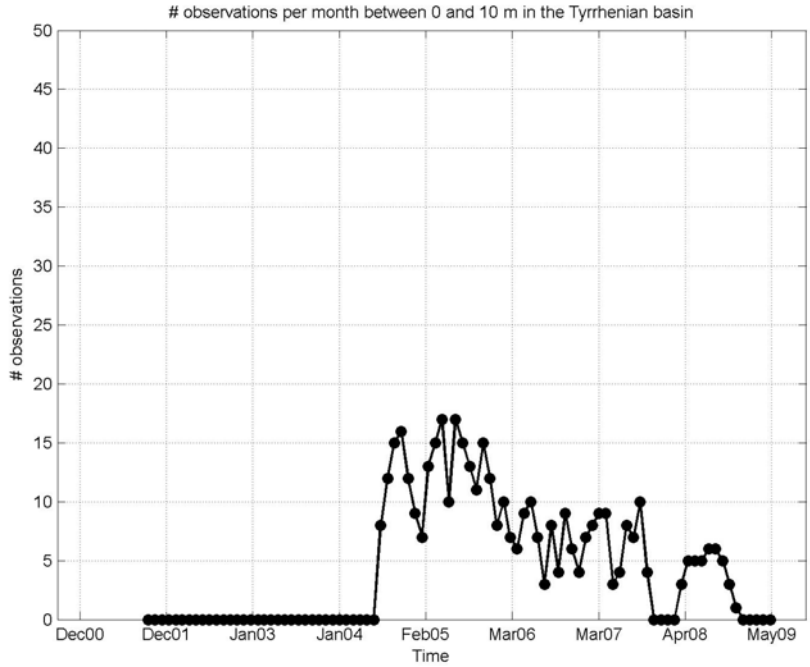

Figure 47. Number of surface observations in the Tyrrhenian sub-basin between December 2000 and June 2009.

The monthly means of θ and S near 600 m are displayed in Figures 48 and 49, respectively. Vertical bars denote the standard deviations and the standard errors. The corresponding numbers of observations are shown in Figure 50.

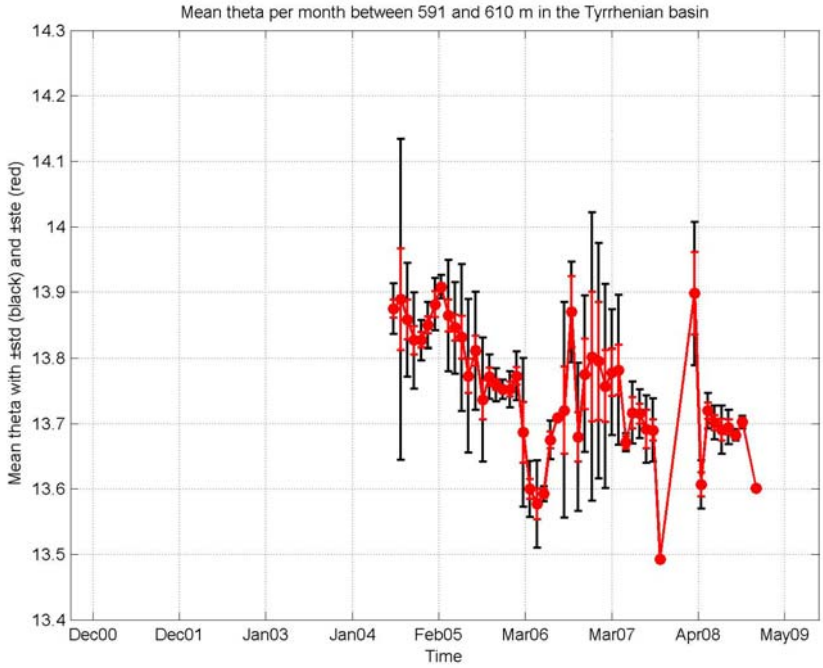

Figure 48. Monthly mean of θ near 600 m in the Tyrrhenian sub-basin between December 2000 and June 2009.

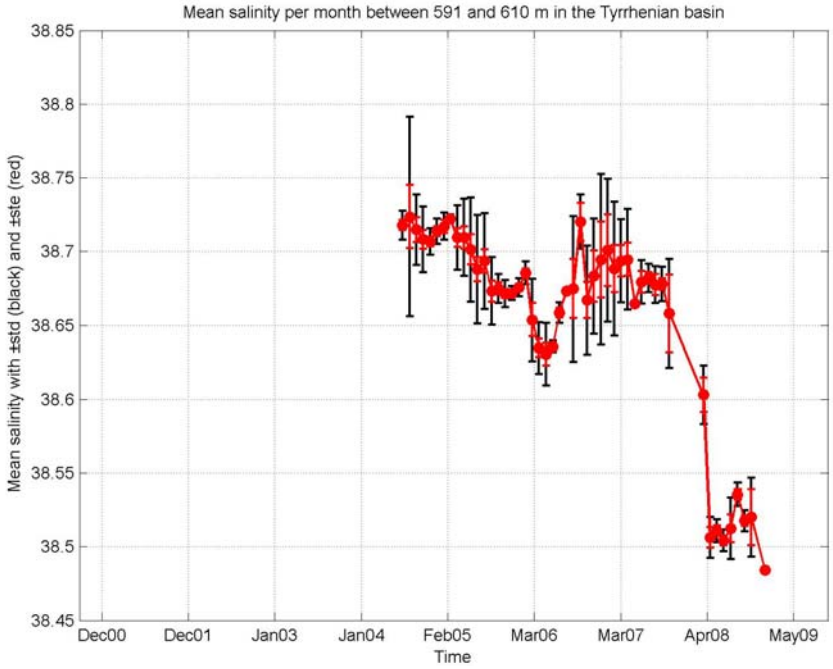

Figure 49. Monthly mean of S near 600 m in the Tyrrhenian sub-basin between December 2000 and June 2009.

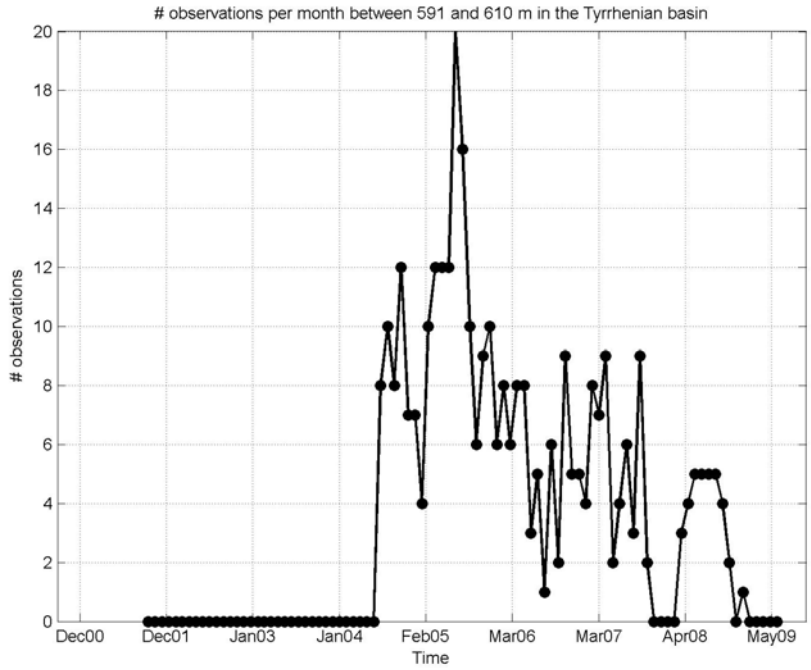

Figure 50. Number of observations near 600 m in the Tyrrhenian sub-basin between December 2000 and June 2009.

The monthly means of θ and S near 2000 m are displayed in Figures 51 and 52, respectively. Vertical bars denote the standard deviations and the standard errors. The corresponding numbers of observations are shown in Figure 53.

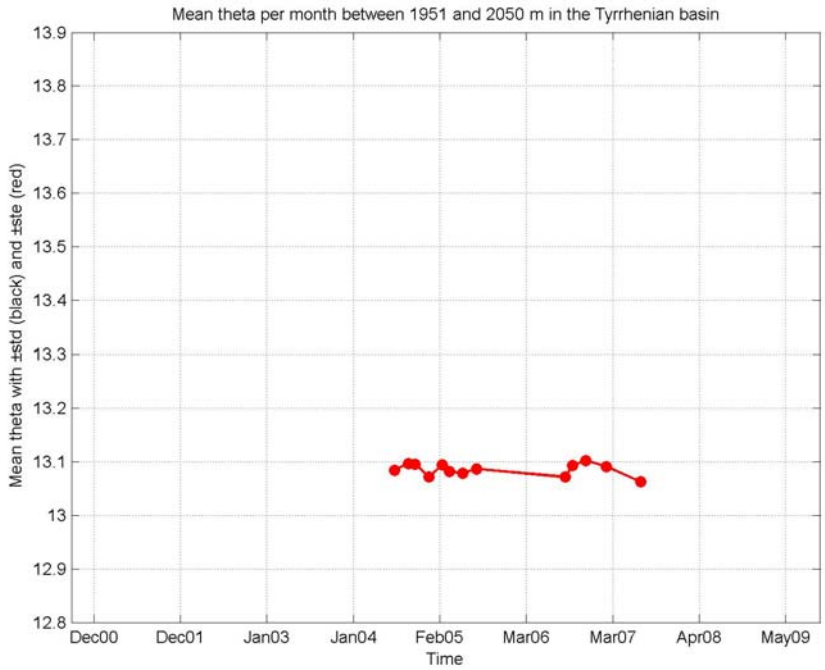

Figure 51. Monthly mean of θ near 2000 m in the Tyrrhenian sub-basin between December 2000 and June 2009.

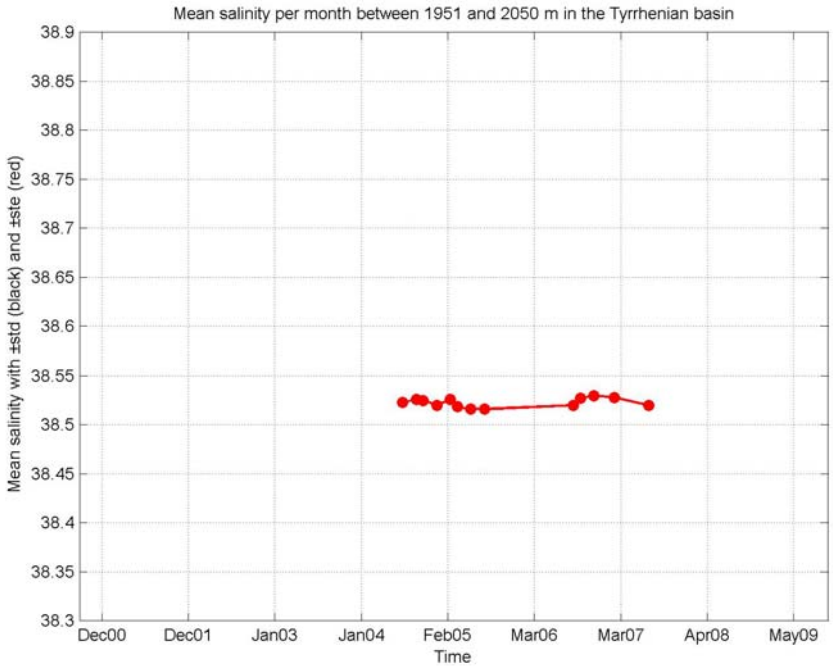

Figure 52. Monthly mean of S near 2000 m in the Tyrrhenian sub-basin between December 2000 and June 2009.

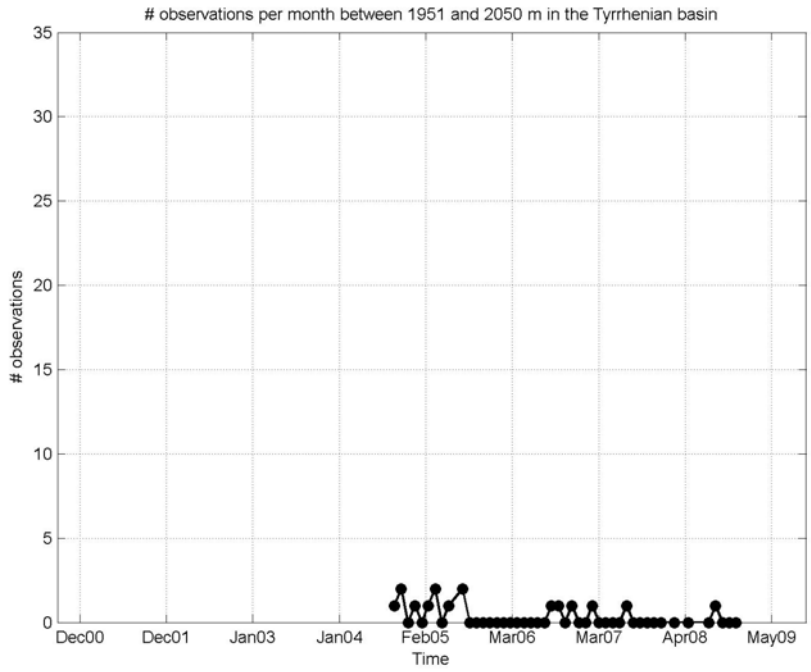

Figure 53. Number of observations near 2000 m in the Tyrrhenian sub-basin December 2000 and June 2009.

The temporal distributions of the monthly mean of the maximum S and the corresponding depth of the salinity maximum are depicted, respectively in Figures 54 and 55.

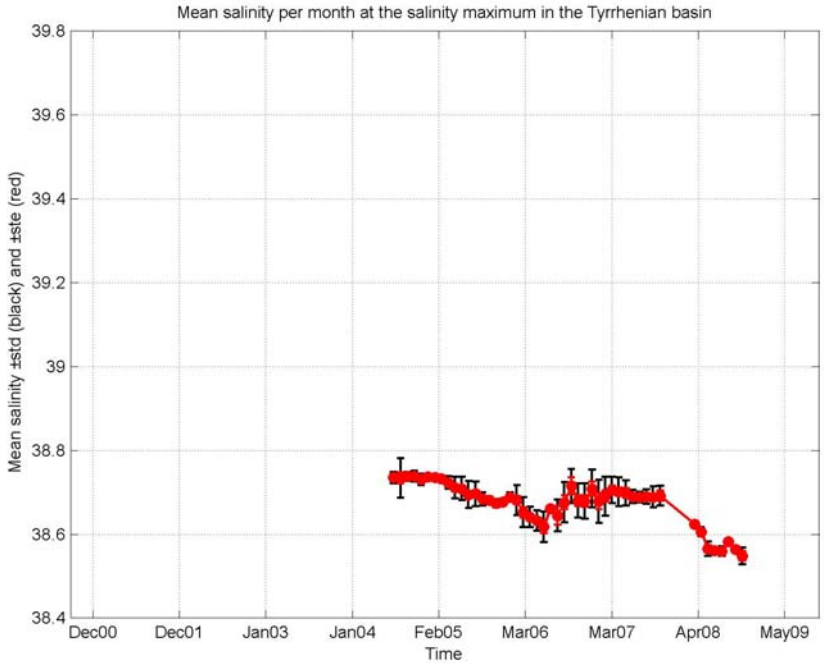

Figure 54. Monthly mean of the maximum S in the Tyrrhenian sub-basin December 2000 and June 2009.

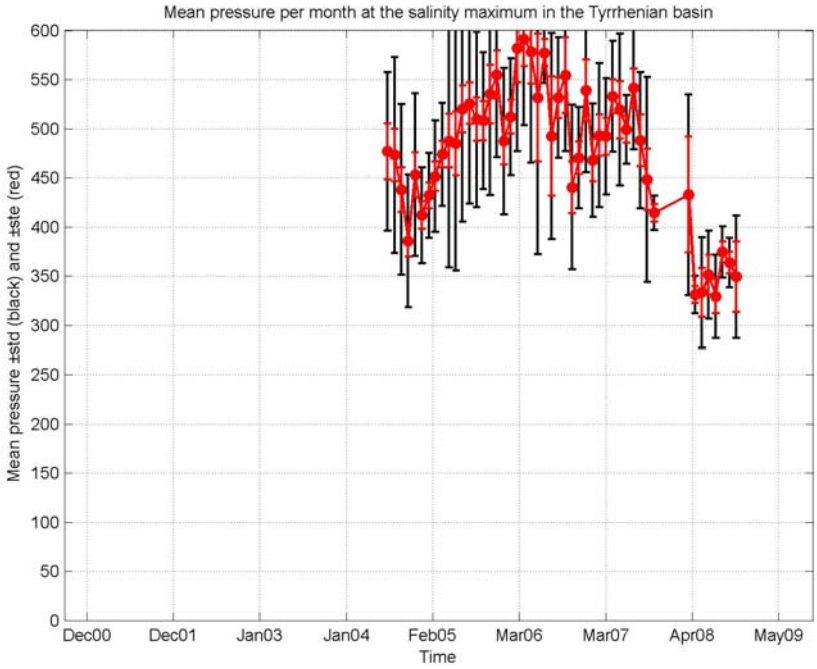

Figure 55. Monthly mean of the depth of the salinity maximum in the Tyrrhenian sub-basin between December 2000 and June 2009.

2.1.5 Ionian sub-basin

Figures 56 and 57 illustrate the temporal distribution of the number of active floats and the number of CTD profiles per month in the Ionian sub-basin, respectively.

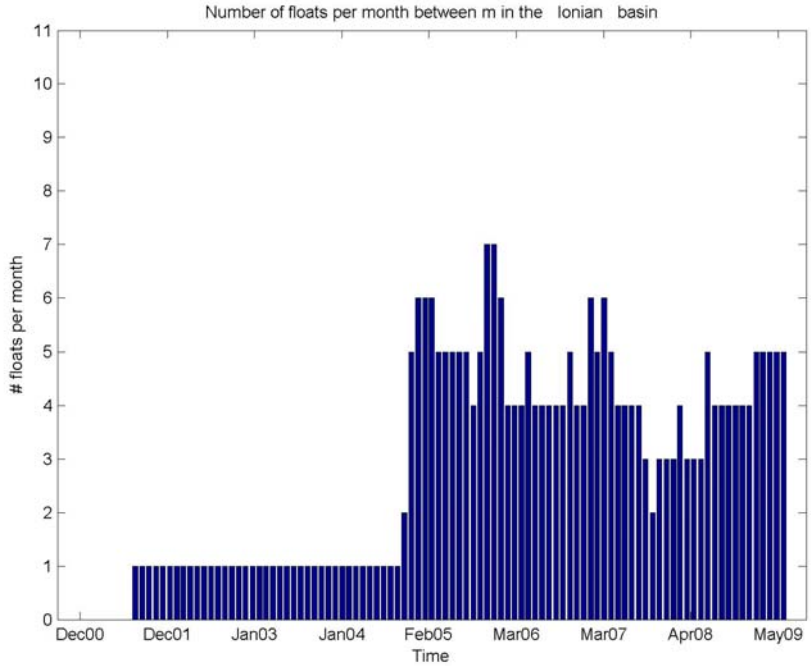

Figure 56. Number of active floats per month in the Ionian sub-basin between December 2000 and June 2009.

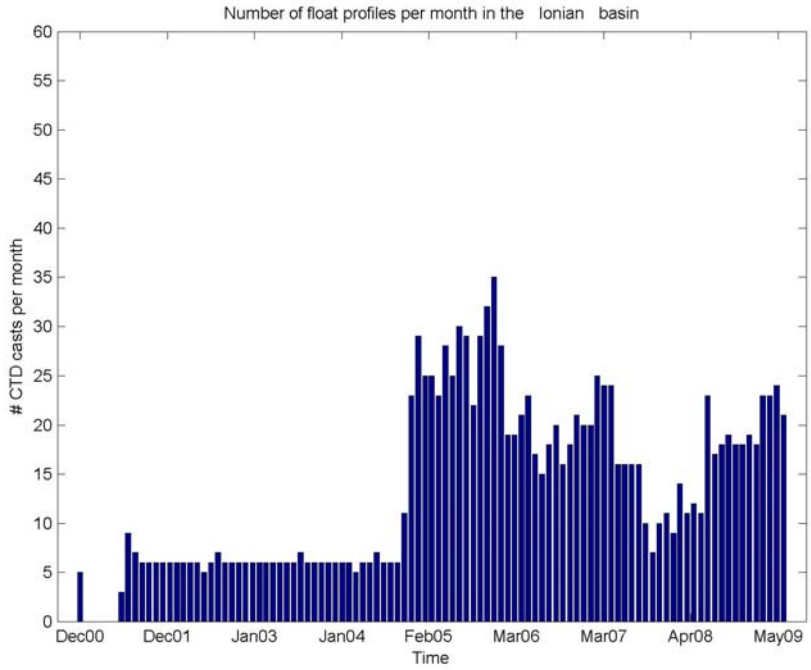

Figure 57. Number of CTD profiles per month in the Ionian sub-basin between December 2000 and June 2009.

The monthly means of θ and S near the surface (0-10 m) are displayed in Figures 58 and 59, respectively. Vertical bars denote the standard deviations and the standard errors. The corresponding numbers of observations are shown in Figure 60.

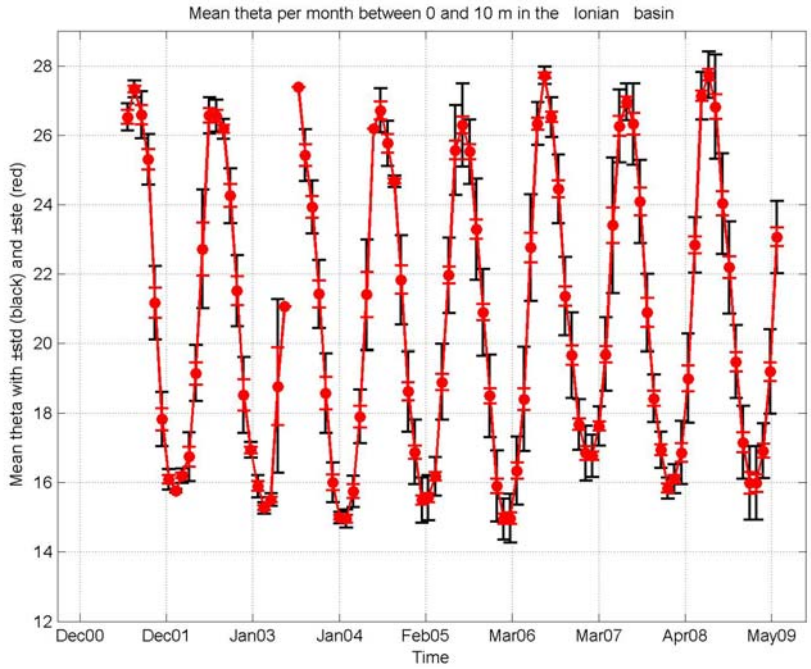

Figure 58. Monthly mean of surface θ in the Ionian sub-basin between December 2000 and June 2009.

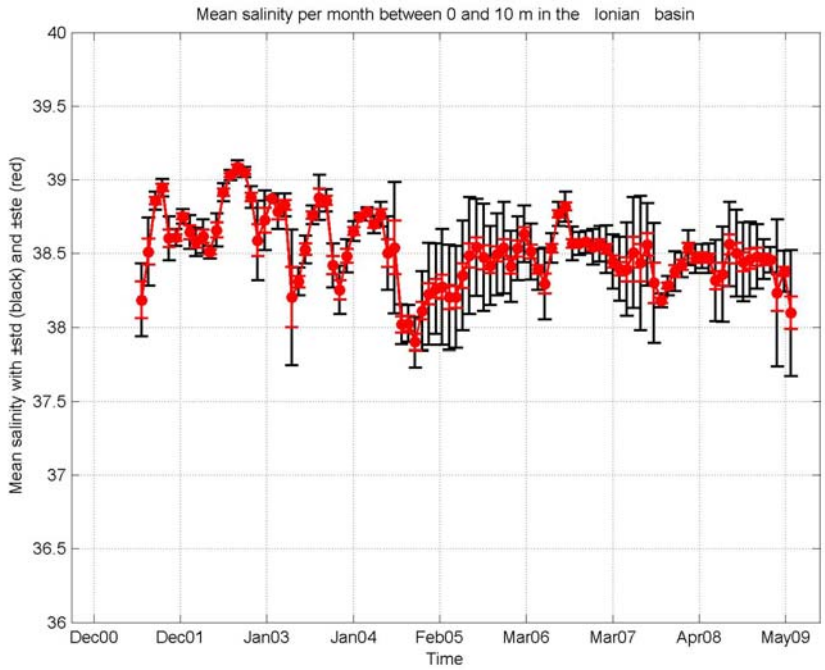

Figure 59. Monthly mean of surface S in the Ionian sub-basin between December 2000 and June 2009.

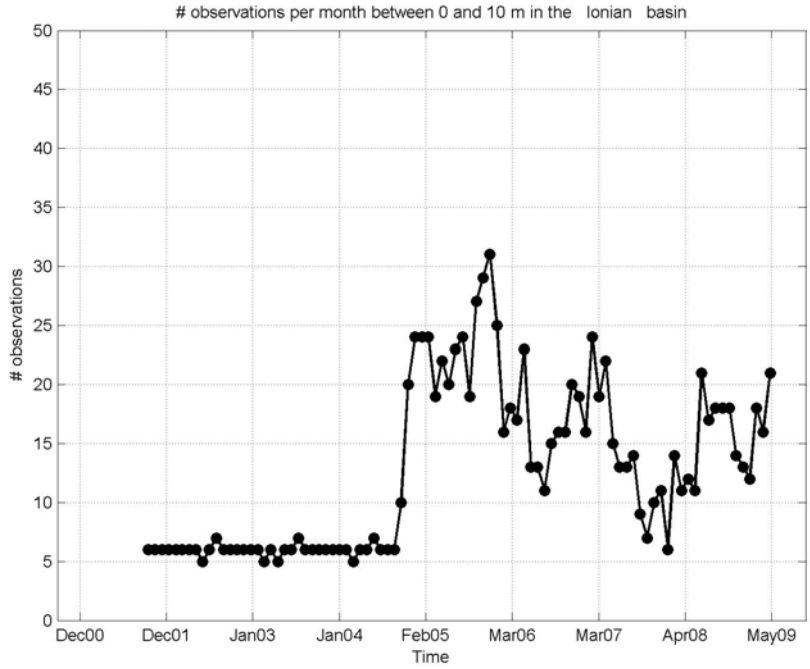

Figure 60. Number of surface observations in the Ionian sub-basin between December 2000 and June 2009.

The monthly means of θ and S near 600 m are displayed in Figures 61 and 62, respectively. Vertical bars denote the standard deviations and the standard errors. The corresponding numbers of observations are shown in Figure 63.

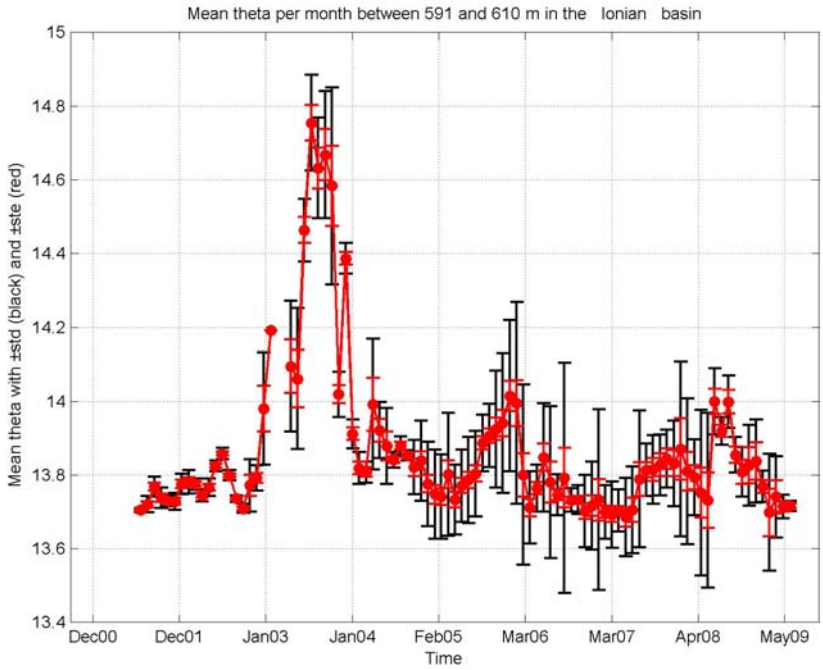

Figure 61. Monthly mean of θ near 600 m in the Ionian sub-basin between December 2000 and June 2009.

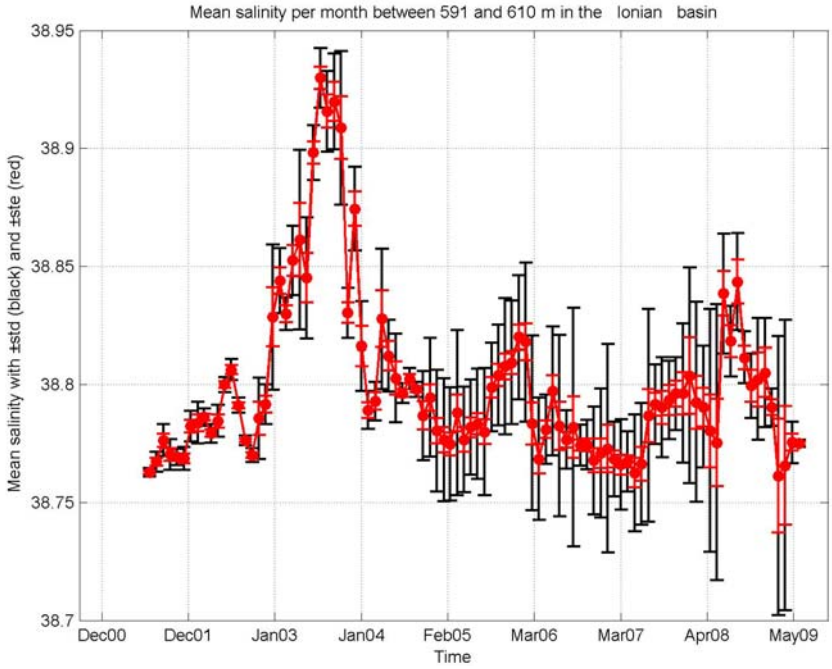

Figure 62. Monthly mean of S near 600 m in the Ionian sub-basin between December 2000 and June 2009.

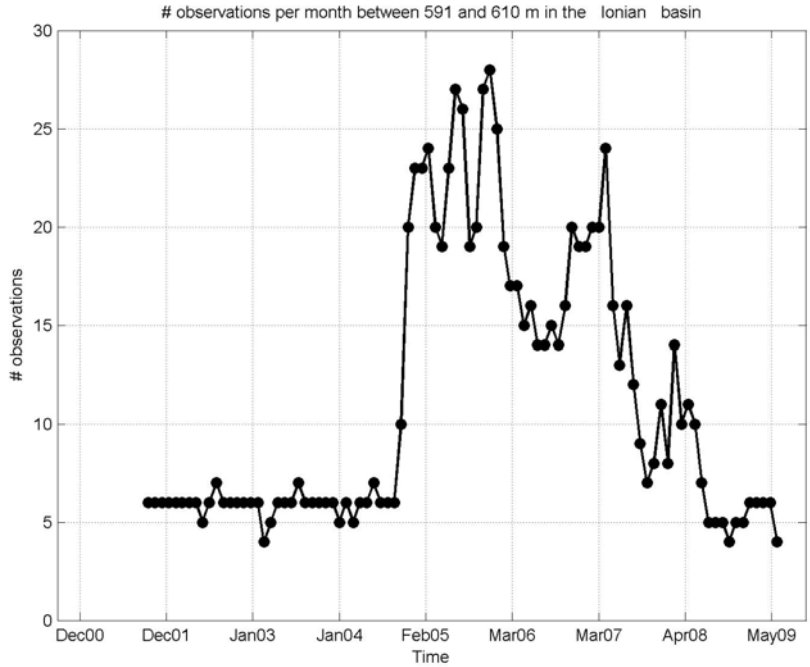

Figure 63. Number of observations near 600 m in the Ionian sub-basin between December 2000 and June 2009.

The monthly means of θ and S near 2000 m are displayed in Figures 64 and 65, respectively. Vertical bars denote the standard deviations and the standard errors. The corresponding numbers of observations are shown in Figure 66.

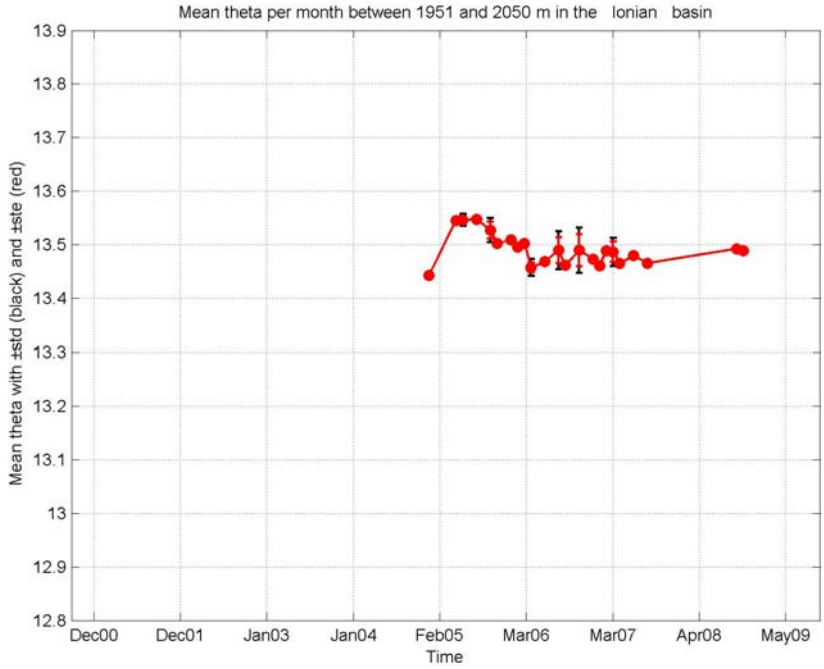

Figure 64. Monthly mean of θ near 2000 m in the Ionian sub-basin between December 2000 and June 2009.

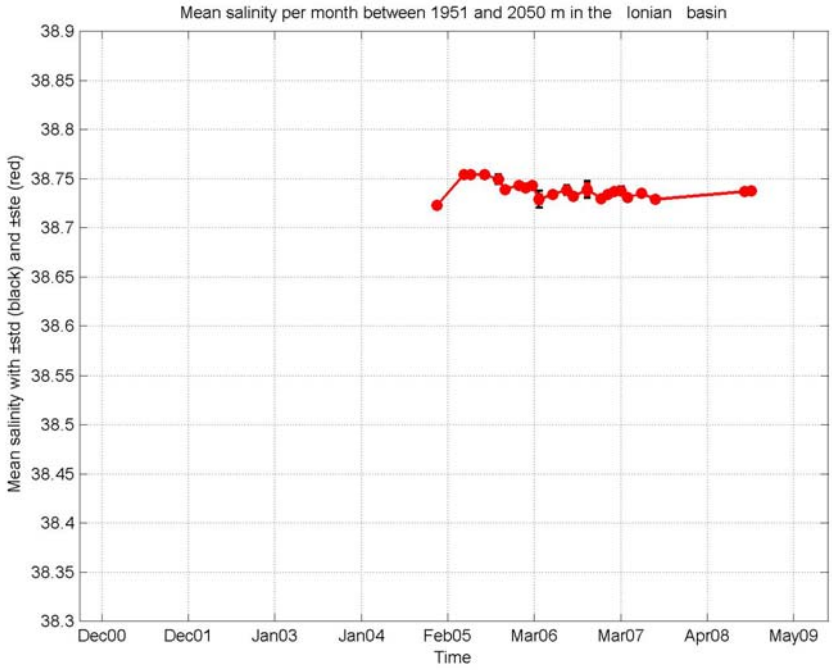

Figure 65. Monthly mean of S near 2000 m in the Ionian sub-basin between December 2000 and June 2009.

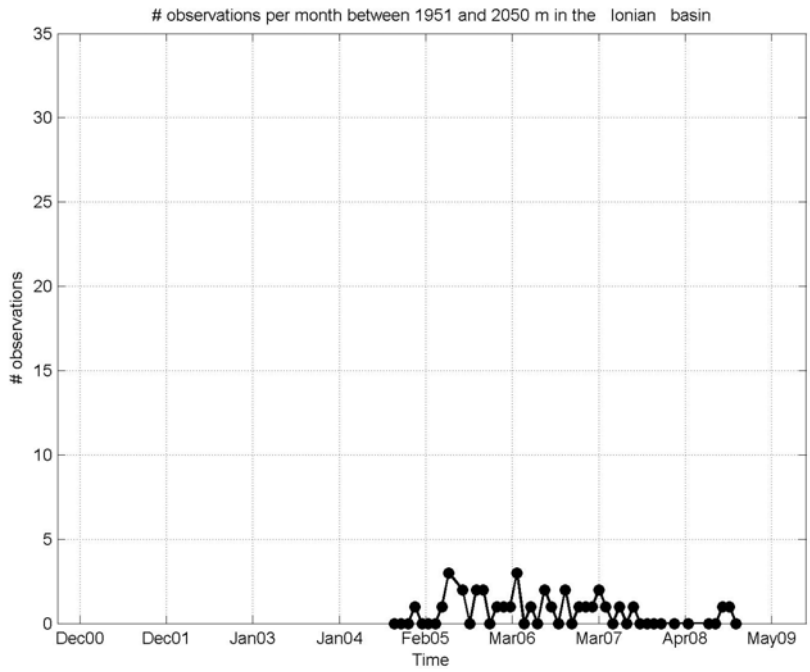

Figure 66. Number of observations near 600 m in the Ionian sub-basin December 2000 and June 2009.

The temporal distributions of the monthly mean of the maximum S and the corresponding depth of the salinity maximum are depicted, respectively in Figures 67 and 68.

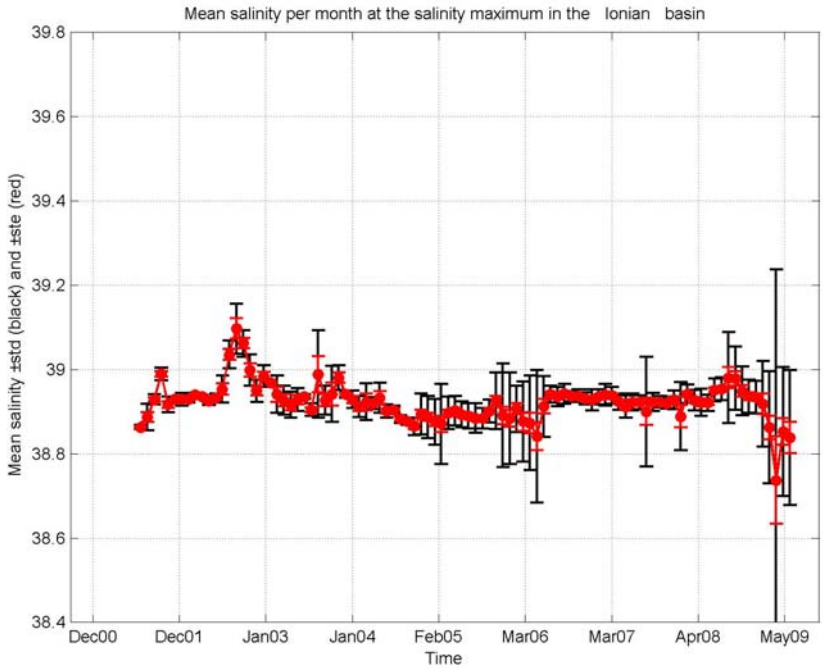

Figure 67. Monthly mean of the maximum S in the Ionian sub-basin December 2000 and June 2009.

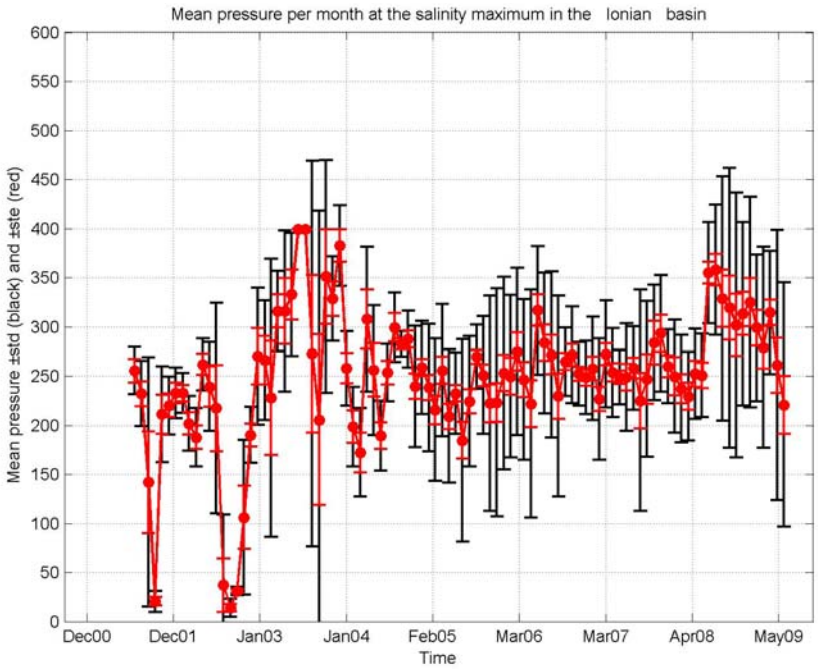

Figure 68. Monthly mean of the depth of the salinity maximum in the Ionian sub-basin between December 2000 and June 2009.

2.1.6 Cretan sub-basin

Figures 69 and 70 illustrate the temporal distribution of the number of active floats and the number of CTD profiles per month in the Cretan sub-basin, respectively.

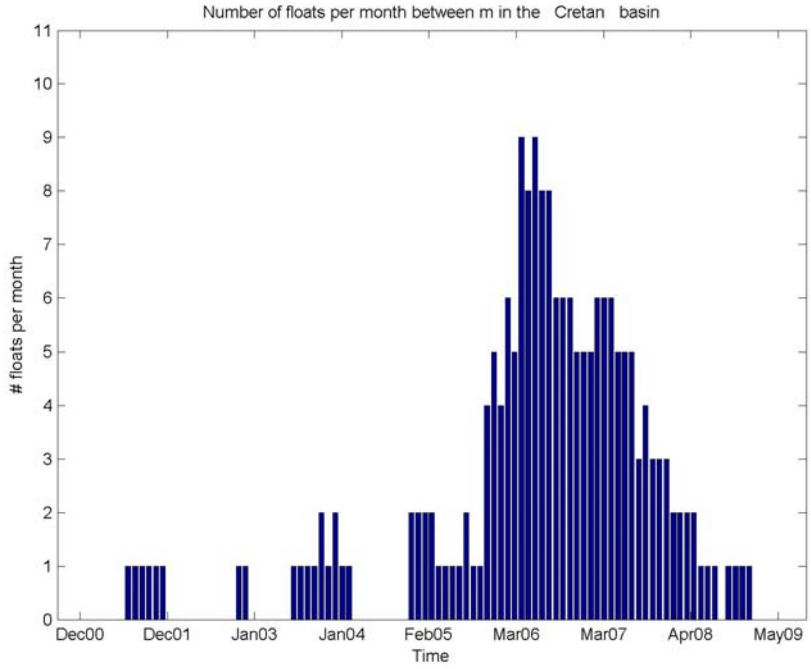

Figure 69. Number of active floats per month in the Cretan sub-basin between December 2000 and June 2009.

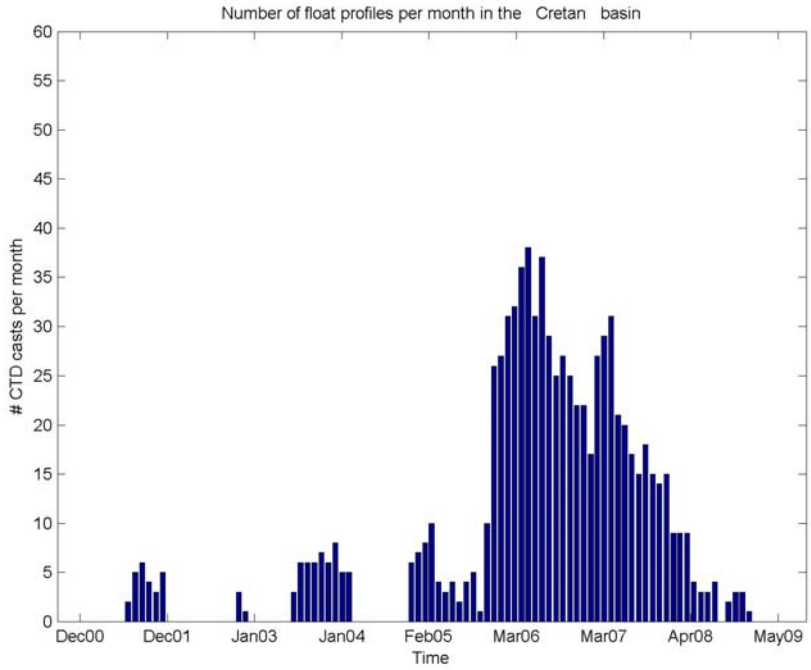

Figure 70. Number of CTD profiles per month in the Cretan sub-basin between December 2000 and June 2009.

The monthly means of θ and S near the surface (0-10 m) are displayed in Figures 71 and 72, respectively. Vertical bars denote the standard deviations and the standard errors. The corresponding numbers of observations are shown in Figure 73.

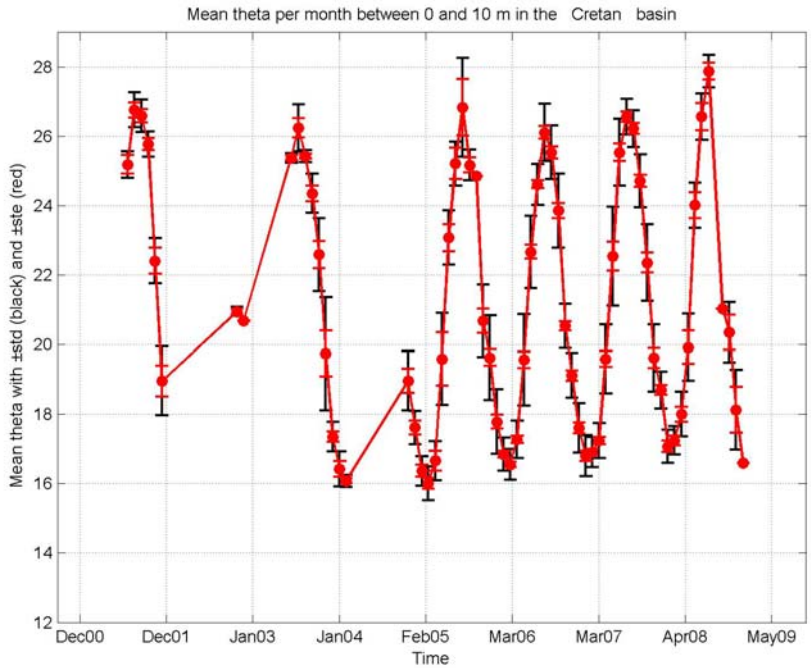

Figure 71. Monthly mean of surface θ in the Cretan sub-basin between December 2000 and June 2009.

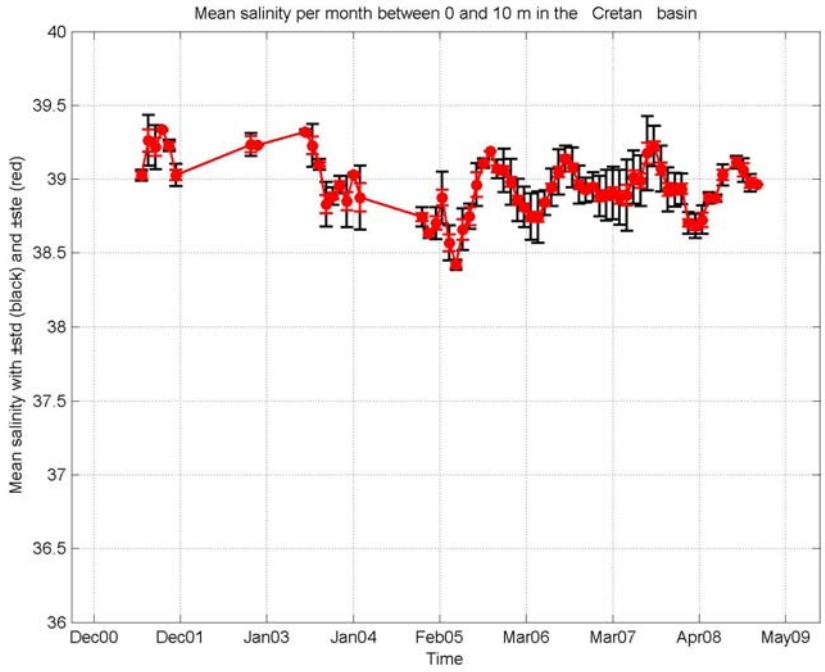

Figure 72. Monthly mean of surface S in the Cretan sub-basin between December 2000 and June 2009.

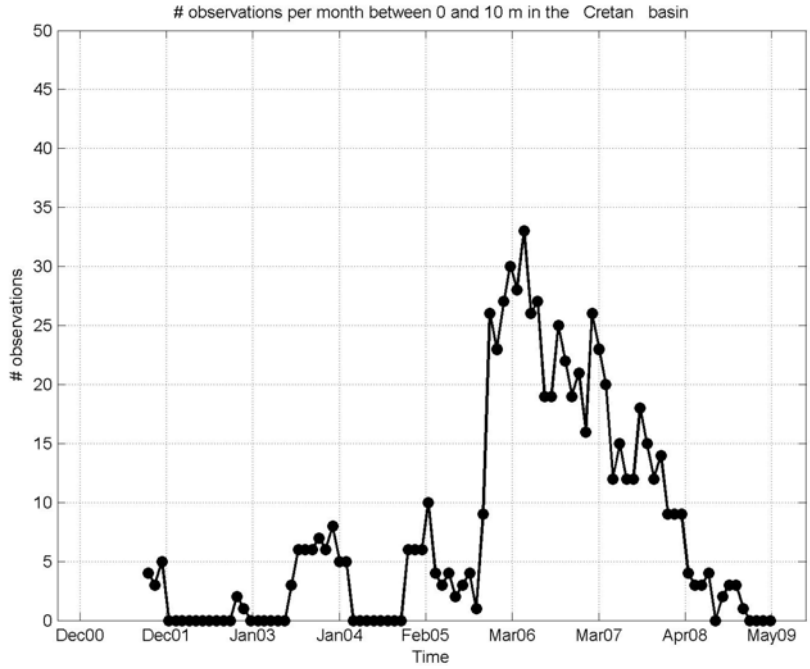

Figure 73. Number of surface observations in the Cretan sub-basin between December 2000 and June 2009.

The monthly means of θ and S near 600 m are displayed in Figures 74 and 75, respectively. Vertical bars denote the standard deviations and the standard errors. The corresponding numbers of observations are shown in Figure 76.

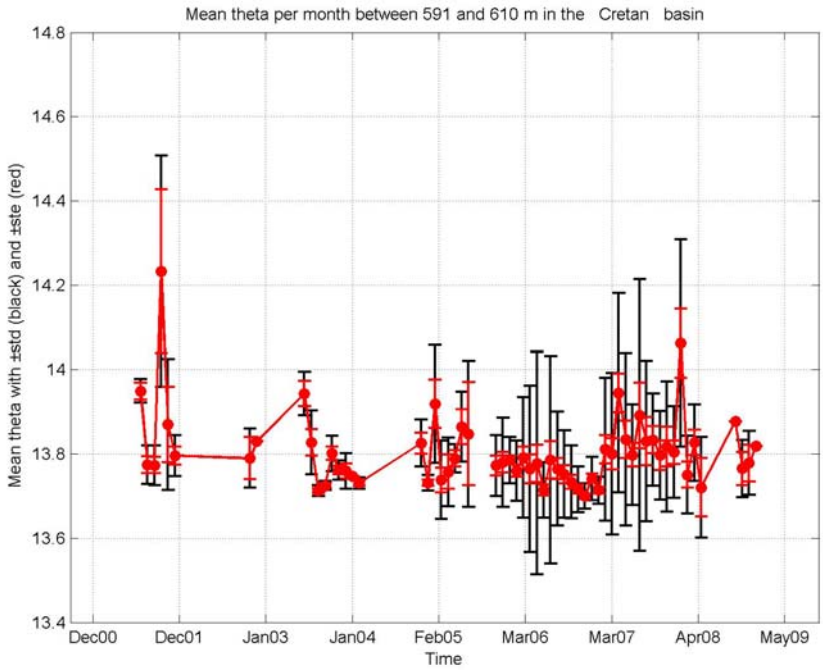

Figure 74. Monthly mean of θ near 600 m in the Cretan sub-basin between December 2000 and June 2009.

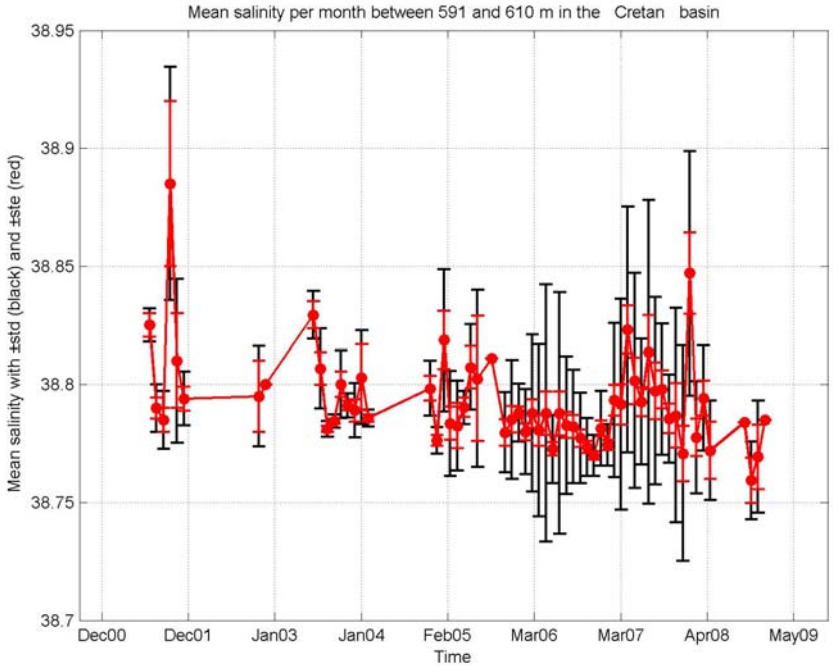

Figure 75. Monthly mean of S near 600 m in the Cretan sub-basin between December 2000 and June 2009.

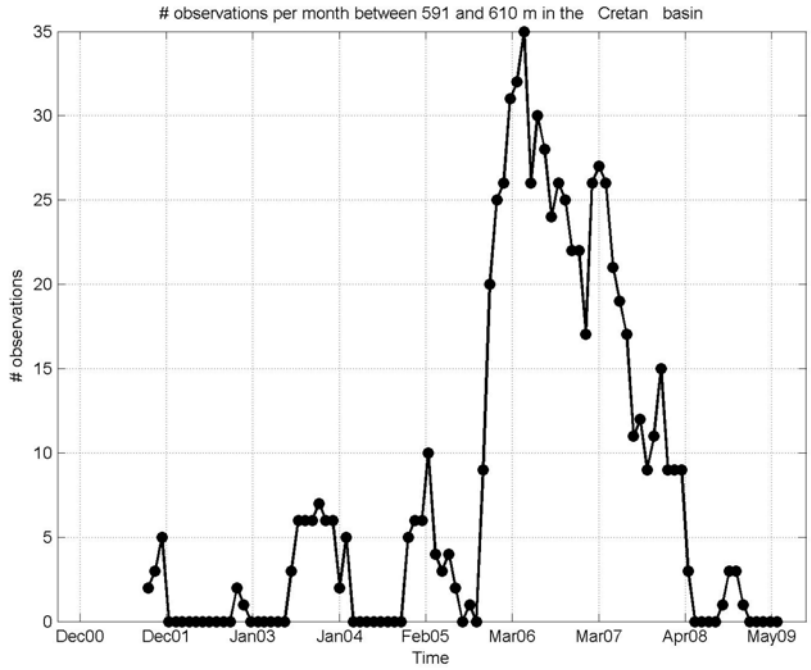

Figure 76. Number of observations near 600 m in the Cretan sub-basin between December 2000 and June 2009.

The monthly means of θ and S near 2000 m are displayed in Figures 77 and 78, respectively. Vertical bars denote the standard deviations and the standard errors. The corresponding numbers of observations are shown in Figure 79.

Figure 77. Monthly mean of θ near 2000 m in the Cretan sub-basin between December 2000 and June 2009.

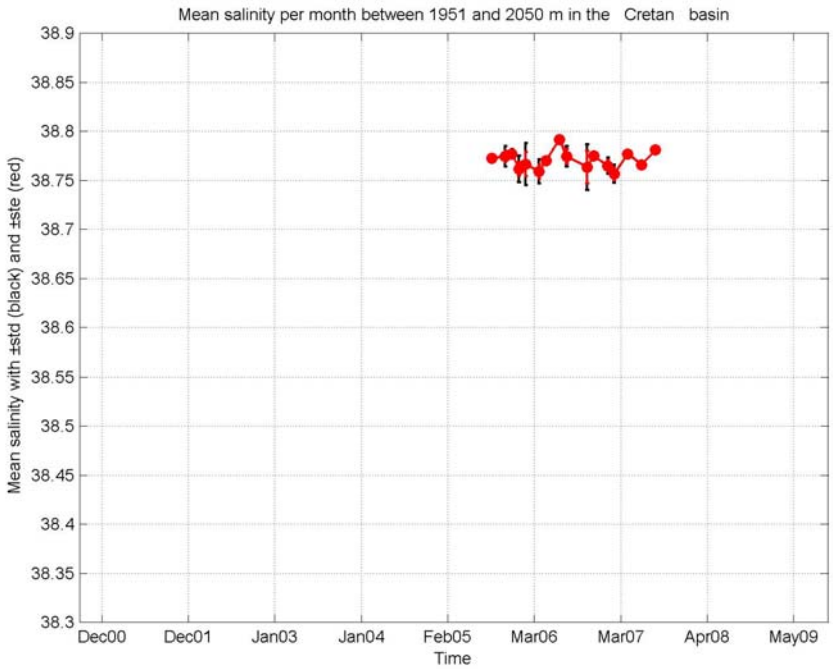

Figure 78. Monthly mean of S near 2000 m in the Cretan sub-basin between December 2000 and June 2009.

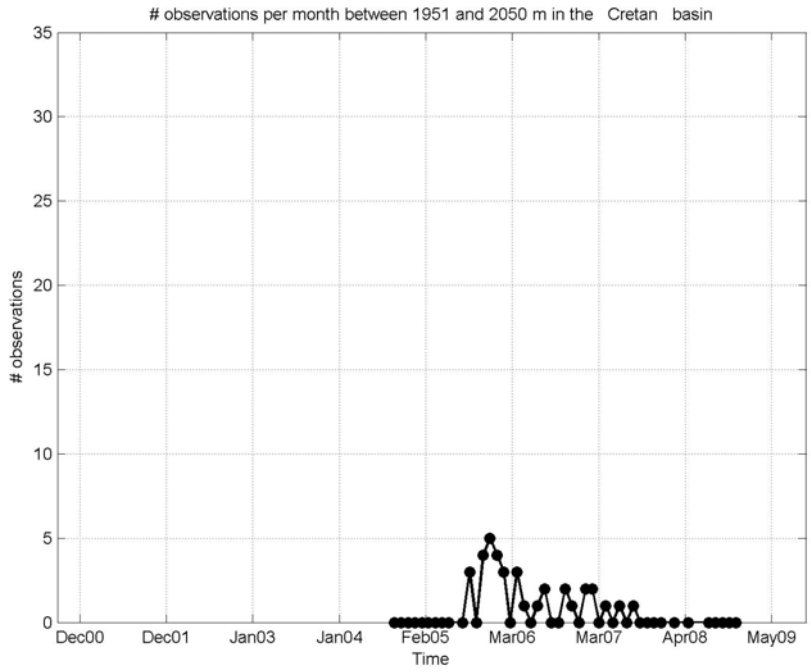

Figure 79. Number of observations near 600 m in the Cretan sub-basin December 2000 and June 2009.

The temporal distributions of the monthly mean of the maximum S and the corresponding depth of the salinity maximum are depicted, respectively in Figures 80 and 81.

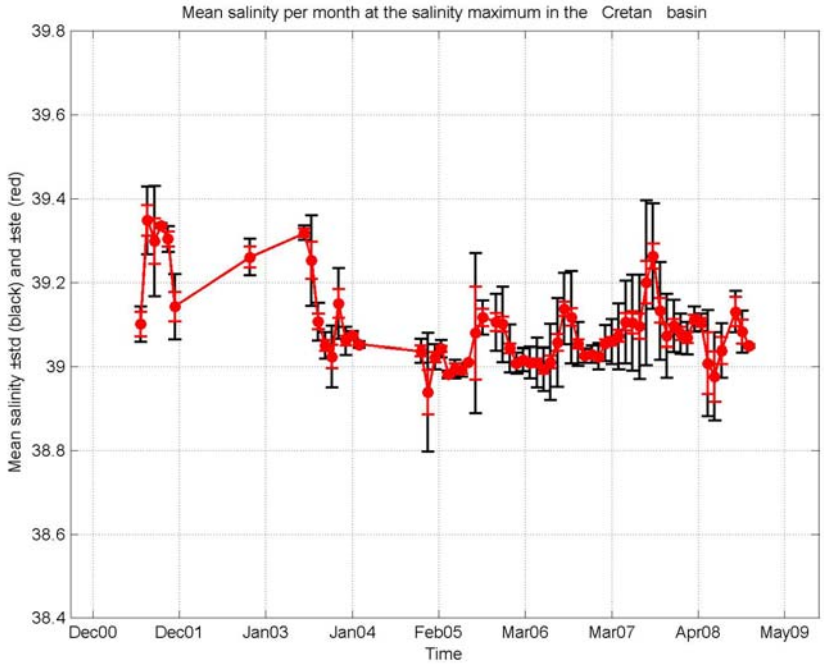

Figure 80. Monthly mean of the maximum S in the Cretan sub-basin December 2000 and June 2009.

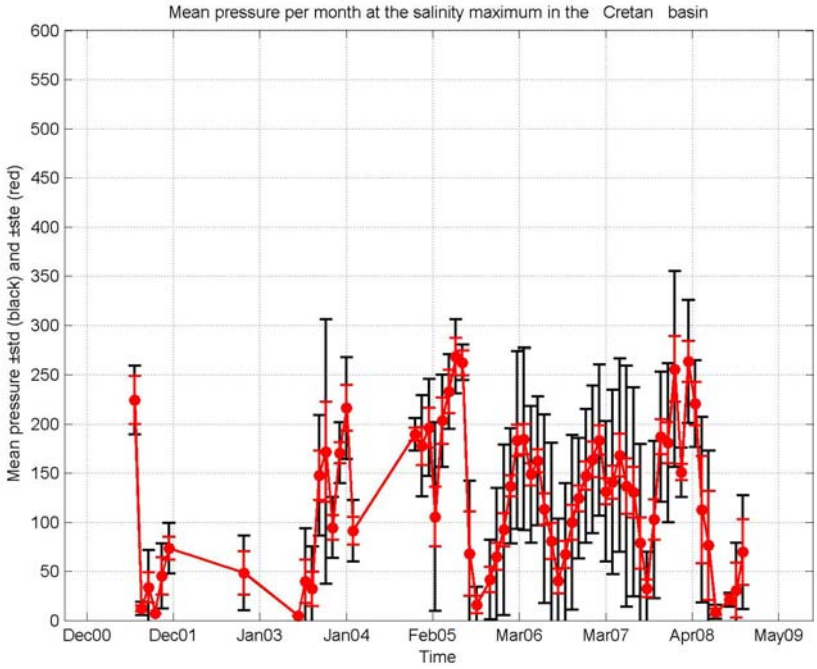

Figure 81. Monthly mean of the depth of the salinity maximum in the Cretan sub-basin between December 2000 and June 2009.

2.1.7 Levantine sub-basin

Figures 82 and 83 illustrate the temporal distribution of the number of active floats and the number of CTD profiles per month in the Levantine sub-basin, respectively.

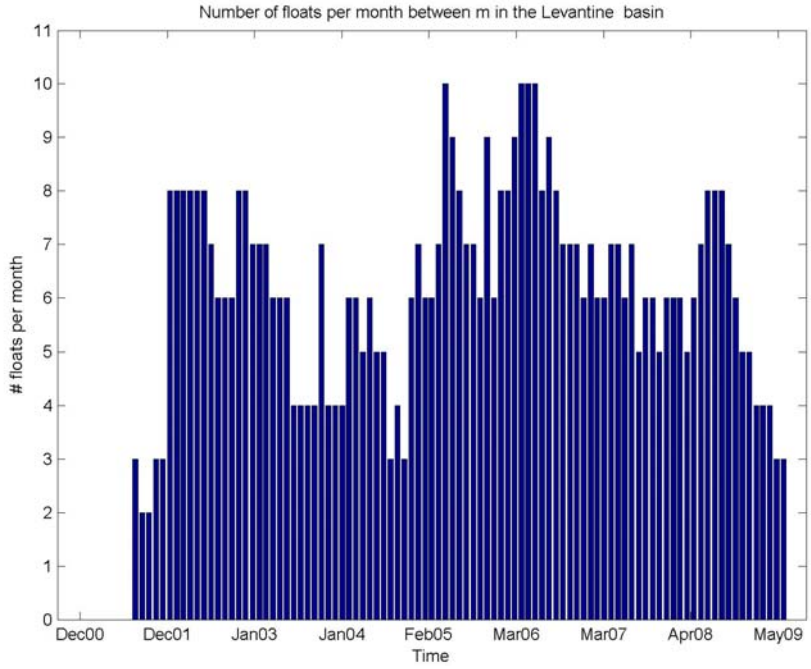

Figure 82. Number of active floats per month in the Levantine sub-basin between December 2000 and June 2009.

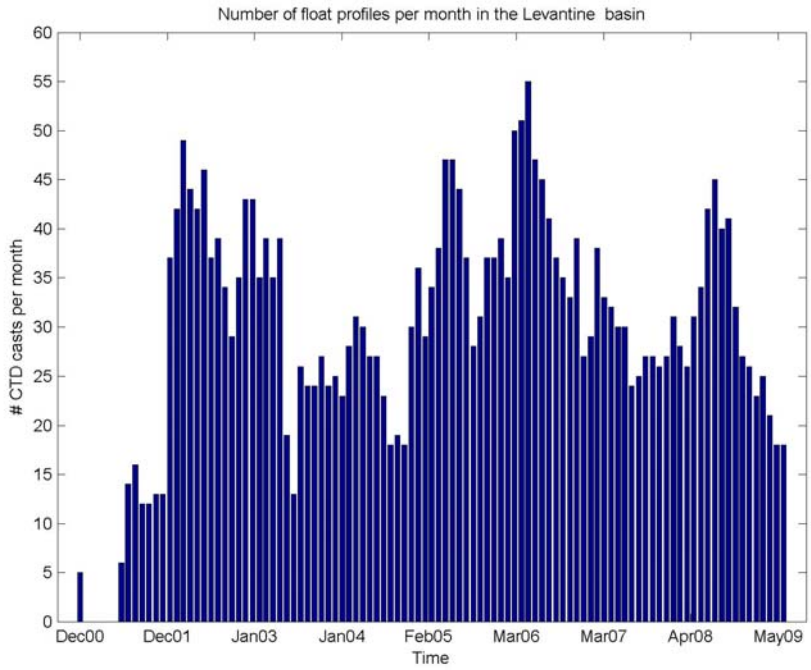

Figure 83. Number of CTD profiles per month in the Levantine sub-basin between December 2000 and June 2009.

The monthly means of θ and S near the surface (0-10 m) are displayed in Figures 84 and 85, respectively. Vertical bars denote the standard deviations and the standard errors. The corresponding numbers of observations are shown in Figure 86.

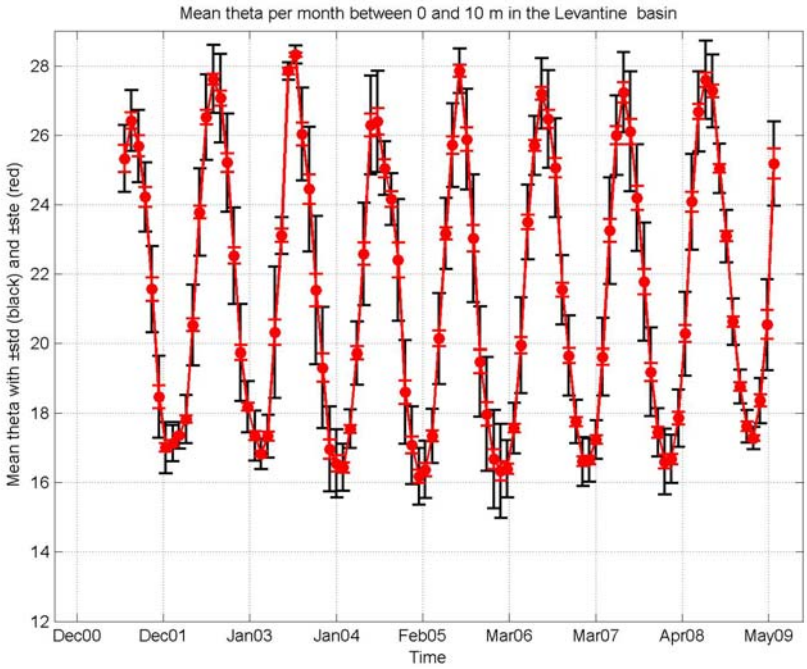

Figure 84. Monthly mean of surface θ in the Levantine sub-basin between December 2000 and June 2009.

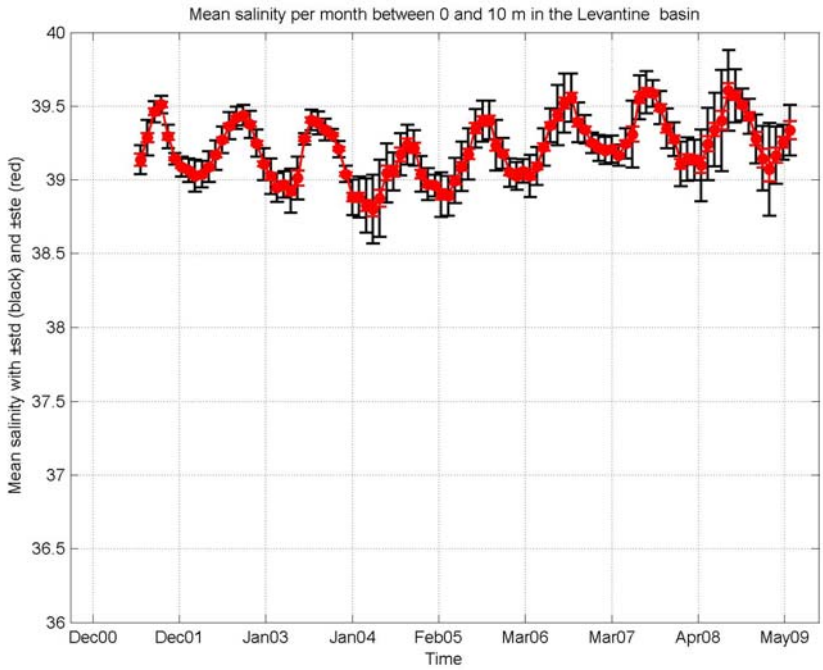

Figure 85. Monthly mean of surface S in the Levantine sub-basin between December 2000 and June 2009.

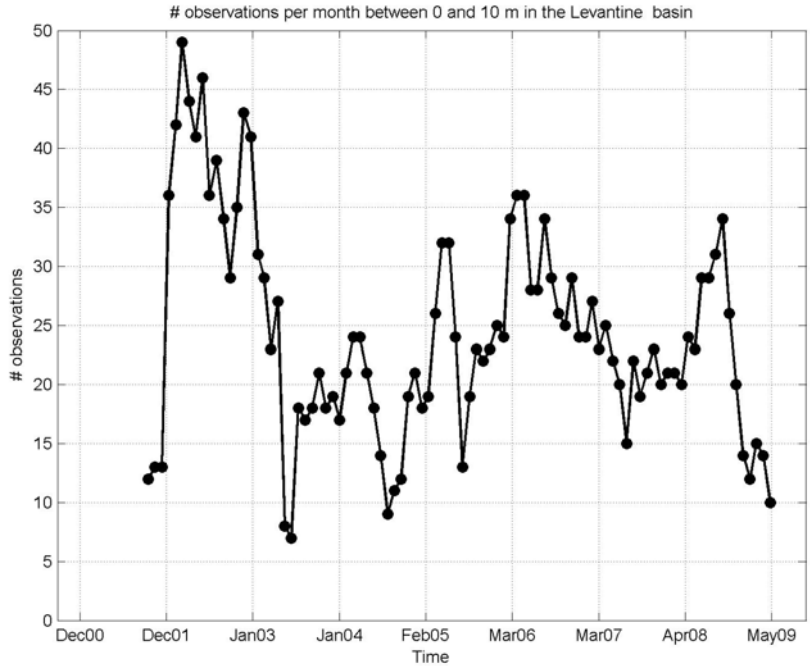

Figure 86. Number of surface observations in the Levantine sub-basin between December 2000 and June 2009.

The monthly means of θ and S near 600 m are displayed in Figures 87 and 88, respectively. Vertical bars denote the standard deviations and the standard errors. The corresponding numbers of observations are shown in Figure 89.

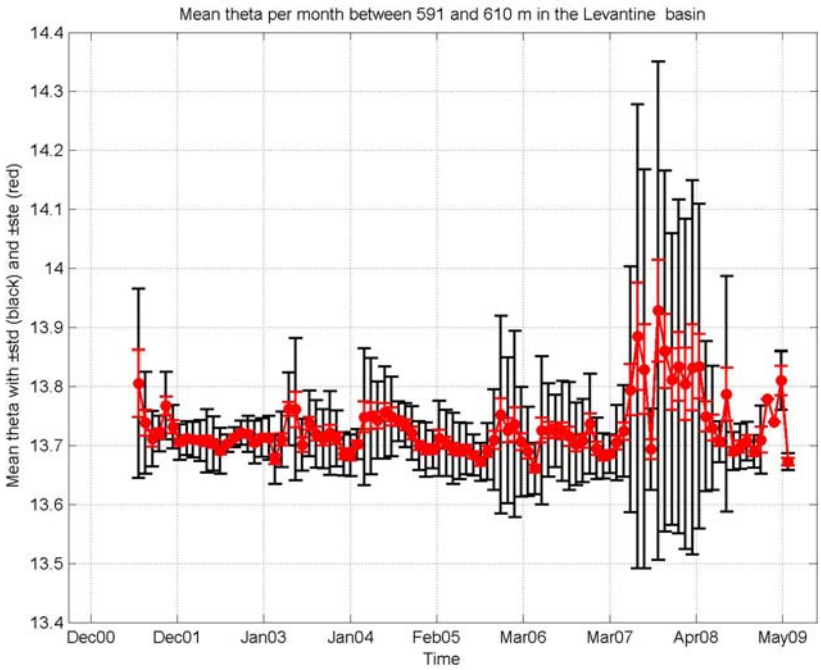

Figure 87. Monthly mean of θ near 600 m in the Levantine sub-basin between December 2000 and June 2009.

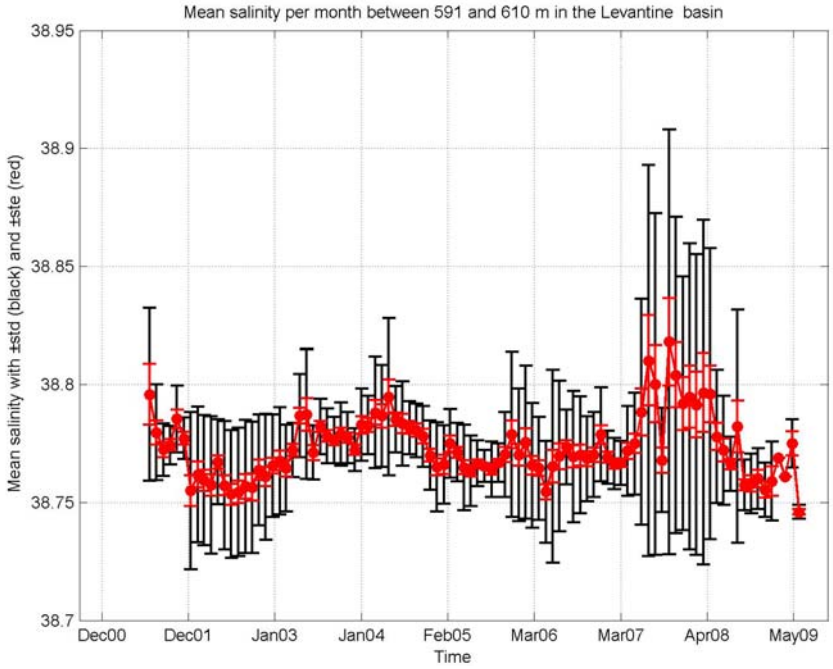

Figure 88. Monthly mean of S near 600 m in the Levantine sub-basin between December 2000 and June 2009.

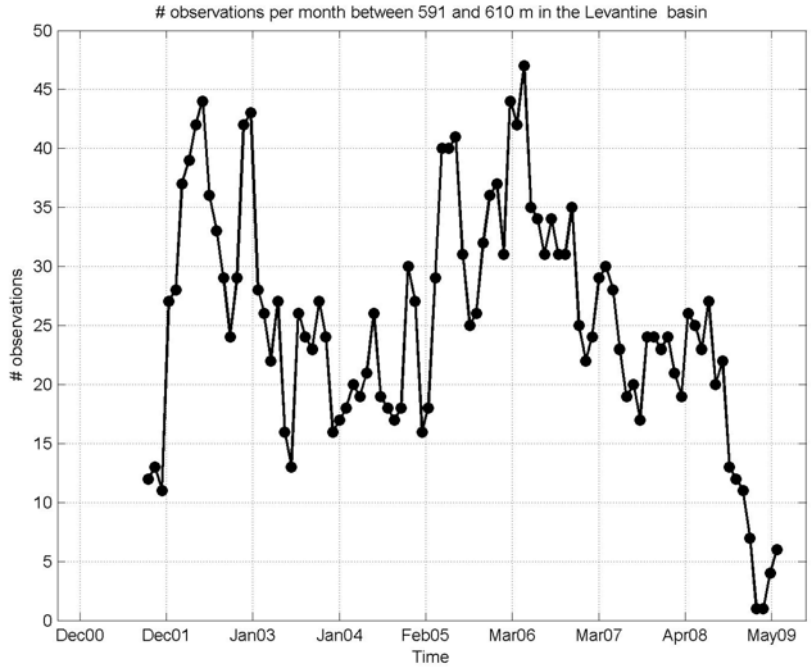

Figure 89. Number of observations near 600 m in the Levantine sub-basin between December 2000 and June 2009.

The monthly means of θ and S near 2000 m are displayed in Figures 90 and 91, respectively. Vertical bars denote the standard deviations and the standard errors. The corresponding numbers of observations are shown in Figure 92.

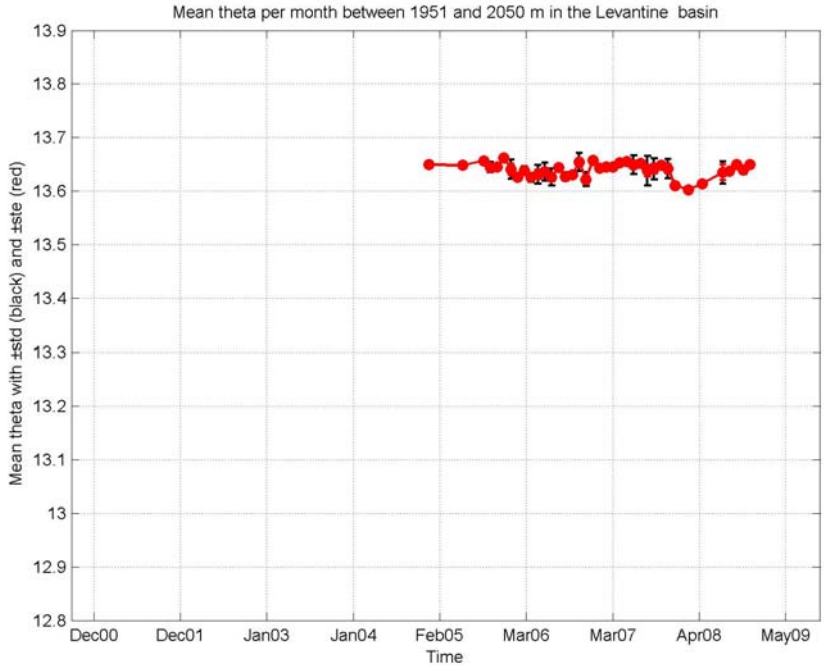

Figure 90. Monthly mean of θ near 2000 m in the Levantine sub-basin between December 2000 and June 2009.

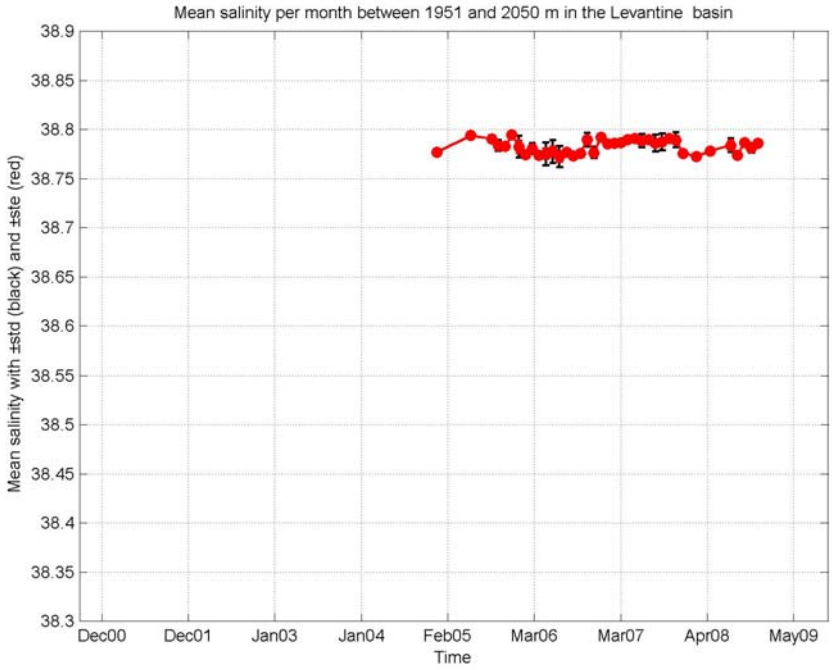

Figure 91. Monthly mean of S near 2000 m in the Levantine sub-basin between December 2000 and June 2009.

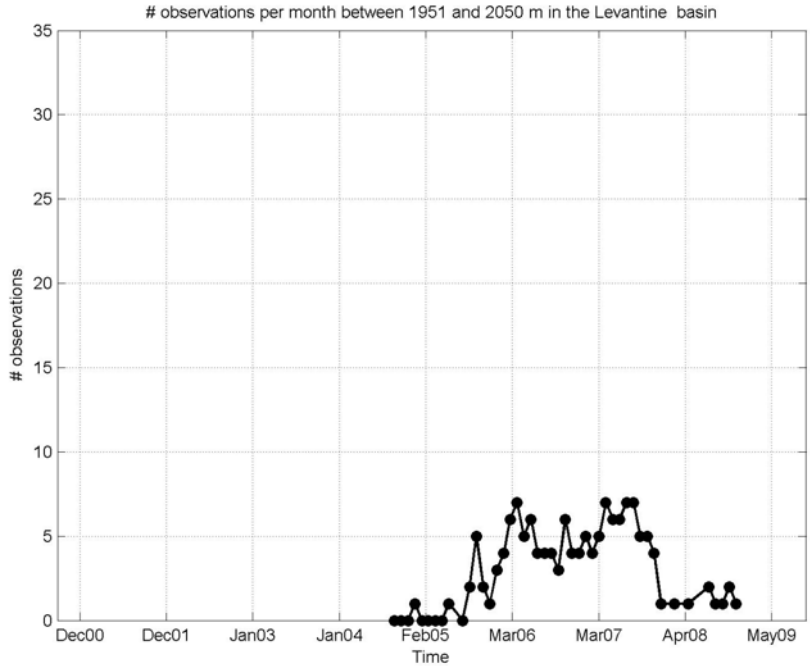

Figure 92. Number of observations near 600 m in the Levantine sub-basin December 2000 and June 2009.

The temporal distributions of the monthly mean of the maximum S and the corresponding depth of the salinity maximum are depicted, respectively in Figures 93 and 94.

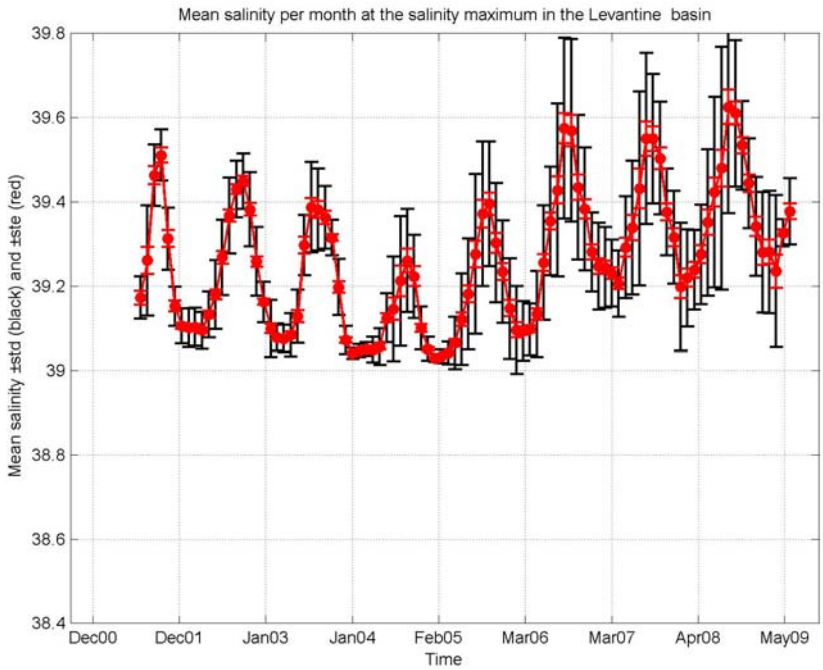

Figure 93. Monthly mean of the maximum S in the Levantine sub-basin December 2000 and June 2009.

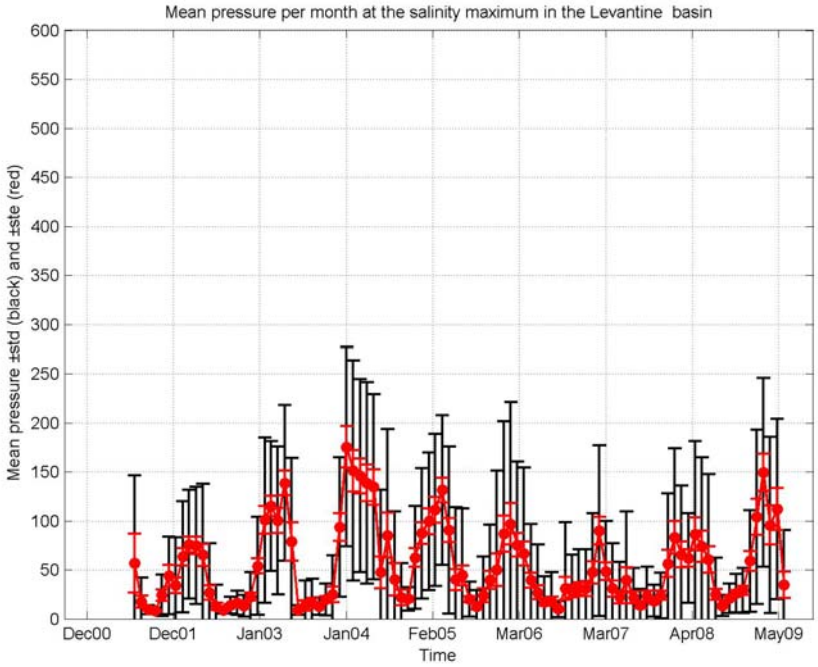

Figure 94. Monthly mean of the depth of the salinity maximum in the Levantine sub-basin between December 2000 and June 2009.

2.1.8 All Mediterranean sub-basins

The statistics of the thermohaline characteristics of the Mediterranean sub-basins are hereafter illustrated in composite figures in order to put in evidence the differences amongst the sub-basins. The temporal evolution of the monthly near-surface temperatures and salinities are displayed in Figures 95 and 96, respectively. The same statistics for the properties near 600 and 2000 m are displayed in Figure 97 to 100. Finally, the mean temperature and salinity at the depth of salinity maximum, as well as the mean depth of this maximum, are displayed versus time in Figures 101 to 102.

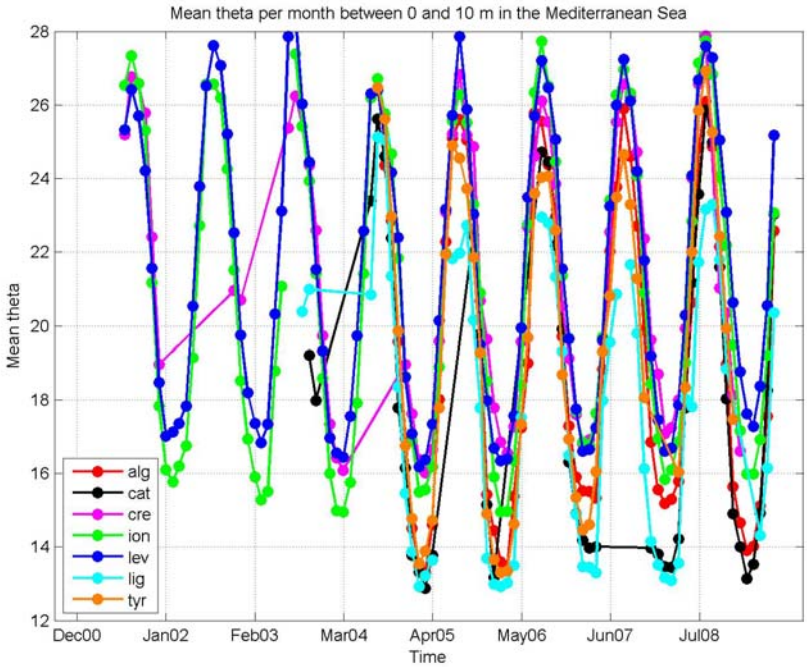

Figure 95. Monthly mean of near-surface θ in the Mediterranean sub-basins between December 2000 and June 2009.

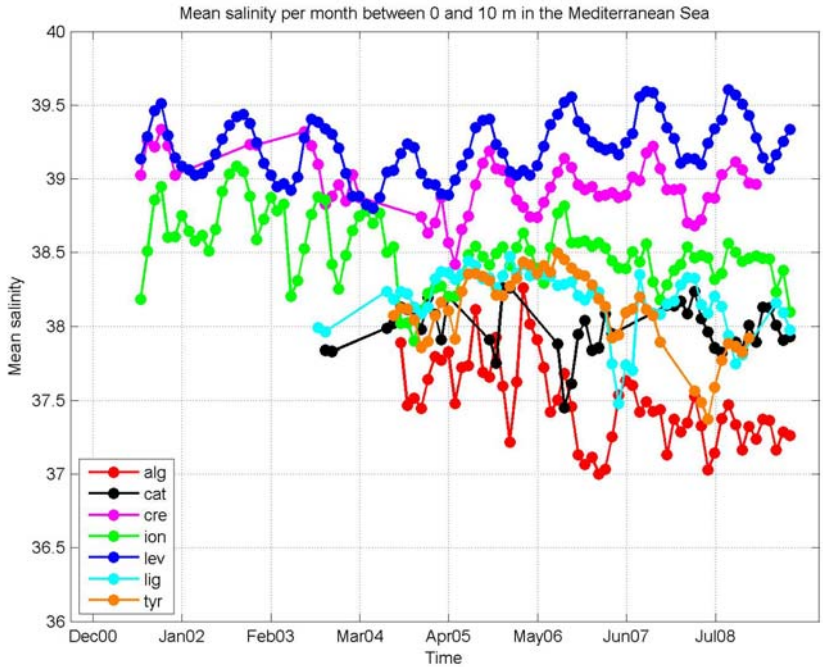

Figure 96. Monthly mean of near-surface S in the Mediterranean sub-basins between December 2000 and June 2009.

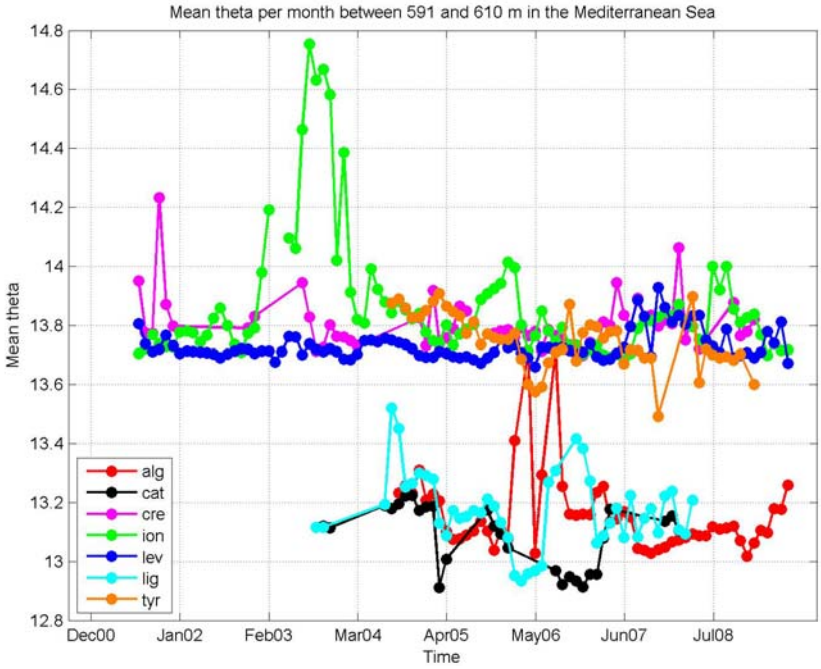

Figure 97. Monthly mean of θ near 600 m in the Mediterranean sub-basins between December 2000 and June 2009.

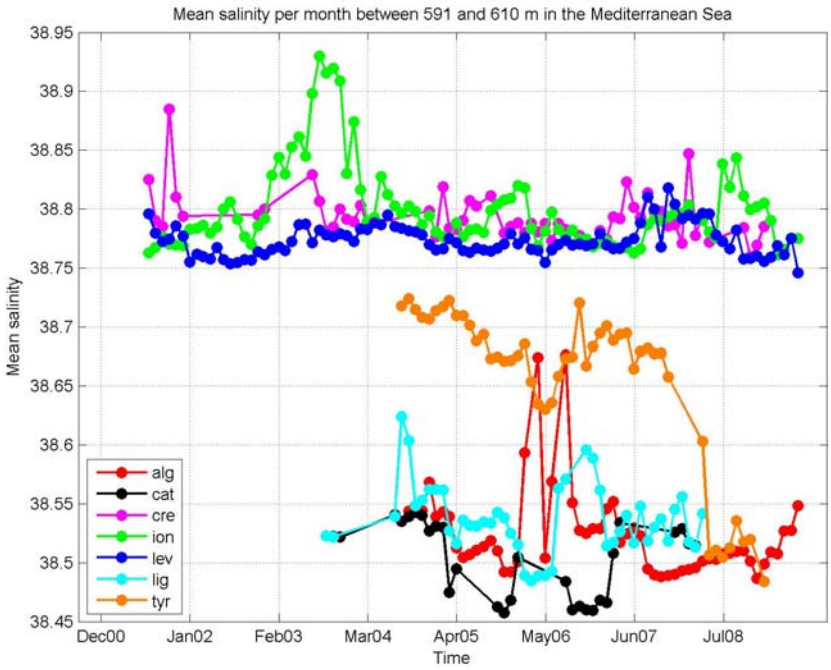

Figure 98. Monthly mean of S near 600 in the Mediterranean sub-basins between December 2000 and June 2009.

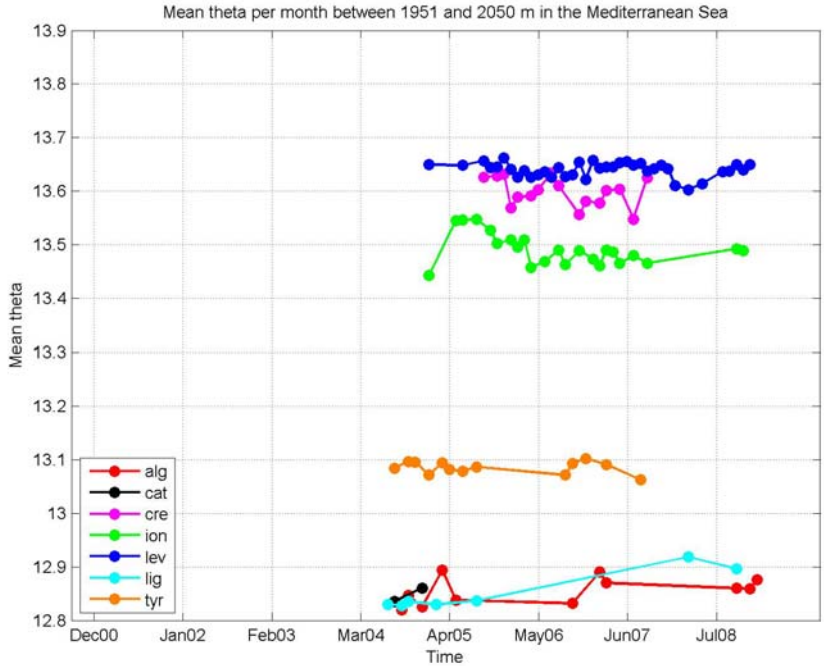

Figure 99. Monthly mean of θ near 2000 m in the Mediterranean sub-basins between December 2000 and June 2009.

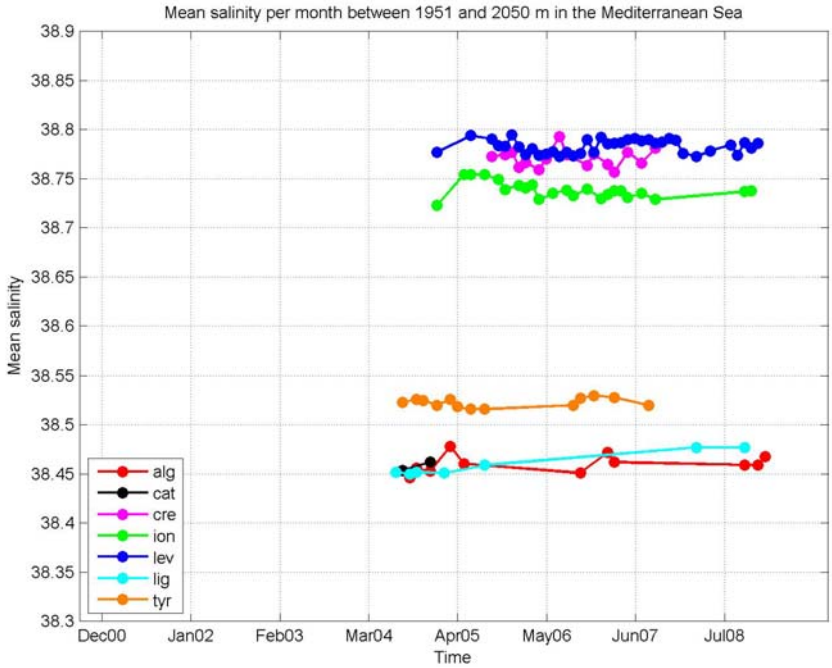

Figure 100. Monthly mean of S near 2000 m in the Mediterranean sub-basins between December 2000 and June 2009.

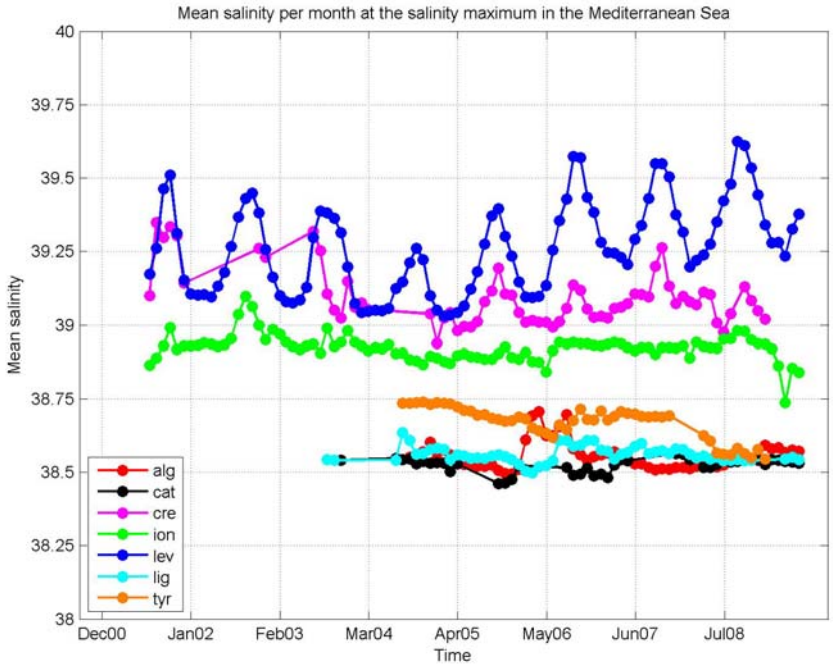

Figure 101. Monthly mean of S at the salinity maximum in the Mediterranean sub-basins between December 2000 and June 2009.

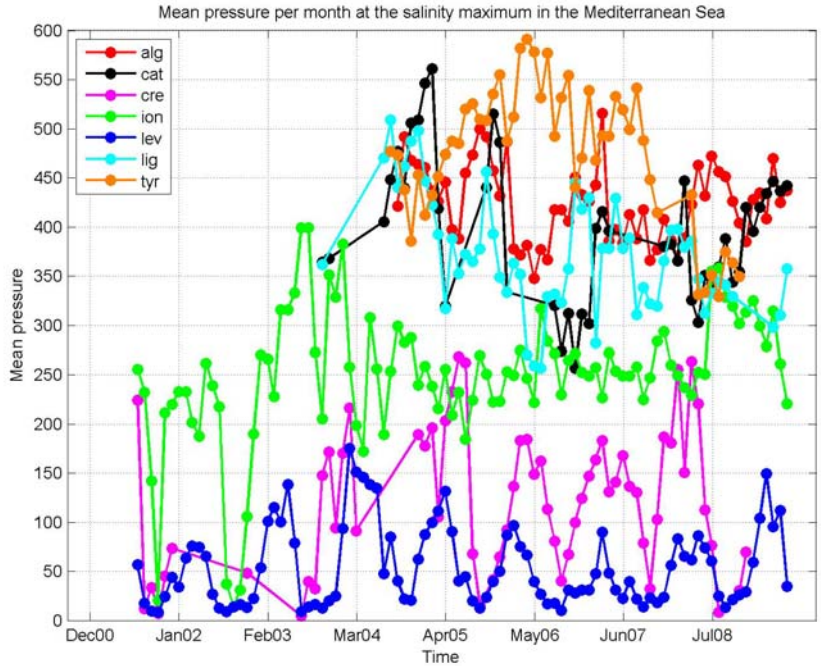

Figure 102. Depth of the salinity maximum in the Mediterranean sub-basins between December 2000 and June 2009.

2.2 Decorrelation scales of temperature and salinity

The time-lagged auto-correlations of temperature and salinity at selected depths were calculated to estimate the decorrelation scales following the floats. For each float, a linear trend was removed from the data time series before computing the auto-correlation, in order to have a realistic measure of the data decorrelation (see example for a float in Figures 103 and 104). The auto-correlations of potential temperature (Figure 105) and salinity (Figure 106) are computed, by using a time step of 5 days. The Lagrangian integral time scale is computed by integrating to the first zero crossing of the autocorrelation function.

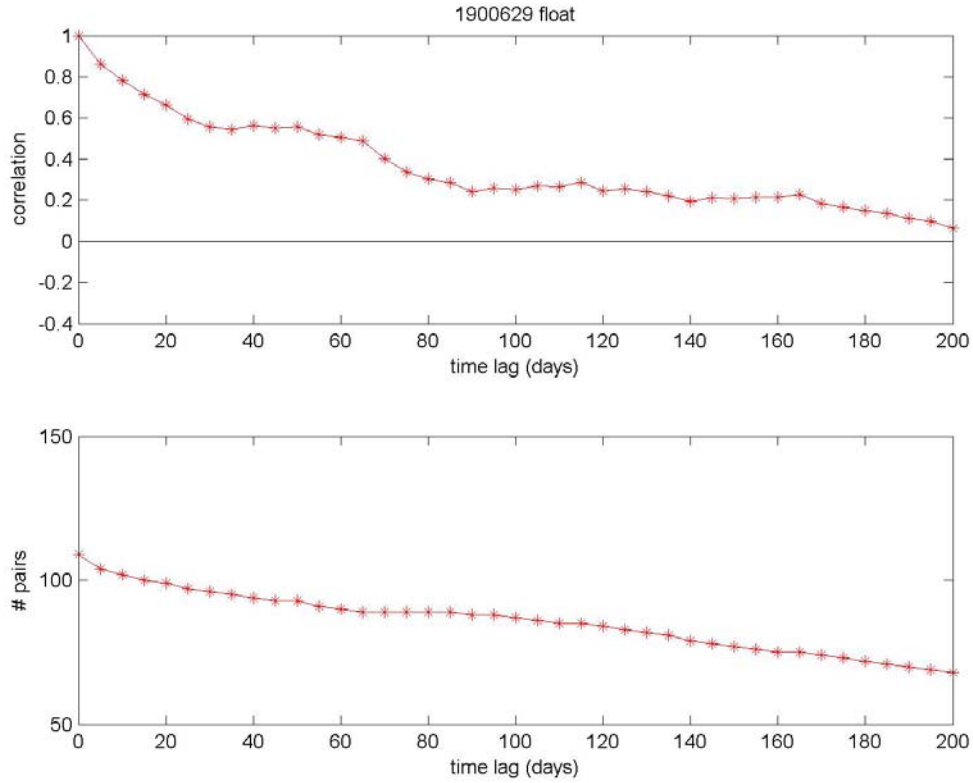

Figure 103. Auto-correlation of temperature (top) and number of pairs (bottom) versus time lag for Argo float 1900629 (trend is not removed from the time series before computing the correlation).

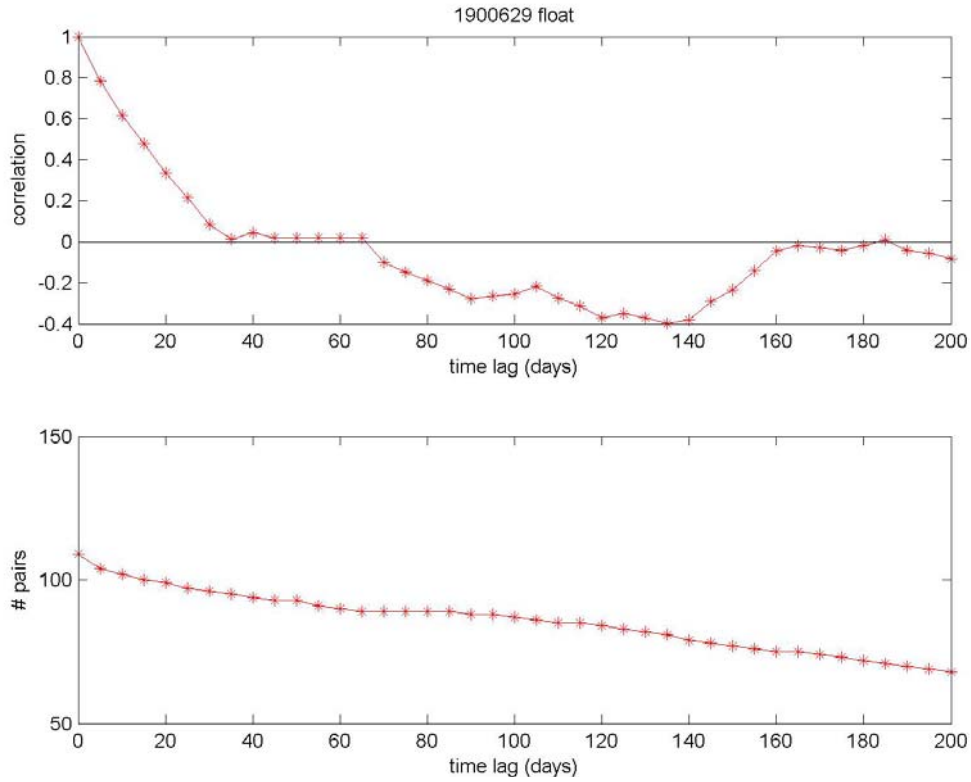

Figure 104. Auto-correlation of temperature (top) and number of pairs (bottom) versus time lag for Argo float 1900629 (trend is removed from the time series before computing the correlation).

At mid-depth (600 m) where most floats have collected data and where the seasonal deterministic signal is reduced, the correlation coefficients for the potential temperature decreases to 0.84 after 5 days, and to 0.75 after 10 days (Figure 105). The zero-crossing occurs after about 140 days, whereas the Lagrangian integral time scale is about 60 days. The results are similar for the salinity at 600 m (Figure 106).

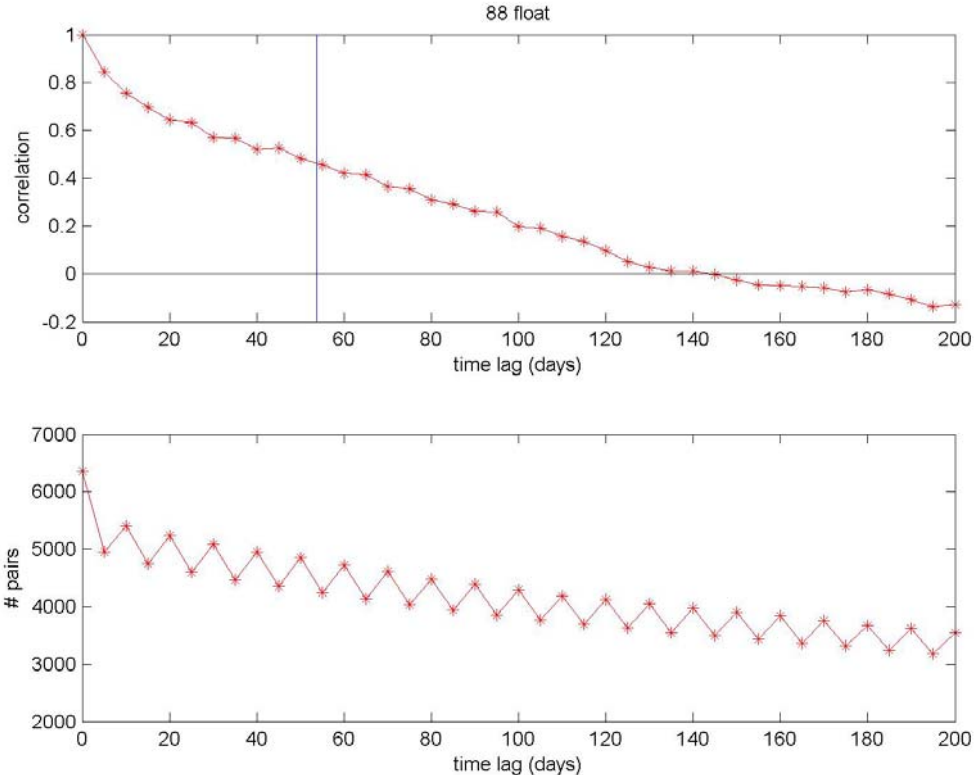

Figure 105. Auto-correlation of temperature and integral time scale (vertical bar) (top) and number of pairs (bottom) versus time lag for all the floats in the Mediterranean (trend is removed from the time series before computing the correlation).

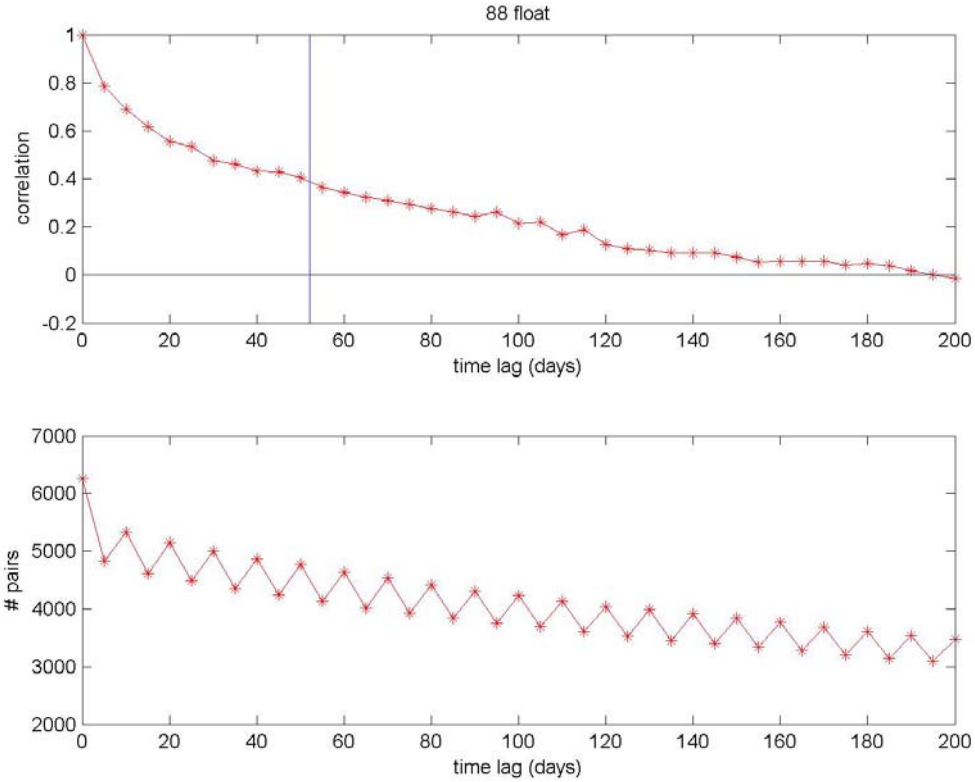

Figure 106. Same as Figure 105 but for salinity.

3. Argo data in the Black Sea

In total, 7 Argo floats have been operated in the Black Sea between March 2005 and June 2009. They have been deployed as part of a joint project between the University of Washington (USA), the Middle East Technical University (Turkey) and the Marine Hydrophysical Institute (Ukraine) (Korotaev et al. 2006). These floats had a cycle length of 7 days and a parking depth between 200 and 1550 m. The data of only 4 units downloaded from the GDAC in June 2009 are considered in this report. Details on the number of floats and profiles are listed in Table 3.

Program/Agency/Country	Number of floats	Number of CTD profiles
UW/METU/MHI	4	626
TOTAL	4	626

Table 3. Number of floats and CTD profiles considered for the Argo program in the Black Sea between March 2005 and June 2009.

Figure 107 shows the geographical coverage of the Argo profiles considered in the Black Sea.

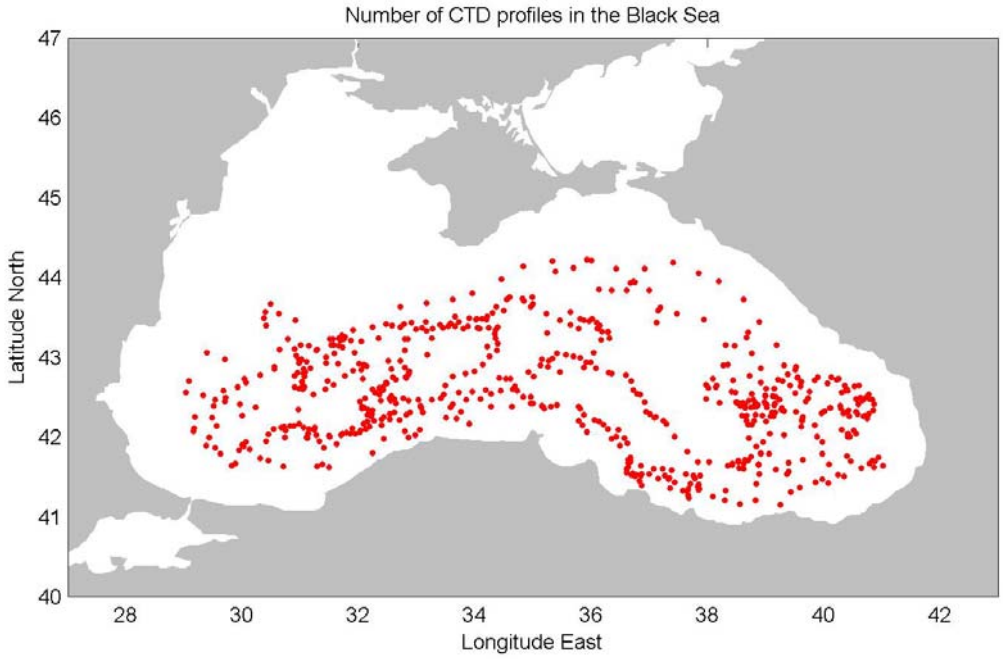

Figure 107. Geographical distribution of the CTD profiles provided by four Argo floats in the Black Sea between March 2005 and June 2009.

Figures 108 and 109 illustrate the temporal distribution of the number of active floats and the number of CTD profiles per month in the Black Sea, respectively.

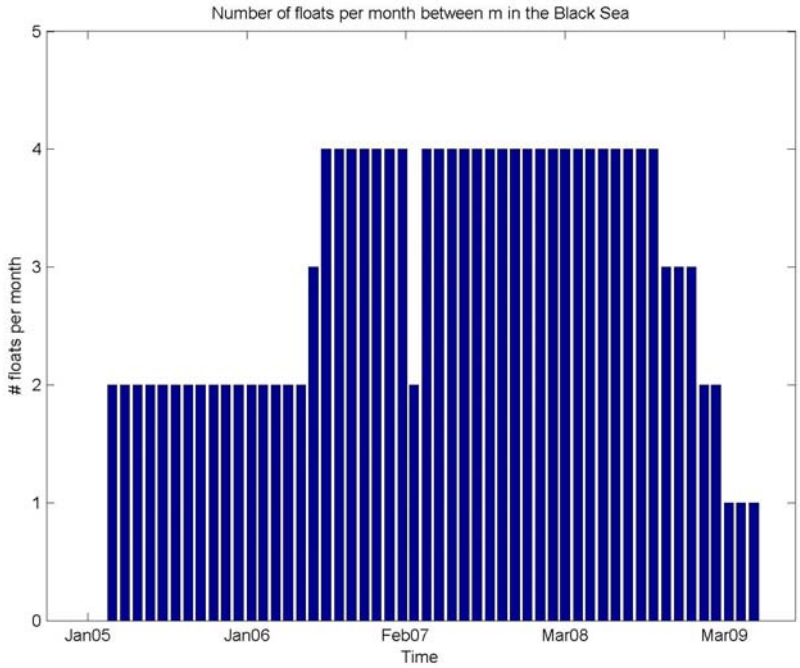

Figure 108. Number of active floats per month in the Black Sea between March 2005 and June 2009.

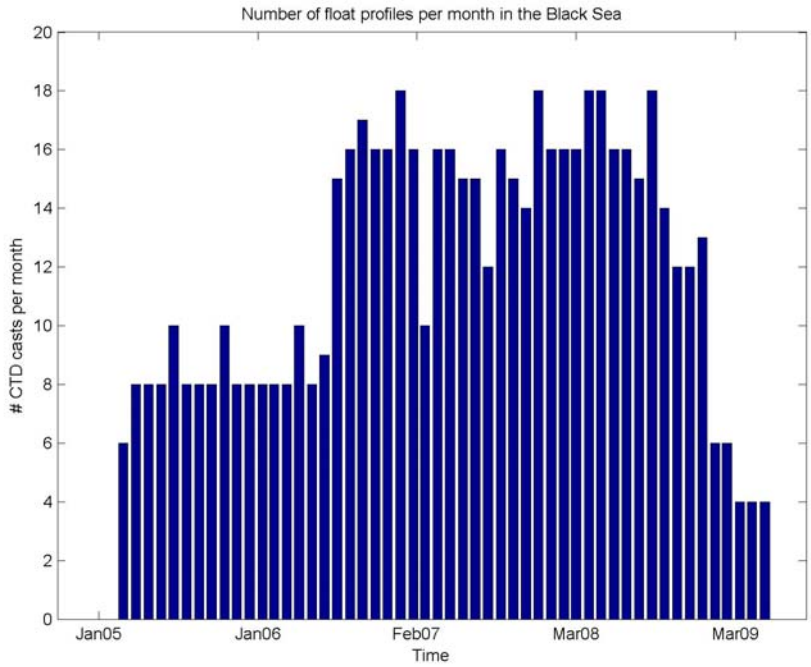

Figure 109. Number of CTD profiles per month in the Black Sea between March 2005 and June 2009.

3.1 Thermohaline characteristics of the Black Sea.

The following statistics have been calculated using the above-mentioned Argo data in the Black Sea:

- number of observations, mean and standard deviation of potential temperature (θ) and salinity (S) near 0, 200 and 1500 m;

The monthly means of θ and S near the surface (0-10 m) are displayed in Figures 110 and 111, respectively. Vertical bars denote the standard deviations and the standard errors. The corresponding numbers of observations are shown in Figure 112.

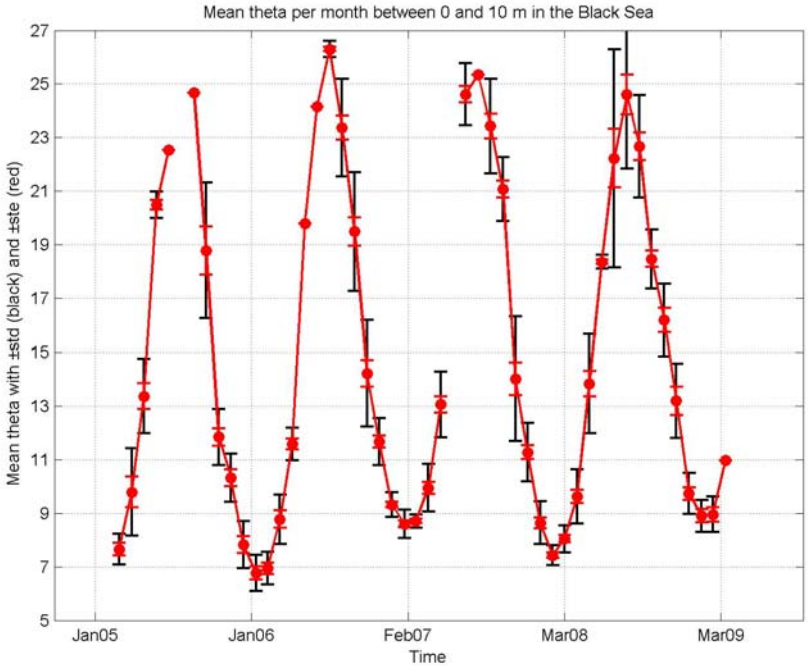

Figure 110. Monthly mean of surface θ in the Black Sea between March 2005 and June 2009.

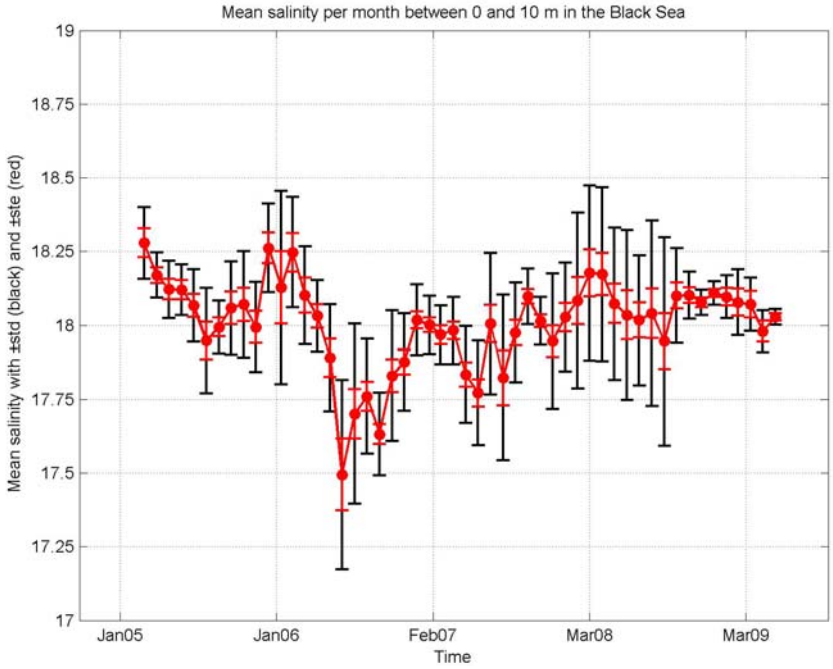

Figure 111. Monthly mean of surface S in the Black Sea between March 2005 and June 2009.

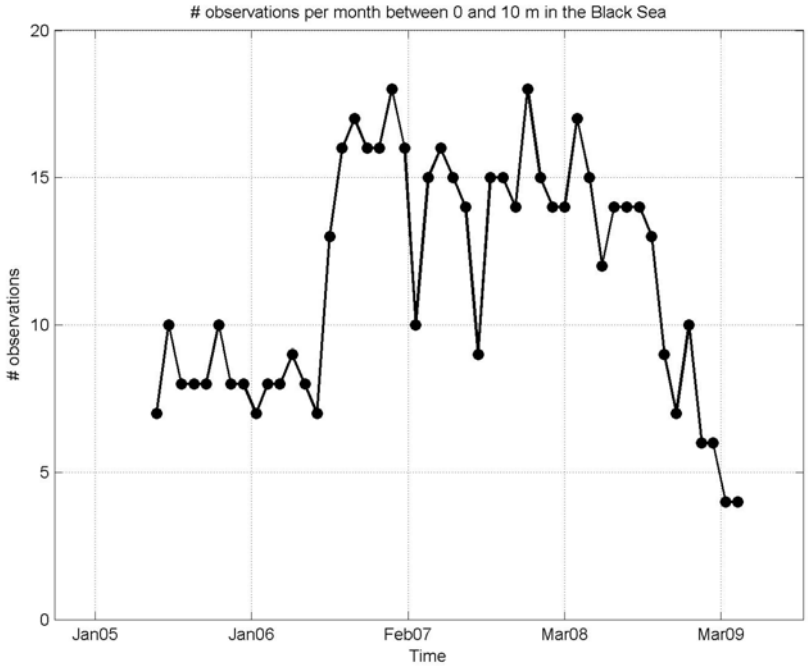

Figure 112. Number of surface observations in the Black Sea between March 2005 and June 2009.

The monthly means of θ and S near 200 m are displayed in Figures 113 and 114, respectively. Vertical bars denote the standard deviations and the standard errors. The corresponding numbers of observations are shown in Figure 115.

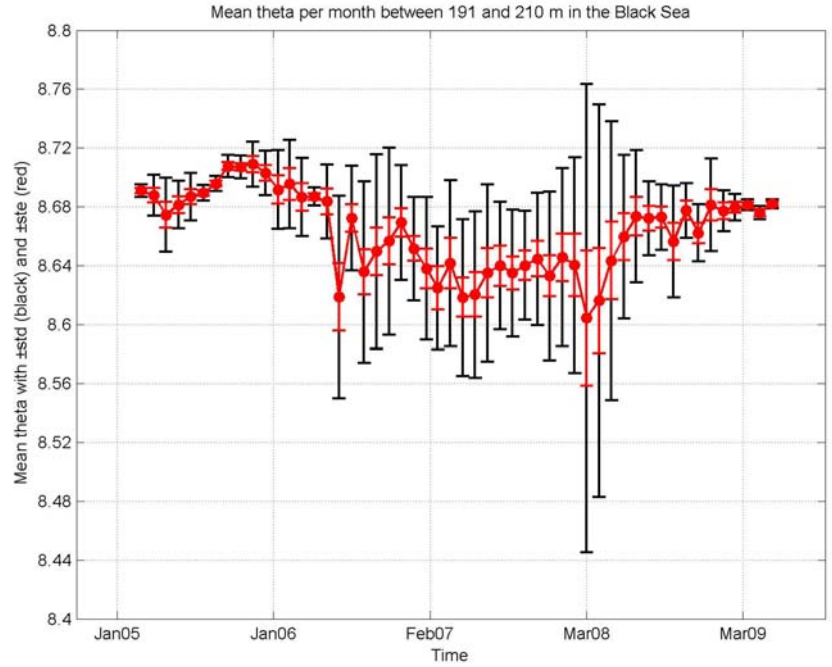

Figure 113. Monthly mean of θ near 200 m in the Black Sea between March 2005 and June 2009.

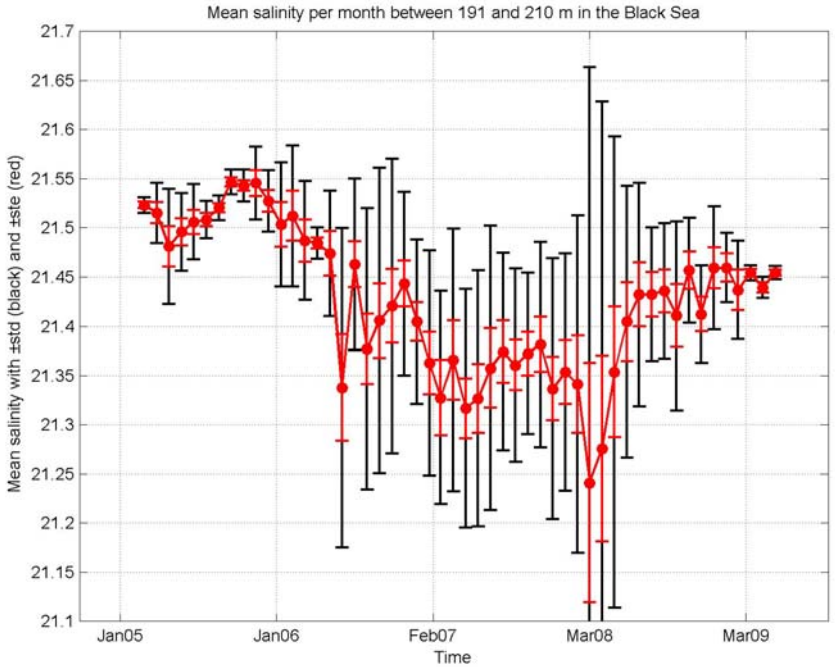

Figure 114. Monthly mean of S near 200 m in the Black Sea between March 2005 and June 2009.

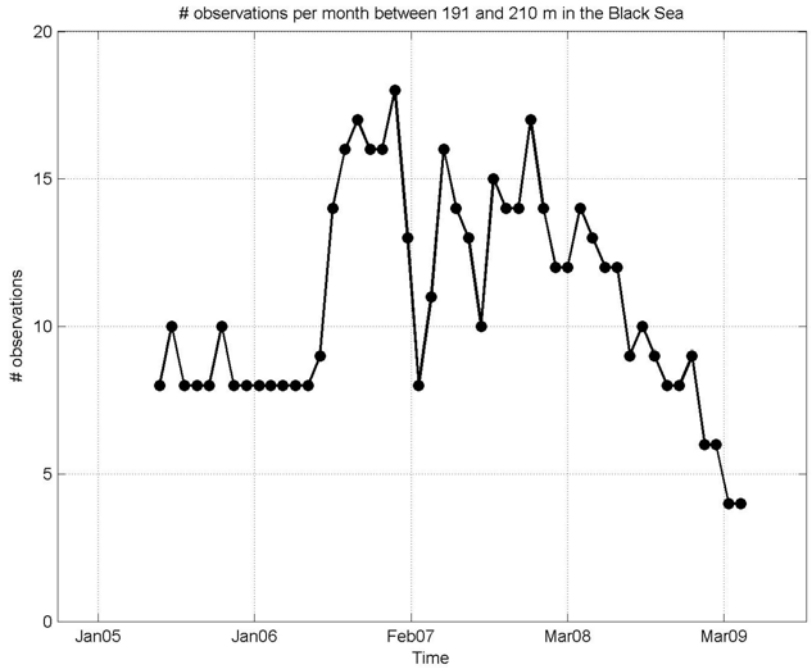

Figure 115. Number of observations near 200 m in the Black Sea between March 2005 and June 2009.

The monthly means of θ and S near 1500 m are displayed in Figures 116 and 117, respectively. Vertical bars denote the standard deviations and the standard errors. The corresponding numbers of observations are shown in Figure 118.

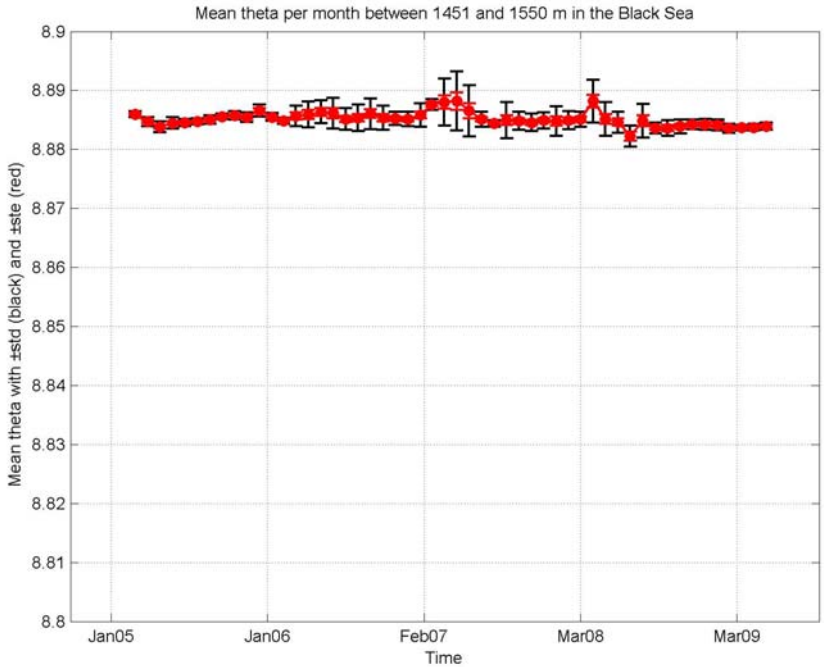

Figure 116. Monthly mean of θ near 1500 m in the Black Sea between March 2005 and June 2009.

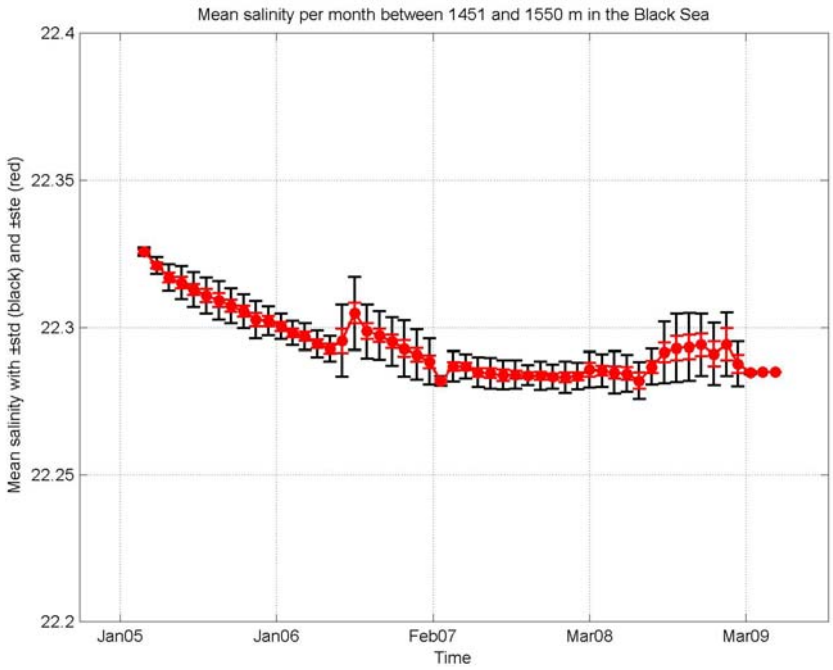

Figure 117. Monthly mean of S near 1500 m in the Black Sea between March 2005 and June 2009.

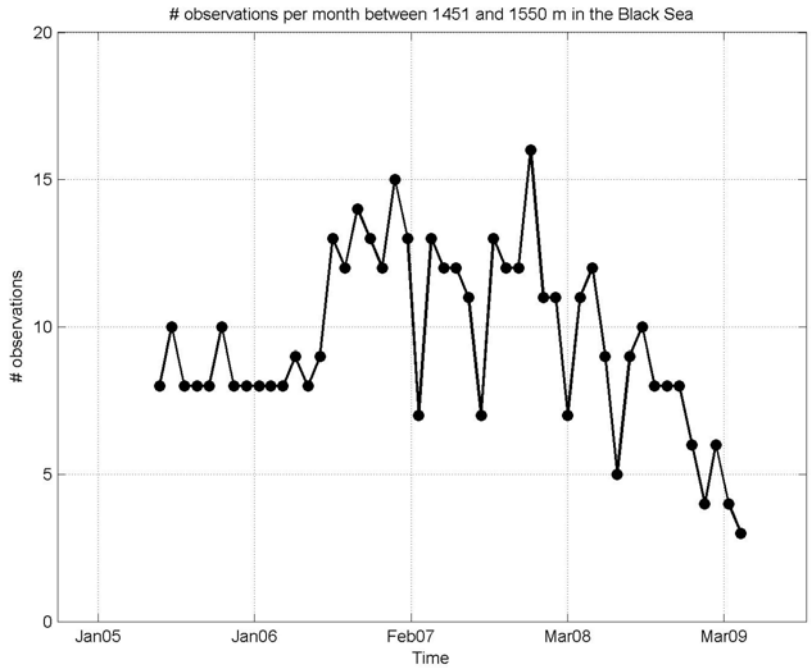

Figure 118. Number of observations near 1500 m in the Black Sea between March 2005 and June 2009.

3.2 Decorrelation scales of temperature and salinity

The time-lagged auto-correlations of potential temperature (Figure 119) and salinity (Figure 120) were computed by using a time step of 7 days. At 200 m where most floats have collected data and where the seasonal deterministic signal is reduced, the correlation coefficients for the potential temperature decreases to 0.84 after 7 days, and to 0.74 after 14 days. The zero-crossing occurs after about 170 days, whereas the Lagrangian integral time scale is about 45 days. The results are similar for the salinity at 200 m.

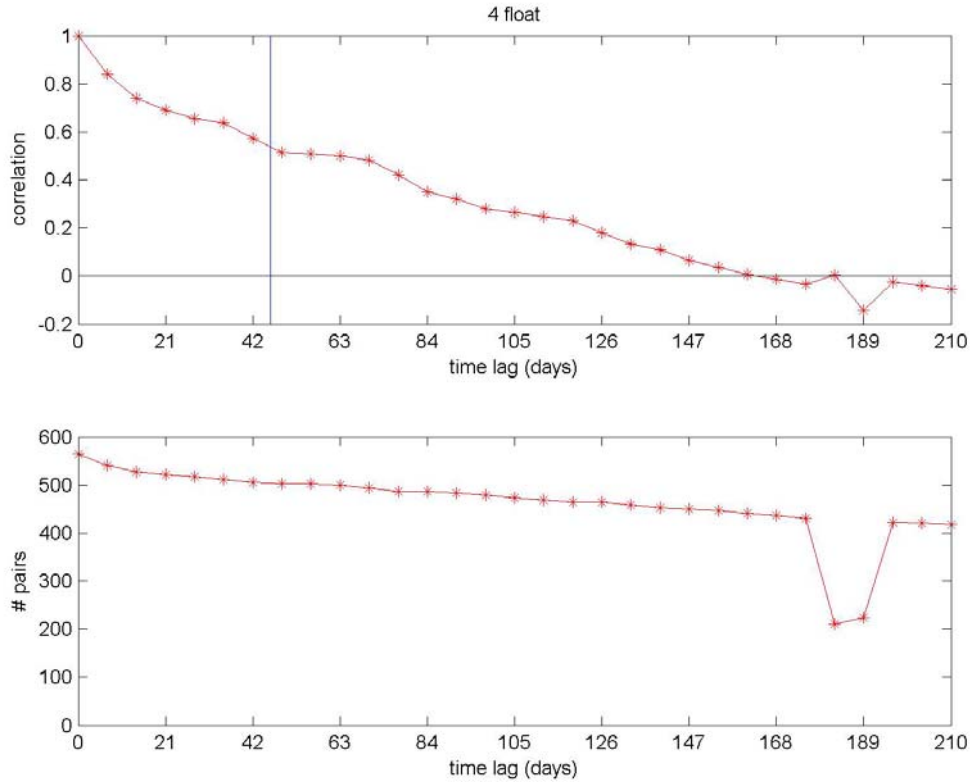

Figure 119. Auto-correlation versus time lag and integral time scale (vertical bar) of temperature at 200 m (top) and number of pairs (bottom) computed from the Argo floats in the Black Sea (trend is removed from the time series before computing the correlation).

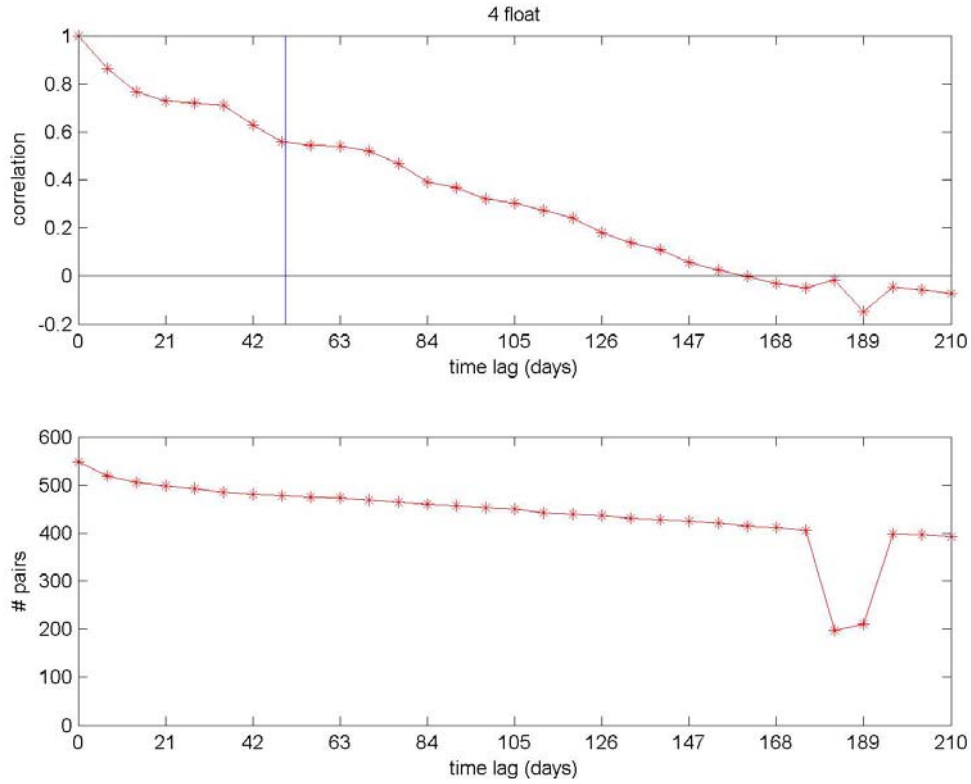

Figure 120. Same as Figure 119 but for salinity at 200 m.

4. Conclusions

In total, 88 Argo floats have been operated in the Mediterranean between December 2000 and June 2009, providing more than 7700 CTD profiles. We have shown that:

- The maximum float density was obtained in May 2006 with 31 floats operating simultaneously.
- The Levantine sub-basin is in general the most populated with data spanning continuously between June 2001 and June 2009.
- The potential temperature exhibits a seasonal cycle near the surface in all the sub-basins, as well as the salinity in the Cretan and Levantine sub-basins.
- The characteristics of the temporal evolution of potential temperature and salinity at 600 and 2000 m show that the sub-basins can be mainly grouped in western and eastern sub-basins.

- trends are evident in the time series of monthly averaged temperature and salinity for some sub-basins, but their interpretation should be very cautious due to the non-uniform sampling of the floats, both in space and time (see for instance the salinity at 600 m in the Tyrrhenian Sea, Figure 49).

- At 600 m the correlation coefficient for the potential temperature decreases to 0.84 after 5 days, and to 0.75 after 10 days. The zero-crossing occurs after about 140 days, whereas the Lagrangian integral time scale is about 60 days.

In the Black Sea, the data for 4 Argo floats between March 2005 and June 2009 (more than 600 CTD profiles) have been used to show that:

- The potential temperature exhibits a seasonal cycle near the surface.

- The potential temperature decreases from the surface to the bottom and salinity reaches its maximum at the bottom layer (about at 1500 m).

- At 200 m the correlation coefficients for the potential temperature decreases to 0.84 after 7 days, and to 0.74 after 14 days. The zero-crossing occurs after about 170 days, whereas the Lagrangian integral time scale is about 45 days.

5. References

Korotaev, G., T. Oguz, S. Riser Intermediate and deep currents of the Black Sea obtained from autonomous profiling floats. Deep-Sea Research II 53 (2006) 1901–1910.

Poulain, P.-M., R. Barbanti, J. Font, A. Cruzado, C. Millot, I. Gertman, A. Griffa, A. Molcard, V. Rupolo, S. Le Bras, and L. Petit de la Villeon (2007) MedArgo: a drifting profiler program in the Mediterranean Sea. Ocean Sci., 3, 379-395.